DELVING INTO THE HEART OF THE MATTER: UNDERSTANDING THE ASSOCIATIONS BETWEEN TGF-β, CTGF AND EARLY MYOCARDIAL CHANGES IN ANGIOTENSIN-II INDUCED MYOCARDIAL FIBROSIS

by

Kok Sum Chloe Wong

Submitted in partial fulfilment of the requirements
for the degree of Master of Science

at

Dalhousie University
Halifax, Nova Scotia
January 2017

DEDICATION PAGE

To my family, friends, and every person I have met along the way that helped me get to this point in my life.

TABLE OF CONTENTS

LIST OF TABLES ..... **vii**

LIST OF FIGURES ..... **viii**

ABSTRACT ..... **x**

LIST OF ABBREVIATIONS USED ..... **xi**

ACKNOWLEDGEMENTS ..... **xvi**

CHAPTER 1 – INTRODUCTION **1**

1.1 Cardiovascular Disease **1**

1.1.1 Heart Failure *1*

1.1.2 Mechanics of Diastolic Heart Failure *2*

1.1.3 Role of Myocardial Fibrosis in Heart Failure *4*

1.1.4 Ang-II and Myocardial Fibrosis *7*

1.2 Cellular Players of Ang-II Induced Myocardial Fibrosis **10**

1.2.1 Resident Caridac Cellular Composition *10*

1.2.2 Resident and Infiltrating Cells in Ang-II Exposed Myocardium *12*

1.3 Molecular Players of Myocardial Fibrosis **13**

1.3.1 Role of TGF-β in Myocardial Fibrosis *14*

1.3.2 Role of CTGF in Myocardial Fibrosis *20*

1.3.3 Biosynthesis and Regulation of Collagen in Myocardial Fibrosis *20*

1.4 Rationale, Hypothesis, and Objectives **22**

1.4.1 Rationale *22*

1.4.2 Objectives *23*

1.4.3 Hypothesis *23*

CHAPTER 2 – MATERIALS AND METHODS 24

2.1 Animals 24

2.2 Saline/Ang-II Infusion and TGF-β Trap Injections 24

2.3 Hemodynamic Measurements 25

2.4 Tissue Harvest and Cell Isolation 25

2.4.1 Cell Isolation – Heart 26

2.4.2 Peripheral Blood Mononuclear Cells (PBMCs) 27

2.4.3 Cell Isolation – Spleen 27

2.5 Flow Cytometry 27

2.6 Tissue Processing and Histological Analyses 29

2.6.1 Hematoxylin-and-Eosin Staining and Analyses 29

2.6.2 Sirius Red/Fast Green Staining and Analyses 30

2.6.3 Immunohistochemistry 30

2.7 *In vitro* Monoculture System 31

2.7.1 Monoculture of NIH/3T3 Fibroblasts 31

2.7.2 NIH/3T3 Fibroblast Exogenous Treatments 32

2.7.3 Immunofluorescence on Fixed In vitro *Cultured Cells 32*

2.8 Proliferation Assay 33

2.9 Gel Electrophoresis and Western Blotting 33

2.10 Relative Real-Time Quantitative Polymerase Chain Reaction (qPCR) .. 37

2.10.1 RNA Extraction and cDNA Synthesis 37

2.10.2 qPCR Reaction and Analyses 38

2.11 Statistical Analyses 38

CHAPTER 3 – RESULTS 40

3.1 Characterization of the Ang-II Model 40

3.2 Early mononuclear cell infiltration precedes significant collagen deposition 41

3.3 Profibrotic factors in the early Ang-II exposed myocardial environment 42

3.4 Mechanistic Link Between Early CTGF Upregulation and TGF-β Activity in the Ang-II Exposed Myocardium 44

3.4.1 Effect of TGF-β Trap on Gene Expression of Pro-fibrotic Factors in vitro *44*

3.4.2 Effect of TGF-β Trap on Early Pro-fibrotic Gene Expression in vivo *45*

3.5 Effect of TGF-β Trap on Early Gross Histological and Cellular Changes in the Ang-II Exposed Myocardium 46

3.6 Role of CTGF on Fibroblast Activation and Proliferation 48

3.6.1 Exogenous CTGF Does Not Appear to Affect Fibroblast Expression of Fibrotic Mediators in vitro *49*

3.6.2 Exogenous CTGF Does Not Appear to Alter Fibroblast Phenotype in vivo *49*

3.7 Characterizing Early Monocytes/Mϕ Composition and Subsets in the Spleen, Blood, and Heart of Ang-II Exposed Mice 50

3.7.1 Mϕ Influx Demonstrated a Pro-Inflammatory Shift in the Ang-II Heart 51

3.7.2 $CD11b^{+}$ Monocytes Were Present in Lower Proportion in Circulation with No Differences in Pro-Inflammatory Phenotype 51

3.7.3 Splenic $CD11b^{+}$ Monocytes Were Reduced After Ang-II Exposure and Consisted of a Higher Proportion of Pro-Inflammatory $Ly6C^{high}CCR2^{+}$ Monocytes 52

3.8 Figures 53

CHAPTER 4 – DISCUSSION 79

4.1 Summary of Findings in the Context of the Literature 79

4.1.1 Early Cellular and Molecular Changes in the Ang-II Exposed Myocardium 80

4.1.2 Mechanistic Link Between Early CTGF Upregulation and TGF-β Activation in the Ang-II Infused Myocardium 82

4.1.3 Gross and Cellular Histological Changes in the Ang-II Exposed Myocardium at 24 Hours 85

4.1.4 Role of CTGF in Fibroblast Activity and Phenotype In vitro *89*

4.1.5 Characterizing Monocyte/Mϕ Composition and Subsets in Ang-II Exposed Mice 90

4.2 Limitations 92

4.3 Future Directions 95

4.4 Concluding Remarks 98

REFERENCES 102

LIST OF TABLES

Table 2.1 Antibody Concentrations, Host, and Source Information..... 35

Table 2.2 Genes of Interest and Primer Sequences..... 39

LIST OF FIGURES

Figure 1.1 Simplified overview of TGF-β activation and signaling 18

Figure 3.1 Hemodynamic and physiological parameters of Ang-II exposed mice 53

Figure 3.2 Collagen deposition in Ang-II myocardium after 24 hours 54

Figure 3.3 Mononuclear cellular infiltration in the myocardium was present at 24 hours after Ang-II exposure 56

Figure 3.4 Myocardium exposed to Ang-II for 6 hours did not display significant cellular infiltration 57

Figure 3.5 Early upregulation of myocardial CTGF and TGF-β transcript levels appeared as early as 6 hours after Ang-II exposure 58

Figure 3.6 Levels of Smad2 phosphorylation was upregulated after Ang-II exposure, indicative of TGF-β activity 59

Figure 3.7 Effect of TGF-β trap on levels of exogenous TGF-β-induced upregulation of pro-fibrotic CTGF, TGF-β and type I collagen transcript levels of NIH/3T3 *in vitro* 61

Figure 3.8 TGF-β trap reduced levels of Ang-II-induced early upregulation of CTGF transcript at 6 hours 63

Figure 3.9 TGF-β trap administration partially reduced Ang-II-induced elevation of Smad2 phosphorylation at 6 hours 64

Figure 3.10 Administration of the TGF-β trap did not affect degree of Ang-II-Induced cellular infiltration observed at 24 hours 66

Figure 3.11 Transdifferentiation into α-SMA^{+} myofibroblasts was not evident after 24 hours of Ang-II infusion 67

Figure 3.12 Ang-II infusion led to significant increase in Ki-67^{+} mononuclear cells In the myocardium after 24 hours, indicative of increased cell proliferation, with no effect after TGF-β trap administration compared to Ang-II hearts 68

Figure 3.13 Exogenous CTGF treatment does not appear to have an effect on NIH/3T3 fibroblast production of pro-fibrotic CTGF, TGF-β, or type I collagen transcript independently or synergistically with exogenous TGF-β incubation *in vitro* 69

Figure 3.14 Exogenous CTGF treatment of NIH/3T3 fibroblasts does not appear to affect differentiation into α-SMA^{+} myofibroblasts independently or synergistically with exogenous TGF-β stimulation *in vitro* 71

Figure 3.15 Ang-II infusion led to significant influx of CCR2^{+}CX$_3$CR1^{+} monocytes/Mϕs in the myocardium at 3 days 73

Figure 3.16 CCR2^{+}CX$_3$CR1^{+} monocytes/Mϕs demonstrated a pro-inflammatory shift towards CD11b^{high}Ly6C^{high} phenotype after 3 days of Ang-II infusion 74

Figure 3.17 Blood CD11b^{+} monocytes displayed CD11b^{low} and CD11b^{high} subpopulations in lower proportions after Ang-II infusion 75

Figure 3.18 Circulatory CD11b^{high} monocytes were mainly pro-inflammatory Ly6C^{high}CCR2^{+} and present in similar proportions after Ang-II exposure 76

Figure 3.19 Splenic CD11b^{+} monocytes displayed CD11b^{high} and CD11b^{low} phenotypes and were present in lower numbers after Ang-II infusion 77

Figure 3.20 Ang-II infusion led to significant shift towards pro-inflammatory Ly6C^{high}CCR2^{+} splenic CD11b^{high} monocytes 78

Figure 4.1 Summary of Findings 100

ABSTRACT

Myocardial fibrosis is the common pathophysiological complication associated with diastolic heart failure. It is characterized by excess extracellular matrix (ECM) protein deposition, which contributes to increased ventricular wall stiffness and impaired relaxation. Transforming growth factor-β (TGF-β) and connective tissue growth factor (CTGF) are well-known to be fibrotic mediators associated with myocardial fibrosis. These cytokines, among others, act on resident and infiltrating cells, such as monocytes and fibroblasts, after cardiac injury or stress and alter cell phenotype and, consequently, the myocardial environment in an effort to repair the injured site. In this thesis, the early molecular and cellular changes associated with hypertension-induced myocardial fibrosis are explored using a model of continuous Angiotensin II (Ang-II) infusion in mice. By using a TGF-β trap able to sequester and neutralize active TGF-β, we demonstrated that TGF-β activity plays a role in CTGF transcript upregulation via TGF-β/Smad dependent signaling prior to cell infiltration after Ang-II infusion. We suggest that this is likely due to latent TGF-β activation in resident cardiac cells, illustrating the close relationship between TGF-β and CTGF implicated in fibrosis. Additionally, monocytes/Mϕs are shown to be key orchestrators of inflammatory and subsequent fibrotic response after myocardial injury. We demonstrated a pro-inflammatory shift in monocyte/Mϕ phenotype in the myocardium and spleen, as defined by $Ly6C^{high}$ expression after 3 days of Ang-II infusion, which may be heavily influenced by early inflammatory and fibrotic mediators produced by myocardial resident and infiltrated cells. This study opens a path towards opportunities for future studies to bridge the knowledge gap between associated mechanisms and the development of myocardial fibrosis.

LIST OF ABBREVIATIONS USED

ABC	Avidin-Biotin Complex
ACE	Angiotensin-Converting Enzyme
ALK5	Activin-Like Kinase 5
Ang-II	Angiotensin II
APC	Allophycocyanin
AT1R	Angiotensin Type I Receptors
A.U.	Arbitrary Units
BCA	Bicinchoninic Acid
BW	Body Weight
C57BL/6	C57 Black 6
CCN	Connective-Tissue-Growth-Factor, Cysteine-Rich-Protein-61, Nephroblastoma-Over-Expressed
CCR2	C-C Chemokine Receptor 2
cDNA	Complementary Deoxyribonucleic Acid
cm	Centimeter
CO_2	Carbon Dioxide
CTGF	Connective Tissue Growth Factor
CVD	Cardiovascular Disease
CX_3CR1	CX3C Chemokine Receptor 1
DAB	3,3'-diaminobenzidine
DAMPs	Damage Associated Molecular Patterns
DDR2	Discoidin Domain Receptor 2

DMEM	Dulbecco's Modified Eagle Medium
DMEM-C	Dulbecco's Modified Eagle Medium Complete
DNase	Deoxyribonuclease
DPBS	Dulbecco's Phosphate Buffered Saline
ECM	Extracellular Matrix
EDTA	Ethylenediaminetetraacetic Acid
EF	Ejection Fraction
EMT	Endothelial-Mesenchymal Transition
EtBr	Ethidium Bromide
FACS	Fluorescence Activated Cell Sorting
FC	Flow Cytometry
FITC	Fluorescein
FSC	Forward Scatter
GAGs	Glycosaminoglycans
GAPDH	Glyceraldehyde 3-Phosphate Dehydrogenase
H&E	Hematoxylin and Eosin
HCl	Hydrogen Chloride
HFpEF	Heart Failure with Preserved Ejection Fraction
HFrEF	Heart Failure with Reduced Ejection Fraction
HW	Heart Weight
ICAM-1	Intercellular Adhesion Molecule-1
IF	Immunofluorescence
IHC	Immunohistochemistry

IL-13	Interleukin-13
IL-1β	Interleukin-1β
IL-4	Interleukin-4
IL-6	Interleukin-6
JNK	C-Jun N-Terminal Kinase
L	Liter
L-Glut	L-glutamine
Ly6C	Lymphocyte Antigen 6C
MAPK	Mitogen-Activated Protein Kinase
MCP-1	Monocyte Chemoattractant Protein-1
MFI	Mean Fluorescence Index
mg	Milligram
MI	Myocardial Infarction
mL	Milliliter
mm	Millimeter
mmol	Millimoles
MMPs	Matrix Metalloproteinases
MΦ	Macrophages
NaCl	Sodium Chloride
NBF	Neutral Buffered Formalin
NGS	Normal Goat Serum
NIH	National Institute of Health
nm	Nanometer

PBMCs	Peripheral Blood Mononuclear Cells
PBS	Phosphate-Buffered Saline
PE	Phycoerythrin
PerCP-Cy5.5	Peridinin Chlorophyll Protein Cyaning 5.5
pSmad2	Phosphorylated Smad2
PVDF	Polyvinylidene Difluoride
qPCR	Quantitative Polymerase Chain Reaction
RAAS	Renin-Angiotensin Aldosterone System
rcf	Relative Centrifugal Force
RIPA	Radioimmunoprecipitation Assay
RNA	Ribonucleic Acid
RNase	Ribonuclease
ROS	Reactive Oxygen Species
RPM	Revolutions Per Minute
rRNA	Ribosomal Ribonucleic Acid
SDS	Sodium Dodecyl Sulfate
SDS-PAGE	Sodium Dodecyl Sulfate Polyacrylamide Gel Electrophoresis
SEM	Standard Error of Mean
SR/FG	Sirius Red/ Fast Green
SSC	Side Scatter
TAC	Transverse Aortic Constriction
TBST	Tris-Buffered Saline with 0.1% Tween-20
TGF-B	Transforming Growth Factor-β

TIMPs	Tissue Inhibitors of Metalloproteinases
TNF-α	Tumour Necrosis Factor-α
TβRI	TGF-β Receptor Type I
TβRII	TGF-β Receptor Type II
TβRII	TGF-β Type II Receptors
U	Enzyme unit
VCAM-1	Vascular Cell Adhesion Molecule-1
Vs.	Versus
WB	Western Blot
WT	Wild-Type
α-SMA	Alpha-Smooth Muscle Actin
µg	Micrograms
µL	Microliters

ACKNOWLEDGEMENTS

To start off, I would like to thank all those before me for their hard work in setting the path for me to take in order to accomplish this degree. Also, thank you to all the brilliant minds I have been surrounded by throughout this journey.

I would also like to thank my committee members Dr. Robert Liwski and Dr. Petra Kienesberger, as well as my past committee member Dr. Timothy Lee, for their constant encouragement and input throughout my degree. A big thank you to Eileen Kaiser for keeping me up-to-date with everything I ended up forgetting to do.

I could not have imagined 2 and a half years without the *Atlantic Centre for Transplantation Research* for openly welcoming me into the family and making my transition from Toronto to Halifax so smooth – namely Tanya Myers, Dr. Alec Falkenham, Qianni Hu, Dr. Julie Jordan, Dr. Jennifer Devitt, Dr. Ananda Venkatachalam, and more recently, Stephanie Legere, Lauren Westhaver, Elyisha Hanniman, and Kareem Gawdat. The amount of knowledge and life-lessons I have gained from this amazing group was more than I could ever imagine. Dr. Alec Falkenham – without his great mentorship, immense support, and friendship, I think I would have been lost running around in circles and never having the confidence to move forward. Tanya Myers – since I first set foot into the Transplant Lab, she has been my teacher, my support, my friend, and everything in between. I started with almost zero knowledge and she trained me without any hesitation. She was, and still is, the friend I needed to settle into a place where I initially knew no one.

To my family and friends back home and in Halifax, thank you for the never-ending support and for always believing in me. In particular, I would like to truly thank

Edwin Leong for constantly being my support during my first year even when he was in Toronto, and for being an even greater support after coming to Halifax. He listened to everything – from all the exciting stories to all the complaints I had bottled up inside. He was there when I needed the extra help in the lab and through all the laborious editing I needed from as simple as emails to this thesis– he just could not say no.

Finally, I would like to greatly thank my supervisor and mentor, Dr. Jean Francois Légaré, for giving me this great opportunity to complete my Master's degree in this lab. I am truly grateful for the never-ending guidance, support, patience, and encouragement JF has given me. He gave me an opportunity I never thought I would be able to have, and he gave me a chance to a fresh start and always pushed me to strive for higher. He taught me how to be independent and to look at disease and research from an alternate perspective I would otherwise have never thought of. JF is always able to see the best in people – and I am so fortunate he was able to see that in me to have me do research in his lab and never giving up on me.

CHAPTER 1 – INTRODUCTION

1.1 Cardiovascular Disease

Whenever I am asked: "What are you studying?", my response would automatically be: "cardiovascular disease" (CVD), just to keep a long story short. CVD is considered to be one of the world's leading causes of death and accounts for approximately 17 million deaths a year worldwide[1]. In fact, CVD is such a general term that it encompasses numerous disorders, such as atherosclerosis, arrhythmias, heart valve disease, strokes, and heart failure[2]. Thus, if I were to narrow it down a little, one of the areas of CVD that I am exploring is heart failure. In this section, the focus of the thesis will be on heart failure.

1.1.1 Heart Failure

In general terms, heart failure is defined as the structural or functional impairment of the heart to efficiently pump blood in or out of the ventricle to and from peripheral tissues and organs[3]. Heart failure is becoming an increasingly common disease that occurs in approximately 1 in 5 Canadians over the age of 40 years[4]. Despite many surgical and therapeutic advances, the prevalence of heart failure and its associated hospitalization and mortality rates still remains elevated, particularly in the elderly patient population[4,5]. In this world of increasing rates of obesity, diabetes and hypertension, the incidence of heart failure continues to be a global disease burden[6-8].

Heart failure is commonly classified into categories based on left ventricular (LV) dysfunction: (1) Heart failure with reduced ejection fraction (HFrEF), otherwise known as systolic heart failure, and (2) heart failure with preserved ejection fraction (HFpEF),

otherwise known as diastolic heart failure[4,9]. LV dysfunction is considered the final pathway of a number of cardiac disorders, such as ischemic heart disease, cardiomyopathy, hypertension, and myocarditis, which ultimately induces both structural and functional changes to the heart[10]. Systolic function refers to the ability of the LV to generate pressure in order to eject blood to the periphery[9], whereas diastolic function refers to the LV's ability to relax and fill with blood[9,11]. Thus, HFrEF tends to be the result of the loss of myocardial tissue that negatively affects the systolic function of the heart and is more common in younger patients with a history of myocardial infarction[4]. In contrast, HFpEF is presented more commonly in elderly patients and tends to be a result of multiple conditions, such as hypertension, LV hypertrophy, obesity, diabetes, and aging among others[4,12]. With the aging population and the rise in cardiovascular risk factors, the prevalence of HFpEF has increased and is now comparable to HFrEF, affecting approximately 50% of patients with heart failure[11,12]. Due to the multiple confounding comorbidities associated with HFpEF, early diagnosis of this condition has become difficult[4,12,13]. To further narrow it down, in this thesis, the focus will be directed towards hypertension induced heart failure, which is thought to contribute to HFpEF.

1.1.2 Mechanics of Diastolic Heart Failure

As mentioned in the previous section, diastolic heart failure is the inability of the LV to efficiently fill with blood largely due to stiffness of the ventricle, otherwise known as HFpEF[13]. This became apparent when observations were evident in patients presenting with symptoms of heart failure, but were diagnosed with normal EF[14]. As a result, this limits the ability of the ventricular wall to eject the appropriate volume of blood to the

peripheral tissues and organs, due to the decreased volume filling the ventricular chamber and ultimately resulting in heart failure.

Diastolic heart failure is characterized as the impaired relaxation and increased stiffness and is often associated with LV remodeling due to hypertension[15]. In the traditional pathophysiological model, pressure overload is thought to lead towards concentric LV hypertrophy, myocardial fibrosis, and finally diastolic dysfunction[15]. Pressure overload is an example of a cardiac stress that can induce ventricular remodeling largely due to long-term hypertension[16]. In response, the myocardium undergoes compensatory changes in order to adapt to the increased vascular resistance and pressure and results in hypertrophy[16]. Cardiac hypertrophy is characterized by increased cardiomyocyte size as a result of enhanced protein synthesis and the parallel addition of sarcomeres[16,17]. Often accompanying hypertrophic changes in the myocardium is the accumulation of collagen in the extracellular matrix (ECM), termed myocardial fibrosis[8,15,16]. In turn, the increase in collagen deposition in the ECM results in increased ventricular wall stiffness and ultimately impairs the proper function of the myocardium.

Alternatively, the emerging pathophysiological model introduces the concept of pro-inflammatory cardiovascular and noncardiovascular conditions, such as obesity, diabetes and metabolic syndromes in addition to hypertension. This results in the accumulation of endothelial inflammation and dysfunction and thus results in cardiac inflammation and ultimately progression towards fibrosis[15]. Taken together, cardiac dysfunction from various stresses converges on the progression towards myocardial fibrosis, which is the final pathophysiological condition that leads towards diastolic heart failure.

1.1.3 Role of Myocardial Fibrosis in Heart Failure

Myocardial fibrosis is the common pathophysiological complication of many cardiovascular conditions, such as hypertension, and is believed to partake in the final pathway towards diastolic heart failure[15,18]. It is characterized by the excess production and deposition of ECM proteins, thus resulting in increased scar tissue formation, largely due to increased fibrillar collagen deposition[18,19]. As mentioned previously, this accumulation of ECM proteins renders the myocardium dysfunctional due to increased wall stiffness and impaired relaxation[20,21]. Despite numerous advances in medicine, there remains limited therapies that address the burden of diastolic heart failure. Additionally, the fundamental underlying mechanisms leading towards myocardial fibrosis and ultimately heart failure remains incomplete, thus highlighting the importance in bridging this knowledge gap.

Under normal steady state conditions, the myocardial ECM is essentially a meshwork of proteins that forms a scaffold of fibers that keeps the structure of the myocardium, consisting of cardiomyocytes, cardiac fibroblasts, resident leukocytes, and the vasculature, intact[22]. While in the past the myocardial ECM was viewed as only an inert scaffold providing structure to myocardial cells, the myocardial ECM is now recognized as a dynamic entity that is constitutively being remodeled through a tightly regulated process[22,23]. Cardiac fibroblasts are the primary source of ECM protein turnover in the myocardium, of which type I collagen constitutes approximately 80% of the total myocardial collagen content whereas type III collagen is present at about 11% of the total myocardial collagen[24-26]. In addition to these collagens, the other main fibrous proteins in

the ECM include elastins, fibronectins, and laminins, of which all interact with one-another in a cohesive manner[23,27]. Beyond these structural proteins, matricellular proteins, glycosaminoglycans (GAGs), and proteoglycans are also found in the cardiac ECM that play structural and/or nonstructural roles and are tightly regulated under normal homeostatic conditions[22].

Under mechanical stress, or other forms of cardiac injury, cardiac inflammation and the subsequent cardiac remodeling response is associated with an imbalance of ECM regulation, whereby the tightly regulated balance of ECM protein deposition and degradation process is altered[28]. ECM proteins are susceptible to proteolytic degradation by proteolytic enzymes in the ECM, among which some are termed matrix metalloproteinases (MMPs)[29]. Under pathophysiological conditions, the proteolytic processing of the ECM can reveal the otherwise masked epitopes of ECM proteins and expand their functionality, thereby becoming involved in a feed-forward process of propagating cardiac remodeling[22,29].

MMPs are regulated by their physiological inhibitors, termed tissue inhibitors of metalloproteinases (TIMPs)[30]. In the diseased heart, the balance between MMPs and TIMPs are altered and therefore affects the balance of ECM protein degradation and deposition that is otherwise tightly controlled under homeostatic conditions[31]. The changes in the expression of MMPs and TIMPs are induced by growth factors, such as fibroblast growth factor (FGF), platelet derived growth factor (PDGF), transforming growth factor-β (TGF-β) and cytokines such as IL-6, TNF-α, and IL-1β, among others[30,32,33]. More recently, it has been recognized that in the setting of hypertensive heart disease, the quality of fibrosis, as measured by the degree in collagen cross-linking,

rather than total collagen amount, is associated with increased myocardial stiffness and thus may be more predictive for hypertensive heart failure[34,35]. Taken together, the stress induced in the myocardium leads to the imbalance of ECM protein degradation and deposition, resulting in feed-forward mechanisms whereby accumulation of mature collagen cross-linking stiffens the ventricular walls. Consequently, the otherwise contractile myocardium essential for proper function becomes incontractile due to the accumulation of ECM proteins and ultimately develops into diastolic heart failure[28,35,36].

Long-believed to be a quiescent organ after birth, cardiomyocytes were thought to have negligible regenerative capacity and upon ischemic injury in the myocardium, cardiomyocyte loss is replaced by incontractile scar formation. However, recent advances in cardiac regeneration revealed that postnatal generation of cardiomyocytes occur at low rates, but this concept is still relatively unclear[37,38]. Nevertheless, as part of the normal healing process, the term "cardiac remodeling" was initially coined for the process that occurs after an acute ischemic injury, such as myocardial infarction (MI). Other forms of cardiac injury are now recognized, such as pressure overload, inflammation, cardiomyopathy, and volume overload, and they all share similar processes that collectively results in the development of myocardial fibrosis[28]. This accumulation of collagen can be categorized into: (1) "reparative" fibrosis, which largely occurs in ischemia-induced cardiac injury and involves the replacement of cardiomyocyte loss in order to maintain structural integrity, and (2) "reactive" fibrosis, which largely occurs in non-ischemic heart disease whereby interstitial and perivascular fibrosis develops without the requirement for cardiomyocyte loss and is often thought of as more of an insidious progression towards heart failure[39,40].

Whereas much of the advances have been developed in ischemic models of heart disease, such as a MI, non-ischemic models of heart disease, such as that developed from hypertension, have not been explored to the same extent[41-43]. Nonetheless, the scientific advances in understanding molecular and cellular mechanisms in MI-induced models of heart disease has provided a very strong base support in understanding underlying mechanisms in non-ischemic heart disease. Thus, the focus of this thesis will explore the underlying mechanisms involved in Angiotensin-II (Ang-II)-induced hypertensive heart disease. This model of non-ischemic induced myocardial fibrosis involves the continuous infusion of Ang-II into rodents and provides a unique opportunity in studying underlying mechanisms without the presence of confounding factors as seen in MI models, such as tissue necrosis.

1.1.4 Angiotensin-II and Myocardial Fibrosis

Ang-II is a vasoactive peptide and is the main effector molecule in the renin-angiotensin aldosterone system (RAAS)[44]. Traditionally, RAAS is known to play an important role in the cardiovascular system by regulating blood pressure, sodium intake and potassium excretion in order to maintain body fluid homeostasis[44,45]. Briefly, renin is produced in the kidneys and cleaves its substrate angiotensinogen to generate angiotensin I[46]. Ang-II is produced by the angiotensin-converting enzyme (ACE) through mediating the cleavage of Angiotensin I and the biological effects of Ang-II are initiated by binding to either the G-protein coupled receptor angiotensin type I receptor (AT1R) or the angiotensin type II receptor (AT2R)[44,47]. Non ACE-mediated pathways can also cleave angiotensin I into its effector Ang-II, such as chymase, which is primarily produced by

mast cells[46,48]. Beyond its role in the endocrine system, Ang-II has emerged as an important hormone in the function of virtually all organs in the body, such as in the kidney, heart, brain, and vasculature[44]. Whereas acute stimulation of Ang-II plays a homeostatic role in regulating body fluid volumes, long-term exposure of Ang-II is now recognized to play a more vital role in inflammation, immunology, and remodeling[44,45,47].

Accumulating evidence has implicated the important role of Ang-II in the development of myocardial fibrosis[44,45,49-52]. Beyond its hypertensive effects, Ang-II can promote inflammation and tissue injury by signaling via AT1R on a number of different myocardial cell types, such as immune cells, vascular smooth muscle cells (VSMCs), fibroblasts, and endothelial cells[45]. In the context of aging, Ang-II levels are found upregulated in the murine myocardium, while the long-term blockade of Ang-II via AT1R blockers or ACE inhibitors protected rats from age-related myocardial fibrosis and diastolic dysfunction[53,54]. Additionally, disruption of the AT1R gene resulted in less cardiac and vascular injury, likely through the attenuation of oxidative stress, and promoted the longevity of these mice[55]. In the context of inflammation, Ang-II increases vascular permeability and induces expression of vascular adhesion molecules, such as promoting expression of P- and L-selectins, vascular cell adhesion molecule-1 (VCAM-1), intercellular adhesion molecules-1 (ICAM-1) and integrins[45,56,57]. Additionally, Ang-II induces vascular dysfunction through direct and indirect effects of reactive oxygen species (ROS) production[58,59]. Finally, immune cells such as monocytes/macrophages (Mϕs), dendritic cells, and lymphocytes express AT1R, which contributes to the local activation of the immune system that contributes to inflammation[45,60]. Ang-II can also promote the production of cytokines and chemokines, such as monocyte chemoattractant

protein-1 (MCP-1), IL-6, and TNF-α, all of which enhance the recruitment of inflammatory immune cells to the site of injury[45,50,61-66].

In response to tissue inflammation and vascular injury, Ang-II also plays an equally important role in the subsequent healing response. Considered as the primary effector and producers of ECM proteins, Ang-II can act on cardiac fibroblasts and their activated form, termed myofibroblasts[33,39,64,67-71]. Importantly, Ang-II stimulation can induce increased production of type I collagen either directly or indirectly via intermediate fibrogenic mediators, such as TGF-β and connective tissue growth factor (CTGF), which will be described in more detail in later sections[68,72-76]. Furthermore, there has been evidence suggesting the cooperative interaction between resident cardiac cells and infiltrating immune cells in the progression of myocardial fibrosis[77-81]. For example, in a model of Ang-II induced myocardial fibrosis, macrophages were found to be responsible for the induction of fibroblast production of IL-6, which promotes TGF-β/Smad-dependent signaling via autocrine and/or paracrine interactions *in vitro*, and consequently stimulating myocardial fibrosis[64].

Thus far, the effects of Ang-II have been described as signaling via the AT1R. The other Ang-II receptor, AT2R, is expressed in fetal tissue, but is rapidly reduced in adult tissues unless under pathological conditions[44]. With regards to the myocardium, AT2R is expressed on cardiomyocytes, cardiac fibroblasts, and vascular smooth muscle cells[82,83]. In contrast to AT1R, it is mostly believed that AT2R acts as a counterbalance to the effects of AT1R and is responsible for anti-proliferative and anti-inflammatory effects[44,60]. Xu *et al.* examined the effects of AT2R overexpression in the myocardium using transgenic mice expressing different levels of AT2R and found that overexpression

in mice post-MI had a protective effect by reducing hypertrophy, interstitial fibrosis, and ventricular dysfunction[84]. Furthermore, Xu and colleagues[84] suggested the beneficial role of AT2R in the myocardium is dependent on its expression in the myocardium. However, whether the role of AT2R in the myocardium is beneficial still remains controversial.

Despite separating the effects of Ang-II on the inflammatory response and subsequent tissue remodeling after an injurious stimulus, the initiation of inflammation and subsequent progression towards fibrosis appears to be more of an overlapping process. With the progression of inflammation, there appears to be a simultaneous development and progression of fibrosis[49,64,80,85,86]. It is this complex web of interactions comprised of immune and resident cells, inflammatory and fibrogenic mediators, and the time-dependent changes that has to be considered when understanding a multifactorial disease such as hypertensive-induced myocardial fibrosis. Thus, perhaps the most optimal therapeutic opportunity may be at a point where the pro-inflammatory setting is shifting towards a pro-fibrotic healing environment in order to prevent detrimental effects caused by excessive inflammation[41].

1.2 Cellular Players of Ang-II Induced Myocardial Fibrosis

1.2.1 Resident Cardiac Cellular Composition

Accurate knowledge of the composition of myocardial cells under steady state conditions is critical towards understanding cellular changes that occur in pathological conditions. Under homeostatic conditions, cardiomyocytes account for approximately 25% to 35% of the cells present in the myocardium[77,87-89]. Cardiomyocytes are arranged in close proximity to endothelial cells and the ratio of endothelial cells to cardiomyocytes

is estimated to be 3:1[90,91]. This contradicts the current understanding of the cardiac composition, of which the most abundant noncardiomyocyte cell type in the myocardium is believed to be the cardiac fibroblast[77,92,93]. The reported differences in literature could be attributed to the limited availability of fibroblast-specific markers for accurate identification, of which is expressed by other interstitial cell types, such as endothelial or inflammatory cells[94-96]. Pinto and colleagues[88] conducted a study in which they revisited the cellular composition of the myocardium at steady state and identified endothelial cells as the most abundant non-cardiomyocyte cell type in the myocardium, whereas cardiac fibroblasts were present in smaller numbers than previously described.

Approximately 7% to 10% of non-cardiomyocytes are comprised of leukocytes, with the majority of leukocytes identified as Mϕs[88]. Through lineage tracing and fate mapping techniques, cardiac Mϕs are derived mainly from embryogenesis and express the fractalkine receptor chemokine CX3C motif receptor 1 (CX_3CR1)[97-99]. Currently, the question of whether cardiac Mϕs self-renew or are progressively replaced from circulating monocytes throughout ageing is still unclear. Genetic fate mapping and parabiosis experiments identified that cardiac Mϕs at steady state self-renew[100,101], whereas another study concluded that bone-marrow derived monocytes progressively replace cardiac Mϕs with age[102]. It is implicated that the cardiac resident Mϕ population is inherently reparative in maintaining homeostasis whereas monocyte-derived Mϕs are pro-inflammatory and largely express C-C chemokine receptor 2 (CCR2) and high expression of lymphocyte antigen 6C (Ly6C)[98]. Thus, the ever-changing myocardial environment may play a role in shaping Mϕ polarization and in turn may influence the ability of the myocardium to respond to injury[98,103].

1.2.2 Resident and Infiltrating Cells in Ang-II Exposed Myocardium

Much like the cells involved in ischemia-induced models of myocardial fibrosis, Ang-II infusion promotes the accumulation of cellular infiltrate into the myocardium as well as alters the homeostatic function of resident cardiac cells. Previous work from our laboratory has extensively used the Ang-II infusion model of hypertensive-induced myocardial fibrosis to study cellular and molecular changes. Our laboratory has demonstrated the significant recruitment of mononuclear cellular infiltrate into the myocardium, which were identified to be monocytes using flow cytometry and immunohistochemistry techniques[80,104]. Bone marrow derived cells express AT1R and Ang-II-AT1R signaling has been demonstrated to regulate the mobilization of monocyte progenitor cells upon Ang-II infusion[105]. Epelman *et al.* demonstrated that cardiac Mϕ expansion occurred as early as 2 days after Ang-II infusion and that these Mϕs were predominantly $CCR2^{+}$ and expressed an inflammatory gene profile, playing a role in the inflammatory response immediately after Ang-II exposure[100]. The $CCR2^{+}$ Mϕ subset is thought to be derived from circulatory monocytes and is involved in promoting inflammation during cardiac stress. In a study conducted by Haudek and colleagues[62], CCR2 knockout mice exhibited reduced pro-inflammatory cytokine production and fibrosis during earlier time-points (1 week) after Ang-II infusion. Interestingly, in contrast to these findings, our laboratory demonstrated that earlier (3 day) migration of mononuclear cells in the Ang-II model does not appear to be dependent on CCR2, as CCR2 knockout mice did not differ from wild-type (WT) mice with regards to

mononuclear cell infiltration[106]. These differences could be attributed to the different time-points assessed in the Ang-II infusion model[106].

In addition to the inflammatory changes seen as early as 1 day after Ang-II infusion, our previous work identified molecular changes within the myocardium that occurred prior to cell infiltration. Notably, there was a significant increase in the fibrogenic mediator CTGF as early as 6 hours in the Ang-II exposed myocardium[85]. This suggests that activity of Ang-II stimulation occurred in resident cardiac cells. Although not extensively studied *in vivo*, cardiomyocytes, cardiac fibroblasts, and endothelial cells express AT1R and are potential targets of Ang-II during early Ang-II exposure[107]. Ang-II has been shown to induce endothelial dysfunction through the production of ROS, as well as induce inflammatory cytokine secretion and promote leukocyte chemotaxis and adhesion[44,52,59]. Cardiac fibroblasts respond to Ang-II stimulation via AT1R and are induced to proliferate, differentiate into myofibroblasts, and increase ECM protein synthesis, such as type I collagen, directly or via the TGF-β/Smad dependent pathway[68,83,108]. In combination with the secreted factors in the myocardial environment from Ang-II exposure, Ang-II can exert effects on cardiomyocytes by inducing hypertrophic growth[44]. Thus, the multifactorial effects of Ang-II on a variety of myocardial cells work together in an autocrine and/or paracrine fashion to induce myocardial fibrosis upon cardiac stress.

1.3 Molecular Players of Myocardial Fibrosis

As alluded to in previous sections, the interactions between myocardial cells under stress involves a plethora of molecular mediators, cytokines, and chemokines in a

concerted effort to respond to cardiac stress. The focus of this section will be on the fibrogenic mediators that are upregulated in the early Ang-II exposed myocardium as evidenced in our previous works[49,80,85].

1.3.1 Role of TGF-β in Myocardial Fibrosis

TGF-β is a pleiotropic cytokine that has been well recognized as a key mediator of fibrogenesis and is found upregulated and activated in numerous models of fibrotic diseases, such as in the lung, liver, kidney, and the heart[109-113]. The importance of TGF-β in cardiac remodeling has been implicated in numerous animal studies. In an aging model of myocardial fibrosis, TGF-β deficient heterozygous mice (TGF-$\beta^{+/-}$) exhibited reduced myocardial fibrosis and greater compliance compared to age-matched controls[114]. Additionally, transgenic mice overexpressing TGF-β demonstrated significant myocardial hypertrophy and fibrosis compared to nontransgenic controls[115].

Similar to most tissues, TGF-β is expressed in the myocardium in significant amounts as an inactive form, termed latent TGF-β, and is essentially "stored" in the ECM of the myocardium[116,117]. Briefly, TGF-β is bound to the TGF-β latency associated peptide (LAP) that prevents TGF-β from interacting with its receptors. This complex is bound to the ECM via the latent TGF-β-binding protein (LTBP)[110,116]. In order for TGF-β to exert its effects, proteolytic cleavage from the LAP-LTBP complex is required for its bioactivity[109,116,117]. The exact inducers and mechanism for proteolytic cleavage are still unclear, as the complexity of TGF-β activation *in vivo* has slowed scientific advances[116,118]. Although still unclear in the myocardium, TGF-β activators that have been identified include proteases such as plasmin, MMP-2 and MMP-9, thrombospondin-

1 (TSP-1), mast cell chymase, and integrin $\alpha_v\beta_6$, which have been implicated in the wound healing response *in vivo*[109,110,119].

Once activated, TGF-β has a high affinity for its receptor, the transmembrane serine-threonine kinase TGF-β type II receptors (TβRII), and binding of a small fraction of active TGF-β to its receptor can generate maximal cellular response[116]. Following binding to TβRII, the complex recruits and transphosphorylates the well-characterized TGF-β type I receptor (TβRI), also known as activin-like kinase 5 (ALK5)[110]. Once TβRI is activated, TGF-β signaling requires the Smad family protein phosphorylation, such as Smad2 and Smad3, which is propagated by activated TβRI. Phosphorylation of Smad2 and Smad3, known as receptor Smads (R-Smads), results in the formation of a complex with the common Smad, Smad4, which then as a complex translocates into the nucleus to elicit downstream gene activation or repression, depending on the transcriptional complexes present (Figure 1.1)[110].

Due to the difficulty in identifying active TGF-β in the myocardium, studies have only reported TGF-β upregulation at the transcript level. In the context of myocardial fibrosis, elevated transcript expression of TGF-β have been reported as early as 1 day after Ang-II exposure[49,85]. TGF-β has also been demonstrated to reinforce the hypertrophic effects of Ang-II in cardiomyocytes *in vitro*[76]. In animal models, cardiomyocyte-specific conditional knockouts of TβRII or TβRI were protected against early-onset mortality from MI due to wall rupture as well as induced expression of cardioprotective cytokines, implicating a role for cardiomyocyte-specific TGF-β in adverse remodeling[120]. TGF-β applied to cardiac fibroblasts *in vitro* induces differentiation towards myofibroblasts, enhances ECM protein synthesis, and induces

synthesis of ECM preserving enzymes, such as protease inhibitors[110,121,122]. Additionally, the TGF-β-mediated induction of endothelial-to-mesenchymal transdifferentiation (EMT) has been shown to contribute to the progression of myocardial fibrosis[123]. Finally, TGF-β has been demonstrated to have profound modulating effects on immune cells, such as monocytes/Mϕs, which may play a role in propagation of the fibrotic response in the myocardium[124,125]. Recently, Mewhort *et al.* demonstrated that the interaction between human peripheral blood monocytes and cardiac myofibroblasts induces the TGF-β-mediated myofibroblast production of ECM proteins and involvement in ECM remodeling[126].

The involvement of TGF-β in the pathogenesis of myocardial fibrosis suggests targeting TGF-β to be a therapeutic opportunity. However, due to the pleiotropic, multifunctional, and context-dependent activities of TGF-β, directly targeting TGF-β and/or its receptors have led to unfortunate outcomes[117]. A number of animal studies involving the blockade of TGF-β have demonstrated opposing results, highlighting the complexity of the role of TGF-β in myocardial fibrosis[81,127,128]. Ikeuchi *et al.* demonstrated the importance of time-specific events in the process of myocardial injury and healing by blocking TGF-β using TβRII secreted from TβRII plasmid-infected cells[129]. Ikeuchi and colleagues demonstrated that early post-MI inhibition of TGF-β resulted in exacerbated inflammatory responses, whereas later inhibition of TGF-β post-MI attenuated hypertrophy and interstitial fibrosis[129]. Frantz *et al.* inhibited TGF-β using a pan TGF-β neutralizing antibody post-MI, but that resulted in worsening left ventricular dilatation and contractile dysfunction, thus emphasizing the protective effects of TGF-β in the healing response after MI[130]. A more recent study conducted by Engebretsen and

colleagues used an orally active inhibitor of ALK5, SM16, in animals subjected to pressure-overload induced myocardial fibrosis via aortic banding[131]. Administration of SM16 attenuated fibrosis development in the left ventricle, but resulted in increased left ventricular dilatation likely due to prolonged inflammation, again highlighting the context-dependent actions of TGF-β *in vivo*[131].

With the discouraging results of targeting TGF-β in the treatment of myocardial fibrosis, there has been a shift towards targeting downstream mediators of TGF-β in an attempt to identify biomarkers and targets for development of anti-fibrotic therapies, such as Smad proteins and associated fibrogenic mediators, including CTGF[81,132,133]. In particular, TGF-β signaling has been demonstrated to directly upregulate CTGF production via Smad signaling, which was also shown to correlate with fibrosis progression[85,122,134,135].

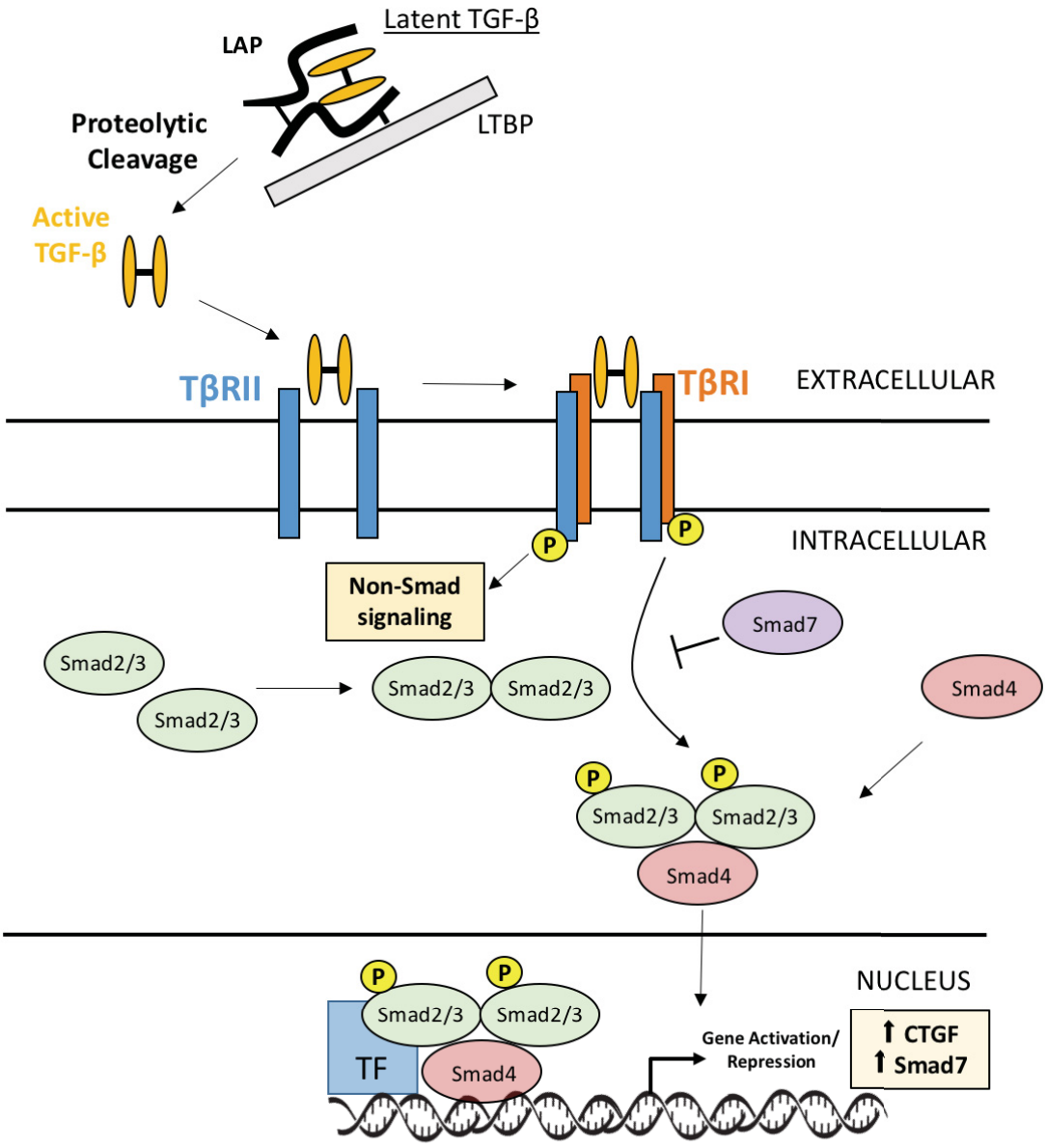

Chen and Dijke 2016, Travis and Sheppard 2014, Dobaczewski 2011, Rosenkkranz 2004

Figure 1.1. Simplified overview of TGF-β activation and signaling. Latent TGF-β is composed of the latency-associated peptide (LAP) and bound to the extracellular matrix by the latent TGF-β binding protein (LTBP). Upon activation, latent TGF-β is proteolytically cleaved into active TGF-β, whereby it binds to its receptor TGF-β type II receptor and subsequently recruits and transphosphorylates TGF-β type I receptor. Once phosphorylated, a sequence of intracellular signaling occurs, one of which involves the

Smad family protein phosphorylation. One such pathway is the phosphorylation of Smad2 (serine 465/467) and Smad3 (serine 423/425), which then results in formation of a complex along with Smad4, allowing for translocation into the nucleus and downstream gene activation or repression dependent on respective transcriptional complexes bound to the promoter region.

1.3.2 Role of CTGF in Myocardial Fibrosis

Although initially named as a growth factor, CTGF does not function as do traditional growth factors by binding through receptors and eliciting downstream signaling, as a receptor for CTGF is unknown. In fact, CTGF is part of the connective-tissue-growth-factor, cysteine-rich-protein-61, nephroblastoma-over-expressed (CCN) family of proteins and is considered a matricellular protein that plays an important role as an adaptor protein in the ECM[136]. Usually not expressed under steady-state conditions, induction of CTGF expression is upregulated in fibrotic conditions, such as myocardial fibrosis[133]. It has been suggested that CTGF alone mediates moderate fibrotic responses, but can also act synergistically with TGF-β to sustain the fibrotic response[137,138]. Despite its association with fibrotic conditions, the exact role of CTGF in myocardial fibrosis is still relatively unknown and whether it is essential for the progression of fibrosis remains elusive[139-144].

1.3.3 Biosynthesis and Regulation of Collagen in Myocardial Fibrosis

The hallmark of myocardial fibrosis is the increased deposition of ECM proteins, and in particular, increased collagen deposition namely fibrillar type I and III collagens[22,39]. The main producers of collagen in the myocardium are cardiac fibroblasts and myofibroblasts and collagen production is likely induced by either direct Ang-II stimulation via AT1R or indirectly via the TGF-β/Smad-dependent pathway[68,73,107,109,110,134,145]. Observations in humans and animal models of hypertension-induced heart failure have shown dysregulation of collagen turnover, favouring increases in type I and III collagen, which lead to the development of fibrosis[19,33,146]. Additionally,

collagen metabolites have been found in circulation and shown to correlate with increased myocardial fibrosis and diastolic dysfunction in patients[21].

Collagen is the most abundant fibrous protein found in the interstitial ECM and is organized in striated fibrils to provide structural integrity and the basis for cell adhesion, migration, and regulation of tissues and organs[23]. To date, there has been 28 types of collagen identified and the majority of collagens are arranged in triple-stranded α-helices[23,147]. Briefly, synthesis of type I collagen involves a number of post-translational modifications, notably proline and lysine hydroxylation, lysine glycosylation, and N- and C-terminal propeptide cleavage[23,148,149]. Type I collagen is composed of two major subunits, α1(I) and α2(I), of which contains two α1(I) and one α2(I) subunits. The main biosynthesis steps include the hydroxylation in the lumen of the endoplasmic reticulum. Prolyl-4-hydroxylase plays a central role in the formation of the triple helix structure by hydroxylation of proline and lysine residues[149]. Following additional modifications such as glycosylation of lysine, the triple helical molecule formed by two α1(I) and one α2(I) chains becomes the procollagen molecule and is packaged and secreted into the extracellular space. The N- and C-terminal propeptides are cleaved to release collagen molecules to the extracellular space[148,149]. These collagen molecules then spontaneously self-assemble into collagen fibrils followed by formation of covalent cross-links initiated by lysyl oxidase[149]. In addition to the lysyl oxidase catalyzed cross-linking of collagen, nonenzymatic reactions can occur between glucose and collagen, which forms advanced glycated end products that has also been shown to contribute to slow turnover of ECM seen in cardiac dysfunction[21]. Taken together, the importance of collagen deposition in myocardial fibrosis has turned to quality of collagen as opposed to quantity of collagen

and the role of lysyl oxidase and collagen cross-linking has been implicated in animal models of ageing and MI-induced cardiac dysfunction[35,150-152].

1.4 Rationale, Hypothesis, and Objectives

1.4.1 Rationale

While the role of TGF-β in the pathogenesis of myocardial fibrosis has been extensively studied in ischemic animal models, its role in the progression of non-ischemic models of myocardial fibrosis has not been explored in-depth[107,120,130,153,154]. In particular, previous work from our laboratory has demonstrated significant mononuclear cell accumulation in the Ang-II exposed myocardium as early 1 day that was associated with subsequent fibrosis seen 3 days after Ang-II exposure[49,80,85,106]. These observations were supported by a study conducted by Duerrschmid *et al.* in which production of inflammatory cytokines, chemokines, and accumulation of bone marrow derived monocytes were observed as early as 1 day after Ang-II infusion, which was later switched to a pro-fibrotic environment after 7 days and characterized by increased pro-fibrotic mediators and bone marrow derived cells[66]. Furthermore, Ang-II has been shown to mobilize splenic monocyte deployment to the myocardium as early as 1 day after exposure and contribute to the pro-inflammatory monocyte/Mϕ pool in the myocardium[61] Notably, our previous work identified significant upregulation of pro-fibrotic CTGF in the Ang-II exposed myocardium at 6 hours, prior to significant production of TGF-β and cell infiltration[85].

Additionally, in collaboration with the Montreal National Research Council, we were able to obtain a soluble TGF-β trap, which was designed as human TβRII with the

ability to sequester active TGF-β in the ECM[155]. Although used in tumour models, Zwaagstra *et al.* demonstrated reduced growth of established 4T1 tumours in mice after administration of the TGF-β trap when compared to the pan TGF-β neutralizing antibody, demonstrating the ability of the TGF-β trap for neutralizing TGF-β[155].

1.4.2 Objectives

The objectives of this study were to: (1) Determine the mechanistic link between TGF-β and CTGF in the early (6 hours) Ang-II exposed myocardium by using the TGF-β trap as a molecular tool, (2) Determine the fundamental role of CTGF *in vitro* in NIH/3T3 fibroblasts alone and in combination with TGF-β, and (3) Identify and characterize monocyte/Mϕ composition and subsets in the myocardium, circulation, and spleen 3 days after Ang-II exposure.

1.4.3 Hypothesis

We hypothesize that the TGF-β trap will efficiently reduce levels of CTGF *in vitro* on NIH/3T3 fibroblasts and in the Ang-II exposed myocardium at 6 hours indicating the close relationship between TGF-β activity and induction of CTGF. Additionally, we hypothesize that Ang-II exposure leads to the accumulation of pro-inflammatory monocytes/Mϕs in the myocardium at 3 days, as well as influences the pro-inflammatory phenotypic shift in splenic and blood-derived monocytes at this time-point.

CHAPTER 2 – MATERIALS AND METHODS

2.1 Animals

All animal experiments were approved by Dalhousie University *Committee on Laboratory Animals* in accordance with the Canadian Council on Animal Care guidelines. Male WT C57BL/6J mice (6 to 8 weeks old) were purchased from Jackson Laboratory (Bar Harbor, ME) and housed within the Carleton Animal Care Facility at Dalhousie University. Mice were provided with food and water *ad libitum* for 1 week prior to experimentation.

2.2 Saline/Ang-II Infusion and TGF-β Trap Injections

Mice were randomly assigned saline (vehicle) or Ang-II (2.8 mg/kg/d; Sigma Aldrich, Oakville, ON, Canada) through the use of subcutaneously implanted Alzet osmotic minipumps (Alzet Corp., Palo Alto, CA) as previously described[49,80,85]. Additionally, some mice were also randomly assigned to receive phosphate-buffered saline (PBS, vehicle) or TGF-β trap (T22d35; 10mg/kg), which was acquired through a material transfer agreement with the National Research Council (NRC) in Montreal[155]. All mice were anesthetized using isoflurane (Baxter Healthcare Corp., New Providence, NJ) in oxygen. Intraperitoneal injections of the TGF-β trap was given to mice prior to a mid-scapular skin incision (approximately 1 to 2 cm) made to implant the osmotic minipump containing Ang-II subcutaneously. The TGF-β trap dosage and delivery method was based on previous work by Zwaagstra *et al.* that demonstrated reduced tumour growth in mice with established 4T1 tumours[155]. All mice were recovered for 6

hours, 24 hours, or 3 days while being provided with food and water *ad libitum* and observed for pain and morbidity.

2.3 Hemodynamic Measurements

Mean arterial blood pressure was measured using a non-invasive tail cuff system (Kent Scientific, Torrington, CT, USA). Mice were trained for blood pressure measurements seven days prior to experimentation in order for acclimatization to prevent artificial blood pressure elevation as previously described[49,156]. Blood pressures were measured immediately prior to osmotic pump implantation for baseline measurements and at 24 hours after Ang-II exposure for a minimum of five consecutive measurements per mice.

2.4 Tissue Harvest and Cell Isolation

Mice were anesthetized with isoflurane in oxygen and sacrificed for tissue harvest as previously described[49,80,85,106]. Isolated hearts from mice that received saline or Ang-II for 6 or 24 hours were flushed with saline, weighed, and divided along the vertical axis into three sections. The base was processed for histological analyses and the remaining two sections were immediately snap frozen for molecular analyses. Isolated hearts from mice that received saline or Ang-II for 3 days were flushed with saline, weighed, and the whole heart was immediately processed for cell isolation and flow cytometry. Cardiac hypertrophy was assessed by dividing heart weight at the time of harvest by the final body weight. Blood was collected via cardiac puncture from mice under anesthesia and placed in heparin containing blood collection tubes. Spleens were harvested from 3-day

saline and Ang-II mice and placed in Corning 35 mm culture dishes (Corning, Corning NY, USA) containing complete Dulbecco's Modified Eagle Medium (DMEM-C; DMEM; 10% heat-inactivated fetal bovine serum, FBS; 2 mmol/L L-glutamine, L-glut; 100 U/mL penicillin; 100 mg/mL streptomycin; Life Technologies Corp., Burlington, ON, Canada).

2.4.1 Cell Isolation - Heart

Mononuclear cells were isolated from the heart under sterile conditions from mice infused with Ang-II or saline for 3 days as previously described with slight modifications[49,80]. In brief, hearts were minced with razors followed by mechanical and enzymatic digestion using collagenase solution (1 mg/mL; Collagenase II, Worthington Biochemical Corp., Lakewood, NJ, USA) in serum-free DMEM containing 2mmol/L L-glutamine, 100 U/mL penicillin, and 100 mg/mL streptomycin at 37°C with agitation for 30 min at 250 RPM. Cell isolates were pressed through a 70 μm filter and washed twice in DMEM-C for 10 min at 400 rcf and 4°C. Following washes, cell isolates were purified over a Ficoll-Paque gradient (GE Healthcare UK, LTd., Buckinghamshire, UK) and centrifuged for 30 min at 400 rcf with no deceleration and minimal acceleration. Mononuclear cells at the interface were collected, resuspended in fluorescence-activated cell sorting (FACS) buffer (Dulbecco's phosphate buffered saline, DPBS; 1% bovine serum albumin, BSA; 0.1% sodium azide, NaN_3), and used for subsequent characterization, as described below in *Flow Cytometry*.

2.4.2 Peripheral Blood Mononuclear Cells (PBMCs)

Isolated blood was diluted in half with FACS buffer and then layered over a Ficoll-Paque gradient and centrifuged for 30 min at 400 rcf with no deceleration and minimal acceleration. The mononuclear cell layer was isolated from the interface, washed twice with FACS buffer for 10 min at 400 rcf and 4°C, and then used for subsequent characterization, as described below in *Flow Cytometry*.

2.4.3 Cell Isolation – Spleen

Harvested spleens were minced using razor blades in Corning 35mm culture dishes in DMEM-C. Minced tissue was pressed through a 70μm filter until virtually all tissue passed through. Cell isolates were washed with DMEM-C for 10 min at 400 rcf and 4°C, and then layered over a Ficoll-Paque gradient and centrifuged for 30 min at 400 rcf, no deceleration, and minimal acceleration for mononuclear cell purification. Mononuclear cells were isolated from the interface, resuspended in FACS buffer, and used for subsequent characterization as described below in *Flow Cytometry*.

2.5 Flow Cytometry

Isolated mononuclear cells from heart, blood, and spleen were washed twice in FACS buffer by centrifuging for 10 min at 400 rcf and 4°C, and then counted using Trypan Blue exclusion (Invitrogen, Carlsbad, CA, USA). All cells were incubated with F_CR block (Biolegend, San Diego, CA, USA) as per manufacturer's protocol for 15 min at 4°C. Following F_CR block, all cells were incubated with the following primary antibodies: fluorescein isothiocyanate (FITC)-conjugated anti-CCR2 (R&D systems,

Minneapolis, MN, USA), phycoerythrin (PE)-conjugated anti-Ly6C (Biolegend, San Diego, CA), peridinin chlorophyll protein cyanine 5.5 (PerCP-Cy5.5)-conjugated anti-CX_3CR1 (Biolegend), and allophycocyanin (APC)-conjugated anti-CD11b (eBioscience, San Diego, CA, USA). Following antibody incubation for 30 min at 4°C, all cells were washed twice with FACS buffer for 5 min at 400 rcf and 4°C, and then fixed with 1% formalin/FACS buffer. Single label controls and isotype controls were used for compensation and negative controls, respectively. See Table 2.1 for details on antibody concentrations and supplier information. Data from all samples were acquired using BD FACSCalibur (BD Biosciences, San Jose, CA, USA) and analyzed using FlowJo (FlowJo, LLC, Ashland, OR, USA).

Monocytes/MΦ were gated on all cells using forward scatter (FSC) and side scatter (SSC). For cell gating on the heart, the monocytes/MΦ FSC/SSC gate was applied to a CCR2 x CX_3CR1 dot plot. The $CCR2^+CX_3CR1^+$ events were gated and applied to a CD11b x Ly6C dot plot for characterization of Ly6C mean fluorescent index (MFI) based on $CD11b^{high}$ expression. For cell gating on blood and spleen cells, the monocytes/MΦ FSC/SSC gate was applied to a CD11b x SSC dot plot. The $CD11b^{low}$ and $CD11b^{high}$ events were gated and applied to a Ly6C x CCR2 dot plot for characterization of the different subpopulations of $CD11b^+$ events. Prior to characterization of the cells, monocytes/MΦ populations were back-gated to the FSC x SSC dot plots in order to enrich the populations for further characterization.

2.6 Tissue Processing and Histological Analyses

Ventricular heart sections were processed for histological analyses by fixing with 10% neutral buffered formalin (NBF) for 24 hours and then paraffin-embedded. Heart cross-section blocks were serially sectioned into 5μm sections using a microtome and placed on microscope slides for further staining, as detailed below.

2.6.1 Hematoxylin-and-Eosin Staining and Analyses

Paraffin-embedded heart sections were stained with hematoxylin and eosin (H&E) for analysis of basic myocardial histology and cellular infiltration. In brief, slides were deparaffinized by subjecting to degrading alcohol gradient consisting of 2x xylene, 2x 100% ethanol, 2x 95% ethanol, and 70% ethanol before submerging into H_2O. Slides were then differentiated in Harris's hematoxylin solution, washed in running tap H_2O to remove excess staining, differentiated in 1% acid alcohol, subjected to Scott's solution for bluing, and then counterstained with 0.5% eosin with 0.5% $CaCl_2$ solution. Slides were dehydrated and mounted with xylene-based mounting medium. Images of ventricular cross-sections were taken with a 5x objective by light microscopy using Zeiss Axiovision 4.6 digital image analysis program (Carl Zeiss, Toronto, ON, Canada) on slides, visualized with AxioCam HRc camera (Carl Zeiss) and analyzed using Adobe Photoshop CS6 by compiling images into whole heart cross-sections. Cellular infiltration was semi-quantified using an established standardized method to assess the compiled whole myocardial cross-sections as previously described[49,85]. In brief, 500x500 pixel grid was overlaid on whole heart cross-sections and a blinded observer counted grids containing cellular infiltrate as well as the total number of grids encompassing the heart.

The percent of affected grids containing cellular infiltrate was calculated over the total number of grids encompassing the heart to obtain the area of foci affected.

2.6.2 Sirius Red/Fast Green Staining and Analyses

Paraffin-embedded heart sections were stained with Sirius Red and counterstained with Fast Green (SR/FG) to assess for collagen deposition. Briefly, slides were deparaffinized in a series of degrading alcohol gradients and fixed in Bouin's solution (Sigma) for 1 hour. Following, slides were washed in running water until Bouin's cleared and then placed in 0.1% Fast Green/ddH_2O for non-collagenous proteins. Slides were then washed in 0.1% acetic acid before staining with 0.1% Sirius red solution for 30 min and then dehydrated and mounted with xylene-based mounting medium. Collagen was semi-quantified using a modified method on Adobe Photoshop CS6 originally described by Underwood *et al.* and established in our previous work[49,85,106,157]. In brief, red pixels were positively selected and summed for a total number of red pixels representing collagen. Nonbackground (green) pixels and red pixels were summed for the total number of heart pixels. Collagen content was measured by calculating the percentage of red pixels by total heart pixels. Consistency was ensured by using the same red colour palette, green colour palette, and by processing all tissues simultaneously.

2.6.3 Immunohistochemistry

Immunohistochemistry was performed on paraffin-embedded heart cross-sections for CD11b (Abcam, Cambridge, MA, USA), α-smooth muscle actin (α-SMA; Sigma Aldrich) and Ki-67 (eBioscience) (see Table 2.1 for antibody concentrations and details).

Heart cross-sections were deparaffinized and subjected to degrading alcohol gradient as described above and then treated for antigen retrieval using a pressure cooker before staining. Briefly, sections were quenched for endogenous peroxidases using 3% hydrogen peroxide (H_2O_2), non-specific staining was blocked using 10% normal goat serum (NGS), and primary antibodies were incubated overnight at 4°C. Following primary antibody incubation, a specific biotin-conjugated secondary antibody was incubated for 1 hour at room temperature (see Table 2.1 for antibody concentrations and details). The antibody complexes were then conjugated to avidin-biotin complex (Vectastain ABC kit; Vector Laboratories Inc., Burlington, ON, Canada) and developed using 3,3'-diaminobenzidine as the chromagen (DAB; Dako-Cytomation, Mississauga, ON, Canada). Images were taken by performing light microscopy using Zeiss Axiovision 4.6 digital image analysis program (Carl Zeiss) on slides, visualized with AxioCam HRc camera (Carl Zeiss), and analyzed using Adobe Photoshop CS6. Quantification of positive α-SMA-stained slides were counted by a blinded observer in five fields of view at 20x magnification and the average number of positive cells was calculated per sample. Quantification of Ki-67-stained heart sections are described below under *Proliferation Assay*.

2.7 *In vitro* Monoculture System

2.7.1 Monoculture of NIH/3T3 fibroblasts

NIH/3T3 (ATCC, Manassas, VA, USA) fibroblasts were cultured as previously described[80]. In brief, NIH/3T3 fibroblasts were maintained in DMEM-C until washed with DPBS and lifted using 0.25% trypsin-ethylenediaminetetraacetic acid (trypsin-

EDTA; Invitrogen, Carlsbad, CA, USA). Cells were counted using Trypan blue exclusion, re-plated at 1.0 x 10^5 cells per well on 0.1% gelatin-coated Corning six-well tissue culture plates in DMEM-C with or without 0.1% gelatin-coated coverslips. Cells were incubated in a humidified chamber at 37°C and 5% CO_2.

2.7.2 NIH/3T3 Fibroblast Exogenous Treatments

Upon 60 – 70% confluency, NIH/3T3 fibroblasts were starved in DMEM containing 1% FBS (1% FBS/DMEM) overnight before being treated with (i) sterile-filtered full-length recombinant human CTGF produced in HEK293 cells (125 ng/mL[85]; CS363B, Cell Sciences, Canton, MA), (ii) sterile-filtered full-length recombinant active human TGF-β1 produced in HEK293 cells (10 ng/mL[137,158]; ab50036, Abcam), (iii) CTGF in combination with TGF-β1, (iv) TGF-β1 plus TGF-β trap (400nM), (v) TGF-β1 plus pan TGF-β neutralizing antibody (1D11; 15 μg/mL; MAB1835, R&D Systems), (vi) TGF-β trap only, or (vii) 1% FBS/DMEM as media control groups for 6 hours and/or 24 hours.

2.7.3 Immunofluorescence on Fixed In vitro *Cultured Cells*

Immunofluorescence staining was performed on 4% paraformaldehyde-fixed fibroblast monocultures for α-SMA. In brief, fixed cells were washed with 1x phosphate-buffered saline (PBS) and then blocked against non-specific antibody binding with 10% normal goat serum (NGS). Primary antibodies against α-SMA (Sigma-Aldrich) were incubated overnight at 4°C, followed by secondary antibody incubation using AlexaFluor488-conjugated (Invitrogen) and AlexaFluor555-conjugated (Invitrogen)

secondary antibodies for 1 hour and nuclei counterstain using Hoechst stain (Sigma-Aldrich). Refer to Table 2.1 for antibody concentrations and details.

Six-well plates containing coverslips were mounted onto slides, visualized using Zeiss Axioplan II MOT (Carl Zeiss) and captured with an AxioCam HRC Colour Camera. The remaining wells were read for fluorescence by using an Infinite M200 Pro plate reader (Tecan, Mannedorf, Germany). α-SMA expression, measured in fluorescence intensity, was standardized to Hoechst fluorescence intensity and then calculated relative to untreated groups (1% FBS/DMEM).

2.8 Proliferation Assay

Relative proliferation was assessed via immunohistochemical staining of Ki-67 as a proliferation marker on heart cross-sections as described in *Immunohistochemistry.* Slides of heart cross-sections were visualized and the images captured upon which nuclei positive for Ki-67 were counted relative to the total number of nuclei in five random fields of view at 20x magnification. Data was expressed relative to saline control.

2.9 Gel Electrophoresis and Western Blotting

Samples were isolated from snap frozen heart samples and used for Western blot experiments as previously described[85,152]. Isolated heart samples were homogenized in radioimmunoprecipitation assay (RIPA) buffer (150 mmol/L NaCl, 50 mmol/L Tris-HCl base, 0.1% SDS, 0.1% Triton X-100, and 0.5% deoxycholic acid) with Pierce Protease and Protease Inhibitor Mini Tablets added (ThermoFisher Scientific, Rockford, IL, USA). Protein concentration was determined using a BCA protein assay kit as per

manufacturer's instructions (ThermoFisher Scientific). Samples were then denatured using Laemmli sample buffer with 2-mercaptoethanol (BioRad Laboratories, Hercules, CA, USA) and boiled at 95°C for 5 minutes. Samples were then separated on a 12% SDS-PAGE gel and transferred to an Immobilon polyvinylidene difluoride membrane (PVDF; Millipore Corp., Bedford, MA, USA).

PVDF membranes were incubated with either 5% skim milk or 5% BSA in Tris-buffered saline with 0.1% Tween-20 (TBST; Sigma Aldrich) for 1 hour to block non-specific binding. Primary antibodies against phosphoSmad2 (pSmad2; Cell Signaling, Beverly, MA, USA), Smad2/3 (Cell Signaling), or actin (loading control; Sigma-Aldrich) overnight at 4°C. Following primary antibody incubation, membranes were incubated with secondary antibody horseradish peroxidase-linked goat anti-rabbit IgG (Vector Laboratories) and developed using Amersham ECL enhanced chemiluminescence kit (GE Healthcare UK, Ltd.). Images were captured using the ChemiDoc^{TM} Touch Imaging System (Bio-Rad Laboratories) and analyzed using Image Lab^{TM} software (Bio-Rad Laboratories). See Table 2.1 for antibody concentrations and details.

Table 2.1 Antibody Concentrations, Host, and Source Information.

List of antibodies used for immunohistochemistry (IHC), immunofluorescence (IF), western blot (WB), and flow cytometry (FC) and their respective concentrations, host species, and source are provided.

Primary Antibodies	**Concentration (µg/mL) /Dilution**			**Host**	**Source**	
	IHC/IF	**WB**	**FC**		**Supplier**	**Cat. No.**
α-SMA	1:1000			Mouse	Sigma	A5228
Actin		1:8000		Rabbit	Sigma	A2066
CCR2-FITC			(15µL)	Rat IgG_{2B}	R&D	FAB5538F
CD11b	1:3000			Rabbit	Abcam	Ab133357
CD11b-APC			2.5	Rat IgG_{2B}	Biolegend	101212
CX_3CR1-PerCP-Cy5.5			2	Mouse IgG_{2A}	Biolegend	149009
Ki-67	1:100 (IHC) 1:250 (IF)			Rat	eBioscience	14-5689-82
Ly6C-PE			1	Rat IgG_{2C}	Biolegend	128008
pSmad2		1:1000		Rabbit	Cell Signaling	3101S
Smad2/3		1:1000		Rabbit	Cell Signaling	3102S
Secondary Antibodies	**Concentration (µg/mL) /Dilution**			**Host**	**Source**	
	IHC/IF	**WB**	**FC**		**Supplier**	**Cat. No.**
Alexa-Fluor488 anti-mouse	1:500			Goat	Invitrogen	A11001
Biotin-anti-mouse	1:500			Goat	Vector Laboratories	BA-9200
Biotin-anti-rabbit	1:500			Goat	Vector Laboratories	BA-1000
Biotin-anti-rat	1:500			Goat	Vector Laboratories	BA-9400
Alexa-Fluor555 anti-mouse	1:500			Goat	Invitrogen	A21434

Secondary Antibodies	Concentration (µg/mL) /Dilution			Host	Source	
	IHC/IF	WB	FC		Supplier	Cat. No.
Peroxidase anti-rabbit		1:5000		Goat	Vector Laboratories	PI-1000
Isotype Antibodies	**Concentration (µg/mL) /Dilution**			**Host**	**Source**	
	IHC/IF	**WB**	**FC**		**Supplier**	**Cat. No.**
FITC-IgG2b			(15µL)	Rat	eBioscience	11-4031-82
PE-IgG2c			1	Rat	Biolegend	400707
PerCP-Cy5.5-IgG2a			2	Rat	Biolegend	400532
APC-IgG2b			2.5	Rat	Biolegend	400612

2.10 Relative Real-Time Quantitative Polymerase Chain Reaction (qPCR)

2.10.1 RNA Extraction and cDNA Synthesis

TRIzol (Life Technologies) was used for total RNA extraction from snap-frozen heart sections and NIH/3T3 cells according to manufacturer's instructions. For snap-frozen heart sections, tissues were placed in TRIzol and homogenized using a rotor stator homogenizer. NIH/3T3 cells were resuspended in TRIzol after treatment and briefly homogenized. RNA was eluted in RNase/DNase free water (Invitrogen) and purity (by assessing A260/280) and concentration of samples were determined by using the NanoDrop 2000c UV-Vis Spectrophotometer (ThermoFisher Scientific). RNA samples were also run on a 1% agarose gel with ethidium bromide (EtBr) to assess for RNA integrity. Samples with an A260/280 ratio between 1.8 to 2.0 and which displayed two sharp bands (28S and 18S rRNA bands) were classified as pure and intact, and was used for downstream complementary DNA (cDNA) synthesis.

First strand cDNA synthesis was performed from extracted RNA using iScript™ Advanced cDNA Synthesis Kit (Bio-Rad Laboratories) as per manufacturer's instructions. The reaction took place in a total volume of 20µL consisting of 1µg of extracted RNA, 4µL 5x iScript Advanced Reaction Mix (Bio-Rad Laboratories), 1µL iScript Advanced Reverse Transcriptase (Bio-Rad Laboratories), and RNase/DNase free water (Invitrogen). The reaction cycle protocol consisted of incubation at 46°C for 20 minutes and 95°C for 1 minute, after which the generated cDNA was used for downstream qPCR reactions and analyses.

2.10.2 qPCR Reaction and Analyses

Real-time qPCR was performed using iQ SYBR Green Supermix (Bio-Rad Laboratories) as per manufacturer's instructions, detected using the Rotor-Gene™ 6000 (Corbett Life Science, San Francisco, CA, USA), and analyzed using the Rotor-Gene Q Series software (QIAGEN Sciences, Germantown, MD, USA). Efficiency curves and no-template controls were accompanied with each run and melt curves were run after cycling for target specificity. Relative expression levels were normalized to reference gene 18S ribosomal gene, and in some cases, also normalized to GAPDH, as well as relative to controls using the Pfaffl method[159]. Primer sequences designed against mRNA sequences are listed in Table 2.2.

2.11 Statistical Analyses

All data are represented as means ± standard error of mean (SEM). All direct comparisons between two groups were evaluated using the student two-tailed *t*-test for changes in relative expression compared to controls. One-way analysis of variance (ANOVA) was performed using the Bonferroni post-test for multiple comparisons to compare experimental groups with the control group and to compare multiple experimental groups. qPCR results were evaluated based on the relative changes compared to the theoretical mean value of 1.000 All statistical comparisons were computed using GraphPad PRISM software version 6 (GraphPad Software, Inc., La Jolla, CA, USA), and significance was determined if $p < 0.05$.

Table 2.2 Genes of Interest and Primer Sequences.

List of genes used in qPCR and their respective forward and reverse primers are provided. Primers were designed against mRNA sequences using PrimerBlast.

Gene of Interest	Forward Primer	Reverse Primer
18S Ribosomal RNA (18S)	TCAACTTTCGATGGTAGTCGCCGT	TCCTTGGATGTGGTAGCCGTTTCT
Collagen Type I-alpha-I (Col-IaI)	CAACAGTCGCTTCACCTACAGC	GTGGAGGGAGTTTACACGAAGC
Connective Tissue Growth Factor (CTGF)	TCAACCTCAGACACTGGTTTCG	TAGAGCAGGTCTGTCTGCAAGC
Glyceraldehyde 3-Phosphate Dehydrogenase (GAPDH)	CCTTCCGTGTTCCTACCCC	GCCCAAGATGCCCTTCAGT
Transforming Growth Factor-Beta (TGF-B)	GCCTGAGTGGCTGTCTTTTG	CTGTATTCCGTCTCCTTGGTTC

CHAPTER 3 - RESULTS

3.1 Characterization of the Ang-II Model

Mice with Ang-II infusion are used as models for myocardial hypertrophy and fibrosis secondary to hypertension[160]. Our previous work using the murine model of Ang-II infusion demonstrated early physiological changes characterized by a rise in mean arterial blood pressure, subsequent series of cellular changes, and ultimately the development of fibrosis and hypertrophy[156,161,162]. In order to better understand the early effects of Ang-II infusion, we focused our attention to the first 24 hours. To confirm the hypertensive effects of Ang-II infusion, mean arterial blood pressure was taken for each animal immediately prior to surgery, labeled as baseline, as well as immediately prior to sacrifice. Ang-II infusion resulted in a significant increase in mean arterial blood pressure after 24 hours compared to their WT counterparts (Figure 3.1A; 133.9 ± 6.5 mmHg vs. 109.3 ± 7.3 mmHg respectively, $p < 0.05$).

In addition to hypertensive effects, previous works have demonstrated that long-term Ang-II infusion can lead to significant cardiomyocyte hypertrophy[139]. Additionally, our previous work measured the heart weight of animals after saline or Ang-II infusion and normalized it to body weight after infusion as an indication of hypertrophy. By using this method, the ratio of heart weight to body weight (HW/BW) was found to be significantly higher in Ang-II animals 7 days after infusion, suggestive of hypertrophy[49,156]. In the first 24 hours of Ang-II exposure, these animals did not exhibit any changes in hypertrophy score at 6 hours or 24 hours (Figure 3.1B).

3.2 Early mononuclear cell infiltration precedes significant collagen deposition

Previous studies by our group have demonstrated that the Ang-II infusion model of myocardial fibrosis results in significant collagen deposition in mice myocardium 3 days after Ang-II exposure[49,80,106]. Earlier cellular and molecular changes that occur within the first 24 hours of Ang-II infusion that are associated with later development of fibrosis have yet to be fully characterized in this model. Thus, we first assessed the gross histological changes in the myocardium within the first 24 hours of Ang-II exposure. Collagen deposition was semi-quantitatively assessed using myocardial cross-sections stained with SR/FG and calculated using an established method of assessing the number of red collagen pixels divided by the total number of myocardial pixels (red and green) per section[49,80,85]. Although there appears to be a trend towards increased collagen deposition of Ang-II exposed hearts at 24 hours, these findings were not significant when compared to saline control (Figure 3.2A-C; 6.8% ± 1.1 vs 5.2% ± 0.3). In support of these findings, type I collagen transcript levels trended towards increased expression but did not reach significance in Ang-II hearts relative to saline at 24 hours (Figure 3.2D).

Prior to the development of fibrosis, our previous work has shown significant mononuclear cell accumulation in the myocardium peaking at 3 days after Ang-II exposure[49,106]. In the present series of experiments, myocardial cross-sections were stained with H&E and assessed based on the percentage of grids containing cellular infiltrate over the total number of grids containing the myocardium. After 24 hours of Ang-II exposure, there was a significant increase in mononuclear cell infiltration compared to saline control (Figure 3.3A-C; 18.3% ± 1.4 vs 0.9% ± 0.1, respectively, $p < 0.0001$). There was little to no polymorphonuclear cells, suggesting little role for

granulocytes in this model (Figure 3.3D). Using immunohistochemical staining for CD11b, our findings were confirmed by demonstrating that a significant number of infiltrating cells were positive for CD11b expression (Figure 3.3E-F).

Together, these results suggest that monocytes/macrophages have populated multifocal areas of the heart prior to significant collagen deposition. Thus, the early inflammatory responses in the heart are suggested to be temporally linked to later tissue remodeling and fibrosis in our model of hypertensive-induced myocardial fibrosis. Additionally, there appears to be no significant cellular infiltration 6 hours after Ang-II infusion (Figure 3.4A-B). As such, we further examined molecular signaling within the first 24 hours after Ang-II exposure.

3.3 Profibrotic factors in the early Ang-II exposed myocardial environment

TGF-β and its downstream mediator, CTGF, have been implicated as predominant pro-fibrotic mediators in many fibrotic conditions[107,133,163-165]. Our model of Ang-II infusion has shown involvement of TGF-β and CTGF in the early fibrotic response to Ang-II[49,85,106]. Importantly, CTGF transcript levels were significantly elevated as early as 6 hours after Ang-II infusion (Figure 3.5A; 19.3-fold ± 5.4 vs saline control, $p < 0.05$) and remained upregulated after 24 hours (Figure 3.5A; 17.0-fold ± 3.1 vs saline control, $p < 0.05$), similar to our previous findings[85]. Although not to the same extent as CTGF levels, TGF-β transcript levels were also elevated at 6 hours (Figure 3.5B; 2.5-fold ± 0.2 vs saline control, $p < 0.01$) and 24 hours (Figure 3.5B; 3.2-fold ± 0.4 vs saline control, $p < 0.001$). These results demonstrate that the induction of CTGF and TGF-β transcript production occurred prior to significant mononuclear cell infiltration,

suggestive of resident cardiac cells – such as cardiac fibroblasts, endothelial cells, or resident cardiac Mϕs – as possible sources of these early pro-fibrotic factors.

CTGF can be directly induced by TGF-β activation via the TGF-β/Smad pathway or through direct activity of Ang-II via its receptor, AT1R[75,166-168]. In order to address whether TGF-β activity is upregulated after 6 hours of Ang-II exposure, Western blot experiments were conducted probing for Smad proteins, as TGF-β signaling directly induces downstream phosphorylation of Smad proteins, specifically phosphorylation of Smad2 (Serines 465/467) and Smad3 (Serines 423/425)[109,169,170]. As expected, Ang-II hearts demonstrated a significant upregulation of phosphorylated Smad2 (pSmad2) levels relative to actin (Figure 3.6A; 5.7-fold ± 1.2, $p < 0.05$) compared to saline control, whereas total Smad2/3 protein levels were not affected (Figure 3.6A). Thus, the ratio between pSmad2 levels relative to total Smad2/3 levels is elevated upon Ang-II exposure, suggestive of increased TGF-β activity (Figure 3.6B, 5.7-fold ± 1.3, $p < 0.05$). Similarly, 24 hours of Ang-II infusion resulted in a trend towards increased pSmad2 levels relative to actin (Figure 3.6C, 3.1-fold ± 0.9, $p = 0.0686$), while total Smad2/3 levels remain unchanged (Figure 3.6C). This resulted in a trending increase in pSmad2 levels relative to total Smad2/3 levels (Figure 3.6D, 4.1 ± 1.3, $p = 0.0722$), indicative of TGF-β activity in the myocardium following Ang-II exposure.

Thus far, our results have demonstrated only the association of upregulated pSmad2 levels, indicative of TGF-β activity, with substantial upregulation of CTGF transcript levels at both 6 hours and 24 hours after Ang-II exposure. Therefore, this prompted us to take one step further towards examining the mechanistic link between TGF-β and CTGF in the myocardium within the first 24 hours.

3.4 Mechanistic Link Between Early CTGF Upregulation and TGF-β Activity In The Ang-II Exposed Myocardium

3.4.1 Effect of TGF-β Trap on Gene Expression of Pro-fibrotic Factors in vitro

In order to examine the role of TGF-β and pro-fibrotic gene expression, we have used a soluble TGF-β trap, designed as TGF-β type II receptors by the National Research Council, that is able to sequester active TGF-β and thus neutralize TGF-β activity[155]. Using a NIH/3T3 fibroblast monoculture, we performed initial experiments (n=3 independent experiments) whereby exogenous TGF-β, TGF-β with TGF-β trap, or TGF-β with pan TGF-β neutralizing antibody (1D11) was incubated with fibroblasts. Exogenous TGF-β resulted in a significant elevation of CTGF mRNA levels in NIH/3T3 fibroblasts after 6 hours (Figure 3.7A; 7.7-fold ± 0.7 vs media control, $p<0.001$). This increase was significantly reduced by 66% when TGF-β was incubated with NIH/3T3 along with 1D11 (Figure 3.7A; 2.6-fold ± 1.0 vs media control, $p<0.01$). Although not to the same extent as 1D11, incubation with the TGF-β trap demonstrated a trending reduction in CTGF transcript levels compared to TGF-β stimulated NIH/3T3 fibroblasts (Figure 3.7A; 4.8-fold ± 0.7 vs media control).

Interestingly, exogenous TGF-β stimulation of NIH/3T3 fibroblasts induced production of TGF-β, as indicated by an elevation of TGF-β transcript levels 6 hours after treatment (Figure 3.7B; 4.1-fold ± 1.1 vs media control, $p<0.05$). Similar to changes in CTGF transcript levels, the TGF-β trap and the 1D11 antibody resulted in a trending reduction in TGF-β transcript levels after 6 hours of treatment (Figure 3.7B; 3.1-fold ± 0.8 and 1.8-fold ± 0.3, respectively). Additionally, exogenous TGF-β stimulation of

NIH/3T3 fibroblasts induced type I collagen production, as indicated by an elevation of collagen-I transcript levels 6 hours after treatment (Figure 3.7C; 1.6-fold ± 0.1 vs media control, $p<0.05$). Treatment with TGF-β trap or 1D11 antibody significantly reduced the TGF-β-induced increase of collagen-I transcript levels of NIH/3T3 fibroblasts (Figure 3.7C; 0.9-fold ± 0.2 and 0.7-fold ± 0.1, respectively).

3.4.2 Effect of TGF-β Trap on Early Pro-Fibrotic Gene Expression in vivo

As shown earlier, CTGF expression was substantially upregulated after Ang-II infusion, particularly at 6 hours *in vivo*. If CTGF expression is directly influenced by TGF-β activity, then the observed early elevation of CTGF at 6 hours is hypothesized to be abolished upon administering the TGF-β trap. The TGF-β trap (10 mg/kg) was administered intraperitoneally either with or without Ang-II infusion. Our results indicate that the TGF-β trap significantly reduced CTGF mRNA levels by 64.2% in Ang-II animals at 6 hours compared to PBS control (Figure 3.8A, left; 19.3-fold ± 5.4 vs 6.9-fold ± 1.6, respectively, $p<0.05$). However, the effect of the TGF-β trap was no longer maintained at 24 hours (Figure 3.8B, left). These results suggest that early CTGF expression in the myocardium is partially dependent on TGF-β activity, possibly through latent TGF-β activation in the myocardium rather than TGF-β independent effects of Ang-II exposure. Interestingly, there appears to be a trend towards elevation in TGF-β expression after TGF-β trap administration at 6 hours, although it failed to reach significance and did not affect levels at 24 hours (Figure 3.8A-B, right).

Administering the TGF-β trap appears to have a significant effect *in vivo*, as demonstrated by a reduction of CTGF transcript levels at 6 hours. In order to confirm that

the reduction of CTGF transcript levels after TGF-β trap administration to Ang-II animals is a result of the TGF-β/Smad-dependent pathway, we performed Western blotting experiments to identify levels of pSmad2. Administration of the TGF-β trap reduced myocardial pSmad2 levels relative to total Smad2/3 protein in animals exposed to Ang-II compared to PBS controls (Figure 3.9A-B; 5.7-fold ± 1.5 vs 2.1-fold ± 0.5, respectively, $p<0.05$). At 24 hours, the levels of pSmad2 relative to total Smad2/3 proteins were not significantly different (Figure 3.9C-D).

Together, these results confirm that elevated TGF-β signaling occurs after Ang-II exposure, likely via latent TGF-β activation in the myocardium, particularly after 6 hours. Thus, elevated TGF-β activity induced the substantial early upregulation of CTGF levels prior to significant increase in TGF-β protein expression through activation of the canonical Smad-dependent pathway.

3.5 Effect of TGF-β Trap on Early Gross Histological and Cellular Changes in the Ang-II Exposed Myocardium

As we were able to provide evidence for molecular changes in the Ang-II exposed myocardium at 6 hours with the administration of the TGF-β trap, we then examined myocardial sections of Ang-II hearts that also received the TGF-β trap for cellular infiltration and collagen deposition using H&E and SR/FG staining. Histological analyses of H&E stained cross-sections demonstrated no significant differences in cellular infiltration in Ang-II hearts that also received the TGF-β trap versus PBS controls (Figure 3.10A-C). This would support that early mononuclear cell infiltration is not dependent on the early action of preformed or active TGF-β. As we did not observe any significant

differences in collagen deposition after Ang-II exposure at 24 hours, the TGF-β trap did not affect differences in collagen deposition as observed in the SR/FG stained myocardial sections (Figure 3.10D-F). Type I collagen transcript levels were also not significantly altered after administration of the TGF-β trap after 24 hours of Ang-II exposure (Figure 3.10F).

Previous work has demonstrated an increase in α-SMA expression, a cell-specific marker for indication of fibroblast transdifferentiation into myofibroblasts, 3 days after Ang-II exposure, which remained highly abundant in the myocardium after 7 days of Ang-II exposure[49,80,156]. We have noted, thus far, that significant molecular changes occurred as early as 6 hours after Ang-II exposure, which preceded significant immune mononuclear cell infiltration, suggestive of an initial activation of resident cells in the myocardium. One of the most abundant non-cardiomyocyte cell types is the cardiac fibroblast, second to endothelial cells[88]. It has been well established in the literature that TGF-β can activate cardiac fibroblasts and induce their phenotypic change into myofibroblasts[110,171,172]. Looking at results from immunohistochemical staining for α-SMA, we did not observe any significant increases in α-SMA$^+$ myofibroblasts compared to saline control within 24 hours of Ang-II exposure after quantification by cell counting (Figure 3.11A-C).

Despite any notable changes in fibroblast phenotype, we next assessed proliferation of mononuclear cells in the myocardium at 24 hours. Our previous work has demonstrated that Ang-II exposure led to a significant increase in proliferative mononuclear cells in the myocardium by 3 days[85,106]. Here, immunohistochemical labeling of Ki-67 was used as an indicator of cell proliferation. Ki-67$^+$ cells were then

counted over the total number of infiltrating cells in five fields of view at 40x magnification and the percentage of Ki-67^{+} cells was calculated over the total number of nuclei. In animals that were exposed to Ang-II for 24 hours, there was a significant increase in Ki-67 positive nuclei relative to saline controls (Figure 3.12A-C; 6.0-fold ± 1.8, $p<0.05$). Upon administration of the TGF-β trap, the number of Ki-67^{+} cells in the Ang-II exposed myocardium remained elevated over saline control (Figure 3.12; 8.0-fold ± 1.0, $p\leq0.01$), with no significant differences between Ang-II animals that received PBS or the TGF-β trap. These results suggest that changes in early cellular proliferation in the myocardium is unlikely to be TGF-β dependent and are likely to be greatly dependent on direct Ang-II effects.

3.6 Role of CTGF on Fibroblast Activation and Proliferation

In previous work, we identified that CTGF is one of the initial pro-fibrotic mediators substantially upregulated after Ang-II exposure in the myocardium[85]. We were able to replicate these findings and confirm that CTGF is upregulated as early as 6 hours after Ang-II infusion, as well as provided further evidence to suggest that this upregulation is partially induced by latent TGF-β activation in the myocardium. While the role of TGF-β has been well-described in literature, the role of CTGF has not been explored to the same extent. In fact, there has been conflicting reports on the importance of CTGF in fibrotic conditions, particularly in the development of myocardial fibrosis[143,144,173,174]. Thus, we sought to examine the fundamental role of CTGF on fibroblast activation, proliferation, and ability to produce pro-fibrotic factors important for fibrosis development. To explore this, we used an *in vitro* NIH/3T3 fibroblast

monoculture system grown in culture and exposed to exogenous CTGF and/or TGF-β to better understand their respective roles on fibroblast activation and phenotype.

3.6.1 Exogenous CTGF Does Not Appear to Affect Fibroblast Expression of Fibrotic Mediators in vitro

NIH/3T3 fibroblasts were grown in monoculture and exposed to exogenous CTGF and/or TGF-β for 6 hours and compared to fibroblasts incubated in media only supplemented with 1% FBS. Exogenous TGF-β treatment induced a significant upregulation of CTGF mRNA in NIH/3T3 fibroblasts (Figure 3.13A; 7.3-fold ± 0.5 vs media control, $p \leq 0.01$), as well as a trending increase towards TGF-β and type I collagen mRNA levels (Figure 3.13B-C). However, exogenous CTGF treatment alone or in combination with exogenous TGF-β treatment did not affect, or have a synergistic effect, on CTGF, TGF-β, or type I collagen mRNA levels (Figure 3.13A-C). These findings suggest that CTGF does not have an important role in propagating fibroblast production of fibrogenic mediators, at least independently or synergistically with TGF-β *in vitro*.

3.6.2 Exogenous CTGF Does Not Appear to Alter Fibroblast Phenotype in vitro

Although exogenous CTGF did not alter fibroblast production of pro-fibrotic mediators, such as CTGF, TGF-β, or type I collagen, CTGF may also promote fibroblast differentiation into myofibroblasts. We next assessed phenotypic changes of NIH/3T3 fibroblasts *in vitro* such as differentiation into α-SMA$^+$ myofibroblasts, which are effector cells of fibrosis development. As expected, exogenous TGF-β treatment for 24 hours induced an upregulation in α-SMA expression, indicative of increased fibroblast

transdifferentiation into myofibroblasts, compared to media control (Figure 3.14A,C,E; 1.9-fold ± 0.2 vs media control, $p \leq 0.01$). Alternatively, exogenous CTGF alone had no effect on α-SMA expression and did not produce a synergistic effect with exogenous TGF-β incubation, suggesting that CTGF does not play an important role in early fibroblast differentiation in this context (Figure 3.14A-B, D-E).

3.7 Characterizing Early Monocytes/Mϕ Composition and Subsets in the Spleen, Blood, and Heart of Ang-II Exposed Mice

Thus far, this thesis has focused on the mechanistic link between TGF-β and CTGF in the early myocardial environment after Ang-II infusion, particularly prior to significant cellular infiltration. In addition, the importance of the role of CTGF was explored fundamentally in a monoculture system of NIH/3T3 fibroblasts and compared to the role of TGF-β. Previous work has also demonstrated the important contribution of monocyte/Mϕ interactions with resident cardiac cells in the progression of myocardial fibrosis in ischemic animal models as well as in nonischemic hypertensive models[64,79,126,175]. Importantly, monocyte/Mϕ infiltration is associated with significant collagen deposition within the myocardium as early as 3 days after Ang-II infusion[80,106]. The early changes of the myocardial environment may heavily influence the composition of the monocyte/Mϕ pool in the myocardium and may promote monocyte phenotype changes beyond the myocardium in potential sources such as the spleen and in circulation. Thus, we set out to examine the murine changes in monocyte/Mϕ composition and phenotype in the setting of Ang-II induced hypertension.

3.7.1 Mϕ Influx Demonstrated a Pro-Inflammatory Shift in the Ang-II Heart

Animals were infused with saline or Ang-II and sacrificed after 3 days. Consistent with previous work, animals that received saline infusion were shown to have a population of $CCR2^{+}CX_3CR1^{+}$ Mϕs in the myocardium (Figure 3.15A-B; 17.4% ± 1.1 of isolated mononuclear cells, 404.1 ± 25.9 cells/mg tissue). Ang-II infusion led to a significant increase in the number of $CCR2^{+}CX_3CR1^{+}$ Mϕs in the myocardium compared to saline control (Figure 3.15A-B; 43.0% ± 3.1 of isolated mononuclear cells, $p \leq 0.0001$; 905.4 ± 92 cells/mg tissue, $p \leq 0.001$). Upon further analyses, this population exhibited a pro-inflammatory shift in Ang-II hearts, as demonstrated by an increase in Ly6C MFI within $CD11b^{high}$ Mϕs (Figure 3.16A-B; 2063 ± 297 MFI vs. 644 ± 50 MFI, $p \leq 0.001$). Additionally, the proportion of $CD11b^{high}$ Mϕs was significantly upregulated upon Ang-II exposure (Figure 3.16C; 64.9% ± 8.7 vs. 23.8% ± 3.2, $p \leq 0.01$), whereas the proportion of $CD11b^{low}$ Mϕs was significantly reduced compared to saline controls (Figure 3.16D; 27.5% ± 7.0 vs 57.7% ± 2.6, $p \leq 0.01$).

3.7.2 $CD11b^{+}$ monocytes were present in lower proportion in circulation with no differences in pro-inflammatory phenotype

Monocyte populations were assessed from circulation using flow cytometry after 3 days of Ang-II infusion. Two subpopulations were observed in circulation – $CD11b^{low}$ monocytes and $CD11b^{high}$ monocytes (Figure 3.17A). Both $CD11b^{high}$ and $CD11b^{low}$ monocyte subpopulations (Figure 3.17A-B; 3.2% ± 0.7 and 6.4% ± 0.6 of isolated mononuclear cells, respectively, $p \leq 0.01$) were present in lower proportion in circulation after 3 days of Ang-II infusion compared to saline control (Figure 3.17A-B; 1.7% ± 0.4

vs. 4.4% ± 0.5 of isolated mononuclear cells, and 3.2% ± 0.7 vs. 6.4% ± 0.6 of isolated mononuclear cells, respectively, $p \leq 0.01$). $CD11b^{high}$ monocytes were mainly pro-inflammatory $Ly6C^{high}CCR2^{+}$ monocytes, but did not differ in percentage after 3 days of Ang-II infusion (Figure 3.18A-B).

3.7.3 Splenic $CD11b^{+}$ monocytes were reduced after Ang-II exposure and consisted of a higher proportion of pro-inflammatory $Ly6C^{high}CCR2^{+}$ monocytes

Mononuclear cells were isolated from the murine spleen after 3 days of Ang-II infusion. In total, there was a decrease in the number of mononuclear cells isolated from the Ang-II spleen compared to saline control (Figure 3.19A; 2.9×10^7 cells ± 6.1×10^6 vs 7.9×10^7 cells ± 1.6×10^7, $p<0.05$). Upon flow cytometry analyses, two subpopulations of $CD11b^{+}$ monocytes were present – $CD11b^{high}$ and $CD11b^{low}$ monocytes (Figure 3.19B). The proportion of splenic $CD11b^{high}$ and $CD11b^{low}$ monocytes were similar in Ang-II spleens compared to saline controls but absolute numbers were lower with both subpopulations (Figure 3.19B-C). Further analyses of the subpopulations of splenic $CD11b^{+}$ monocytes revealed that $CD11b^{low}$ monocytes expressed mainly $Ly6C^{low}CCR2^{low}$ (Figure 3.20A) whereas $CD11b^{high}$ monocytes expressed mainly $Ly6C^{high}CCR2^{+}$ (Figure 3.20B). Interestingly, Ang-II exposure led to an increase in the ratio of the number of $Ly6C^{high}CCR2^{+}$ monocytes to the number of $Ly6C^{low}CCR2^{low}$ monocytes compared to saline control (Figure 3.20B-C; 0.4 ± 0.1 vs. 0.1 ± 0.02, $p<0.05$). These results suggest that the monocyte population in the spleen demonstrated a pro-inflammatory shift after Ang-II exposure, which is likely contributing to the influx of pro-inflammatory monocytes into the myocardium.

3.8 Figures

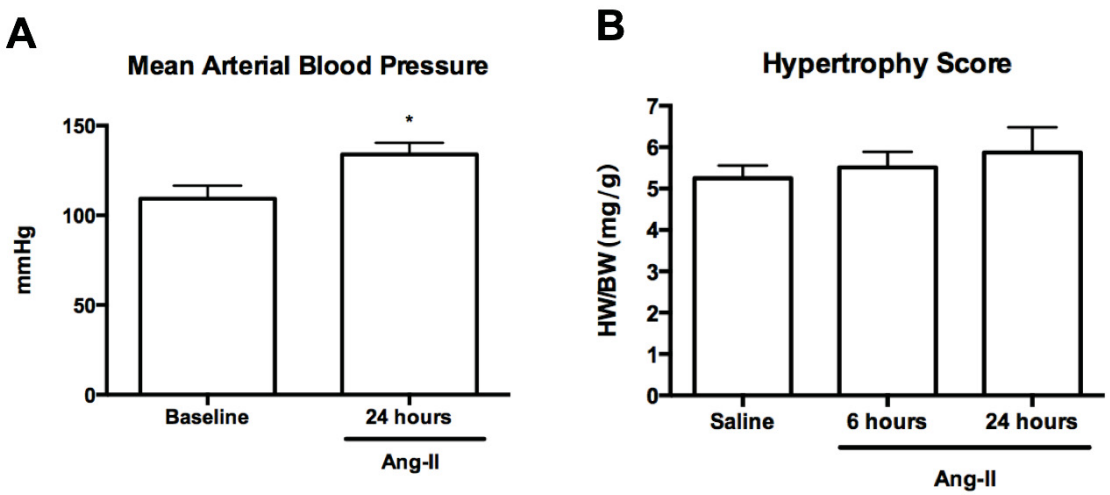

Figure 3.1. Hemodynamic and physiological parameters of Ang-II exposed mice. (A) Ang-II exposure led to an increase in mean arterial blood pressure after 24 hours. **(B)** There was no significant change in hypertrophy score after 6 or 24 hours of Ang-II exposure, as measured by the ratio of heart weight normalized to body weight. Data are expressed as means ± SEM. n=5-8. *$p<0.05$, compared with baseline or saline group. Ang-II, Angiotensin II; BW, body weight. HW, heart weight.

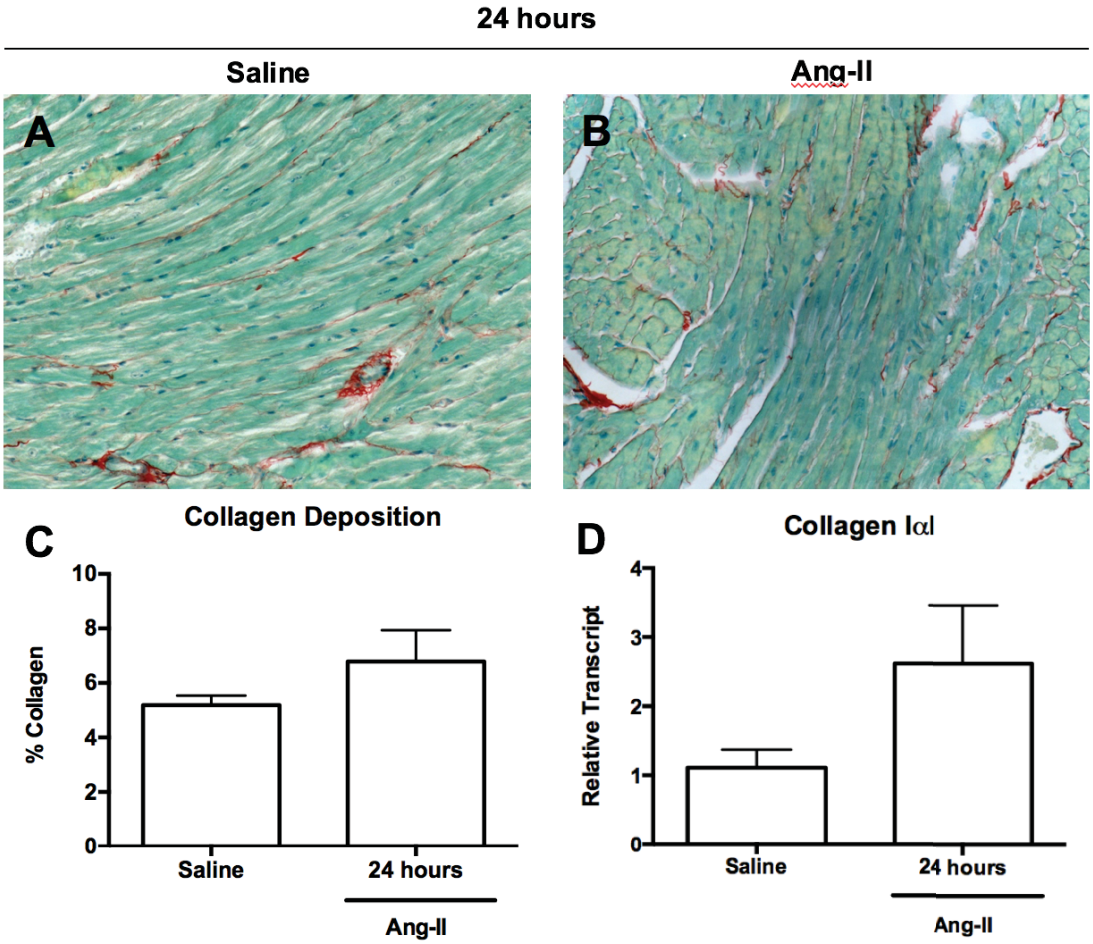

Figure 3.2. Collagen deposition in Ang-II myocardium after 24 hours. Collagen deposition was not apparent within 24 hours of Ang-II exposure. Representative images of myocardial cross-sections stained with Sirius Red and counterstained with Fast Green from an animal that received **(A)** saline or **(B)** Ang-II for 24 hours (collagen, red; cardiomyocytes, green). **(C)** SR/FG cross-sections were semi-quantified for collagen content by collecting number of red pixels over the total number of heart pixels (red and green) of each section. **(D)** Myocardial transcript levels of type I collagen expression after Ang-II infusion relative to saline control for 24 hours. Transcript levels are reported

relative to the reference gene ribosomal 18S. Data are expressed as means ± SEM. n=5. Original magnification: x20. Ang-II, Angiotensin II.

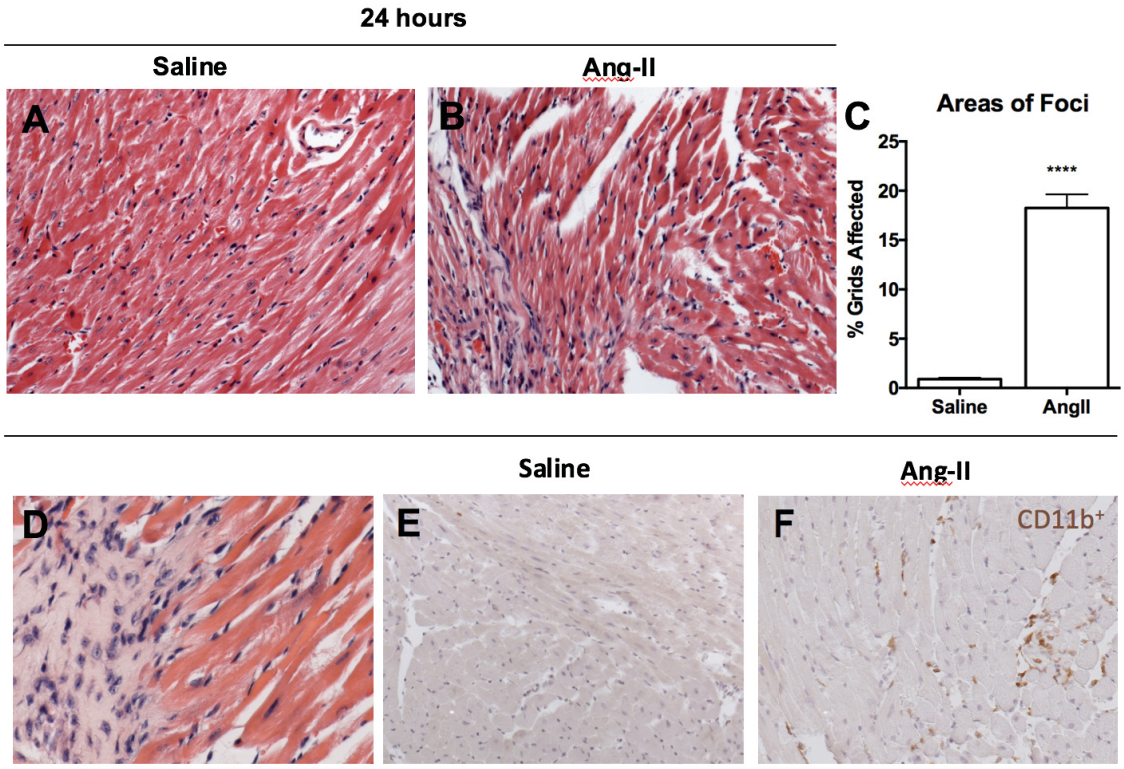

Figure 3.3. Mononuclear cellular infiltration in the myocardium was present at 24 hours after Ang-II exposure. Ang-II exposure led to an increase in mononuclear cell infiltration, primarily $CD11b^+$ monocytes, into the myocardium at 24 hours. Representative images of myocardial cross-sections stained with H&E from an animal that received **(A)** saline or **(B, D)** Ang-II. **(C)** H&E sections were semi-quantified for cellular infiltration in Ang-II animals relative to saline control. Immunohistochemistry was used to characterize mononuclear cell infiltrates as $CD11b^+$ cells. Representative myocardial cross-sections from animals treated with **(E)** saline or **(F)** Ang-II. Data are expressed as means ± SEM. n=5. ****$p<0.0001$, compared with saline control. Original magnification: x20 (A-B, E-F); x40 (D). Ang-II, Angiotensin II; H&E, hematoxylin and eosin.

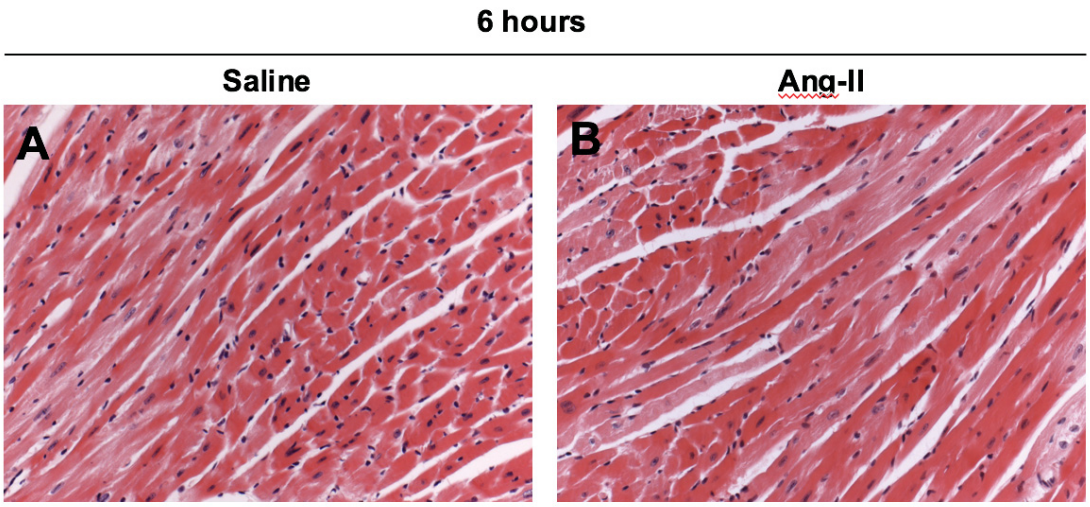

Figure 3.4. Myocardium exposed to Ang-II for 6 hours did not display significant cellular infiltration. Representative images of myocardial cross-sections stained with H&E from an animal that received **(A)** saline or **(B)** Ang-II for 6 hours. Original magnification: x20. Ang-II, Angiotensin II; H&E, hematoxylin and eosin.

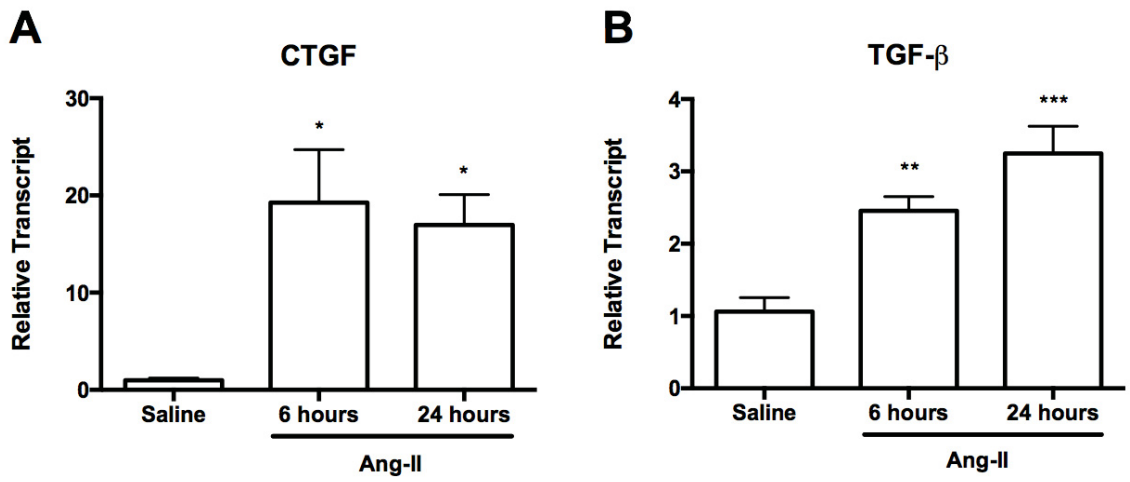

Figure 3.5. Early upregulation of myocardial CTGF and TGF-β transcript levels appeared as early as 6 hours after Ang-II exposure. Myocardial transcript levels of **(A)** CTGF and **(B)** TGF-β after 6 or 24 hours of Ang-II infusion relative to saline control. Transcript levels are reported relative to the reference gene ribosomal 18S. Data are expressed as means ± SEM. n=5-6. *p<0.05, **p<0.01, ***p<0.001, compared with saline control. Ang-II, Angiotensin II; CTGF, connective tissue growth tissue; TGF-β, transforming growth factor-β.

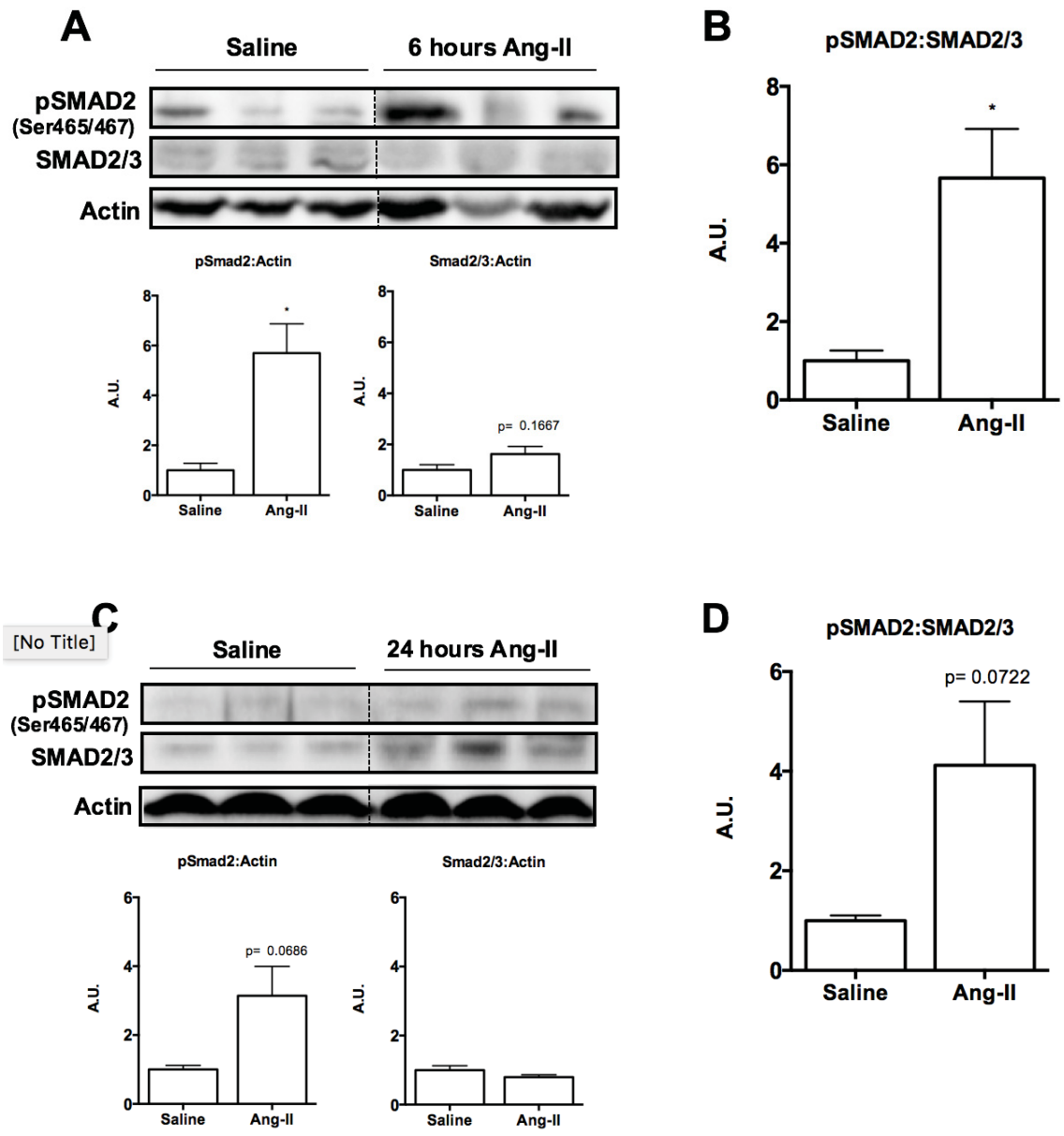

Figure 3.6. Levels of Smad2 phosphorylation was upregulated after Ang-II exposure, indicative of TGF-β activity. **(A)** Representative Western blot images of three animals per group and semi-quantification using densitometry of pSmad2 and total Smad2/3 protein levels relative to actin at 6 hours. **(B)** Densitometry was used for semi-quantification of pSmad2 levels relative to total Smad2/3 protein levels. **(C)** Representative Western blot images of three separate animals (n=3) per group and semi-

quantification using densitometry of pSmad2 and total Smad2/3 protein levels relative to actin at 24 hours. **(D)** Densitometry was used for semi-quantification of pSmad2 levels relative to total Smad2/3 protein levels. Data are expressed as means ± SEM. Samples were run on separate gels with control group present on all gels for normalization. n=5–6. *p<0.05, **p<0.01, compared to saline control. Ang-II, Angiotensin II; A.U., Arbitrary Units; PBS: phosphate-buffered saline; pSMAD2: phosphorylated Smad2; Ser: serine.

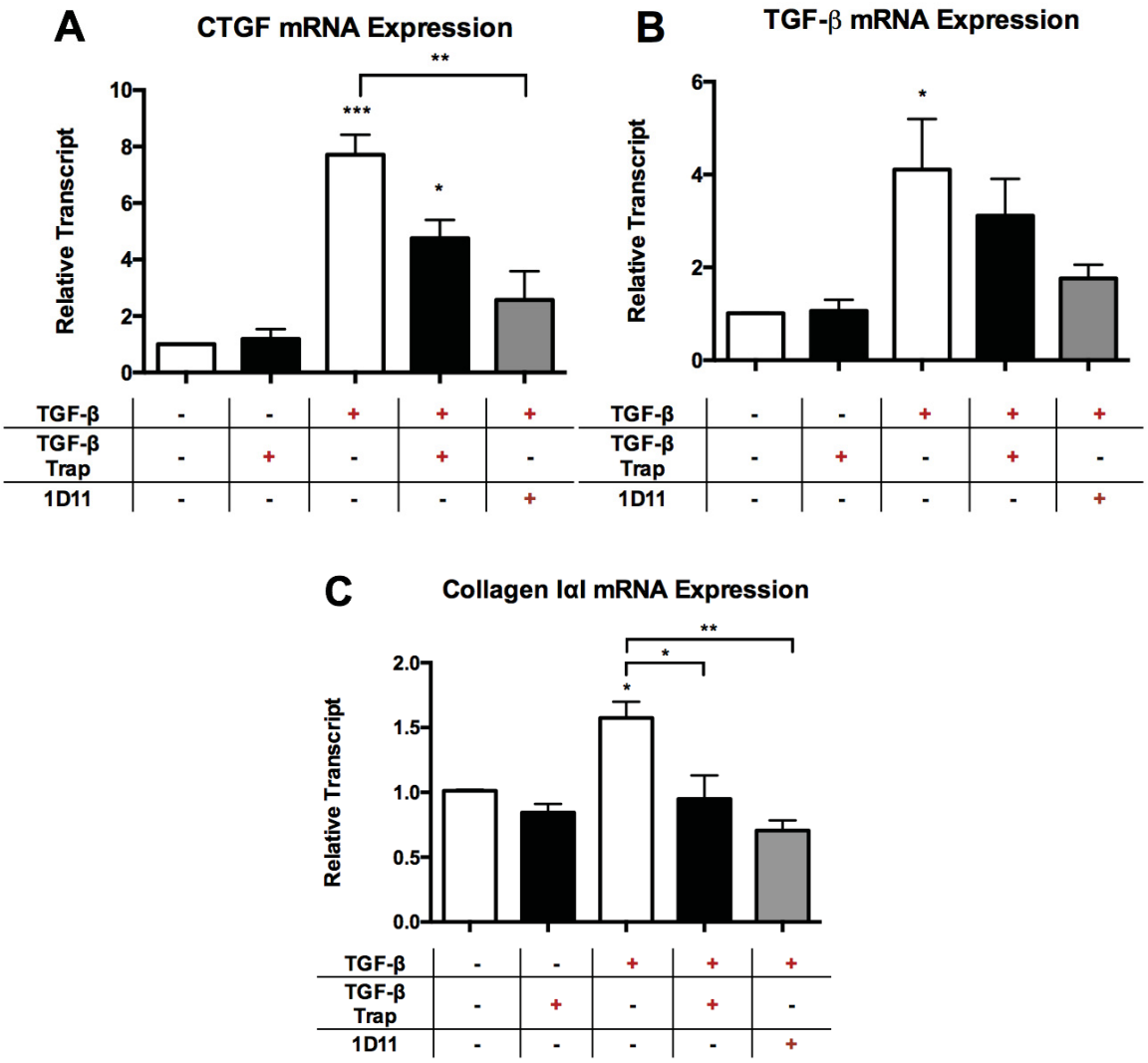

Figure 3.7. Effect of TGF-β trap on exogenous TGF-β-induced upregulation of pro-fibrotic CTGF, TGF-β and type I collagen transcript levels of NIH/3T3 *in vitro*.

NIH/3T3 fibroblasts were incubated with exogenous TGF-β only, TGF-β trap only, TGF-β plus TGF-β trap, or TGF-β plus 1D11 antibody for 6 hours. Transcript levels of **(A)** CTGF, **(B)** TGF-β, and **(C)** type I collagen was obtained using qPCR analyses. Transcript levels are reported relative to both reference gene ribosomal 18S and GAPDH. Data are represented as means ± SEM and expressed relative to media control. n=3 independent

experiments in triplicates. Independent experiments are defined as three separate sets of experiments on different cell passages *$p<0.05$, **$p\leq0.01$, ***$p\leq0.001$. CTGF, connective tissue growth factor; TGF-β, transforming growth factor-β; 1D11, pan TGF-β neutralizing antibody.

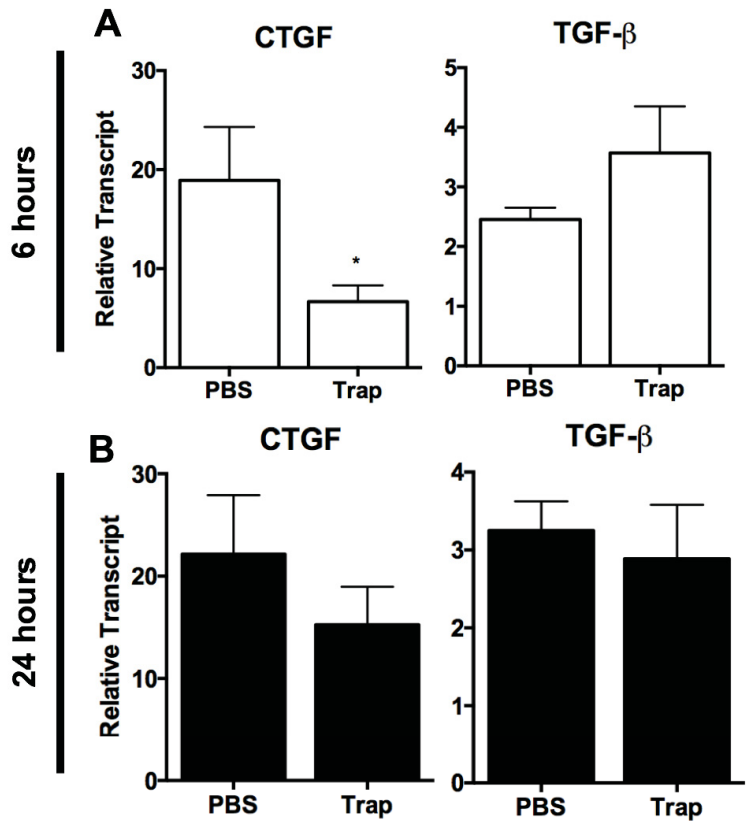

Figure 3.8. TGF-β trap reduced levels of Ang-II-induced early upregulation of CTGF transcript at 6 hours. Myocardial CTGF and TGF-β transcript levels after **(A)** 6 hours or **(B)** 24 hours of Ang-II infusion in animals injected with TGF-β trap or PBS relative to saline control. Transcript levels are reported relative to reference gene ribosomal 18S. Data are expressed as means ± SEM. n=5-6. *p<0.05, compared to PBS group. CTGF, connective tissue growth factor; PBS, phosphate-buffered saline; Trap, TGF-β trap; TGF-β, transforming growth factor-β.

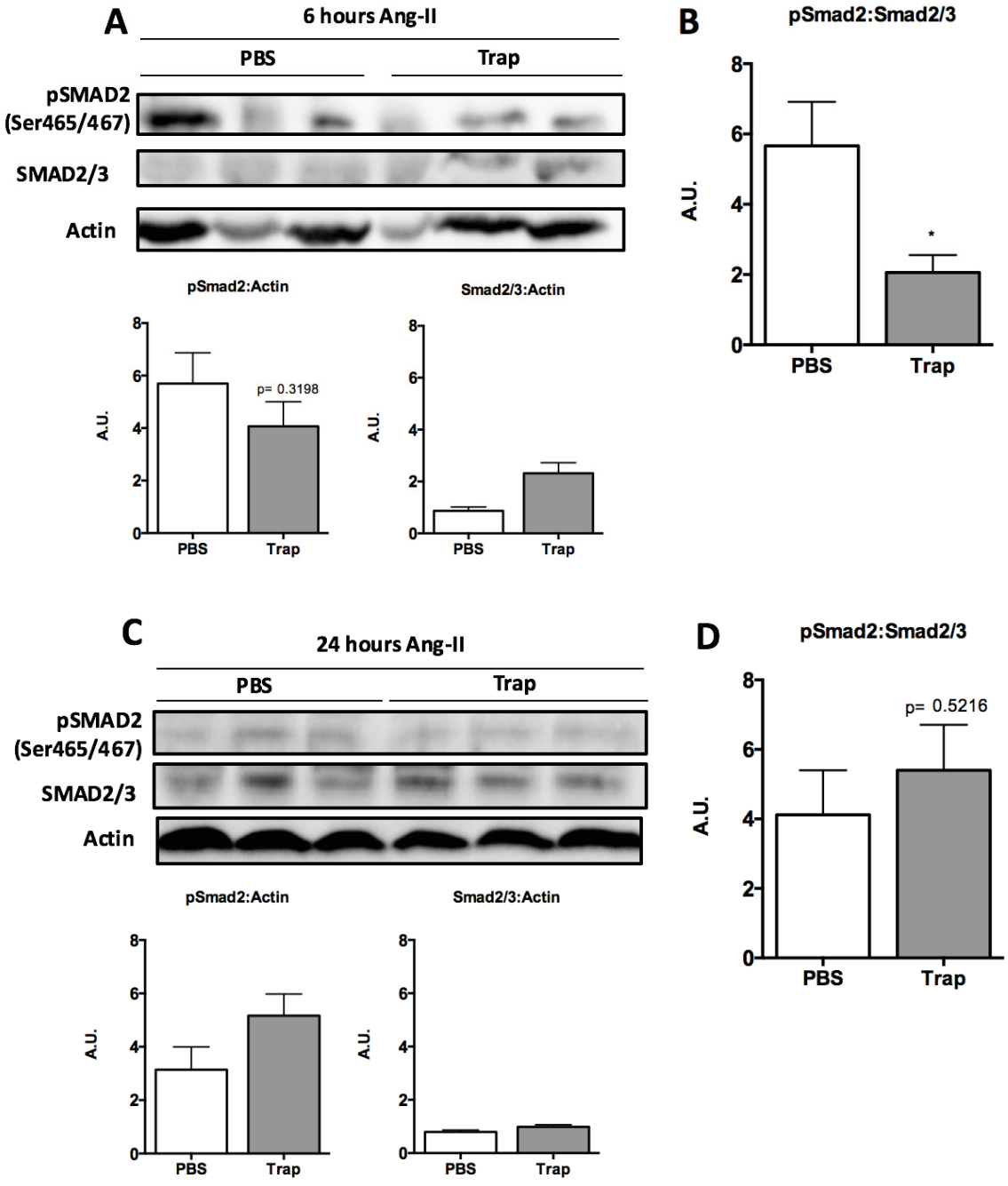

Figure 3.9. TGF-β trap administration partially reduced Ang-II-induced elevation of Smad2 phosphorylation at 6 hours. (A) Representative Western blot images and semi-quantification using densitometry of pSmad2 and total Smad2/3 protein levels relative to actin at 6 hours. Each lane represents a separate animal per group. **(B)**

Densitometry was used for semi-quantification of pSmad2 levels relative to total Smad2/3 protein levels. **(C)** Representative Western blot images and semi-quantification using densitometry of pSmad2 and total Smad2/3 protein levels relative to actin at 24 hours. Each lane represents a separate animal per group. **(D)** Densitometry was used for semi-quantification of pSmad2 levels relative to total Smad2/3 protein levels. Data are expressed as means ± SEM. Samples were run on separate gels with control group present on all gels for normalization. n=5–6. *$p<0.05$, compared to saline control. Ang-II, Angiotensin II; PBS, phosphate-buffered saline; pSMAD2, phosphorylated Smad2; Ser, serine; Trap, TGF-β trap.

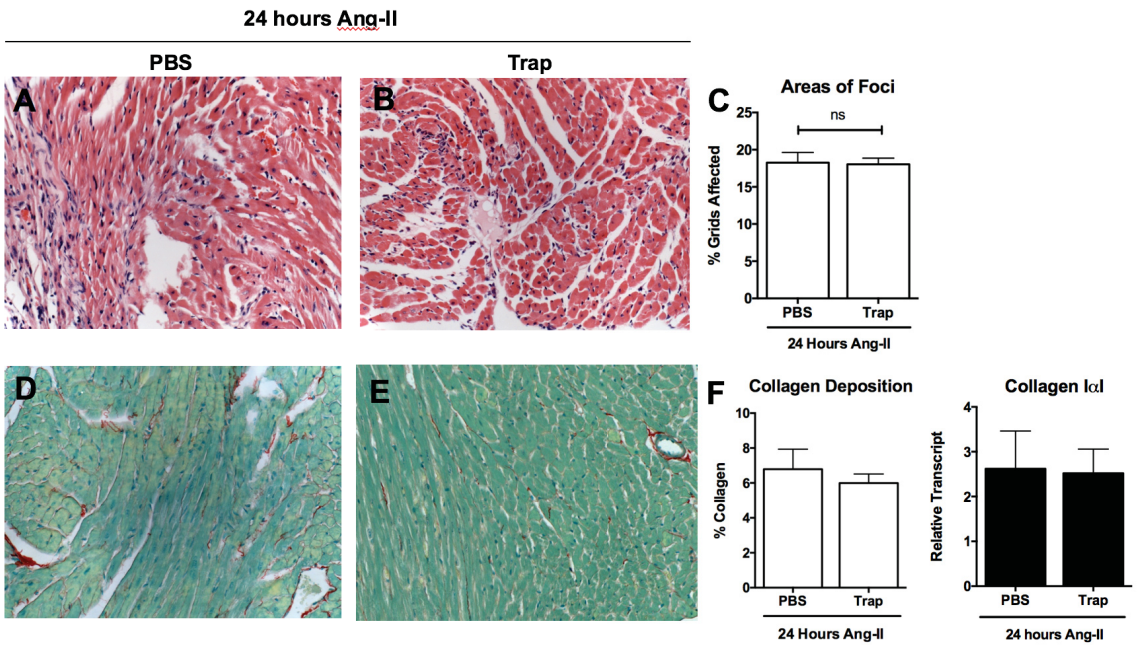

Figure 3.10. Administration of the TGF-β trap did not affect degree of Ang-II-induced cellular infiltration observed at 24 hours. Representative images of Ang-II exposed myocardial cross-sections stained with H&E that also received **(A)** PBS or **(B)** TGF-β trap for 24 hours. **(C)** H&E cross-sections were semi-quantified for cellular infiltration using an established grid-scoring method. Representative images of Ang-II exposed myocardial cross-sections stained with SR/FG that also received **(D)** PBS or **(E)** TGF-β for 24 hours (collagen, red; cardiomyocytes, green). **(F)** SR/FG cross-sections were semi-quantified for collagen content by collecting the number of red pixels over the total pixels (red and green) (left). Myocardial type I collagen transcript levels in Ang-II animals that also received either PBS or TGF-β trap and reported relative to reference gene ribosomal 18S and relative to saline control (right). Data are expressed as means ± SEM. n=5. Original magnification: x20. Ang-II, Angiotensin-II; PBS, phosphate-buffered saline; Trap, TGF-β trap.

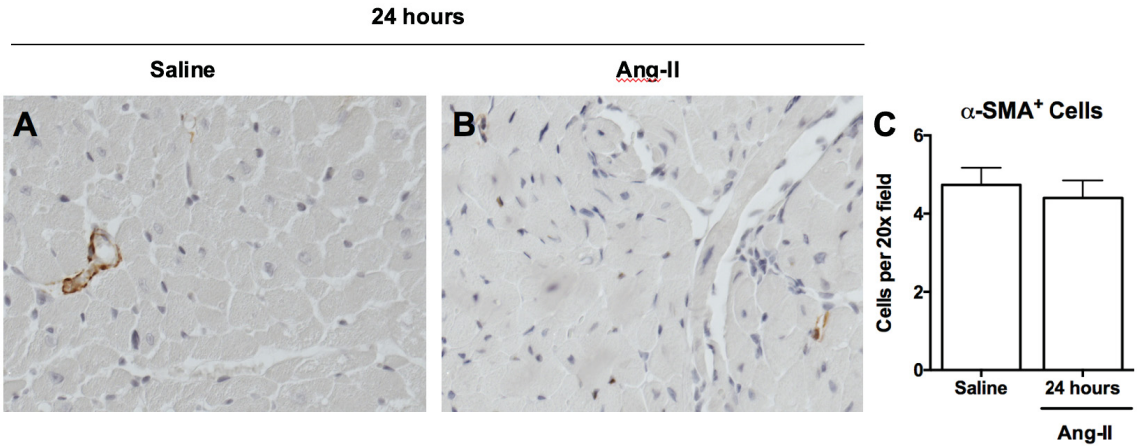

Figure 3.11. Transdifferentiation into α-SMA$^+$ myofibroblasts was not evident after 24 hours of Ang-II infusion. Immunohistochemistry was used to identify α-SMA-positive (brown) cells in myocardial cross-sections of **(A)** saline or **(B)** Ang-II mice. **(C)** Cells were counted at 20x magnification in five random fields of view per sample. Data are expressed as means ± SEM. n=5. Original magnification: x20. α-SMA, alpha-smooth muscle actin; Ang-II, Angiotensin-II; PBS, phosphate-buffered saline; Trap, TGF-β trap.

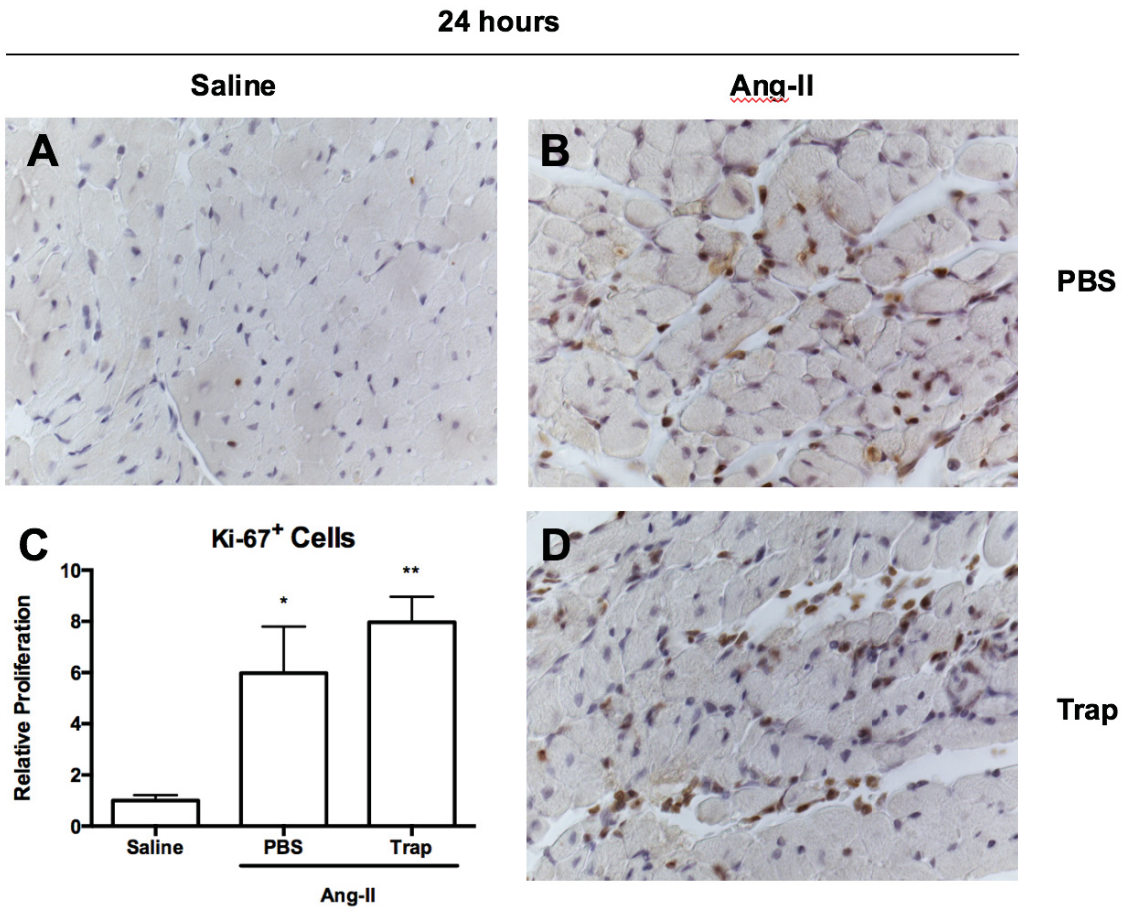

Figure 3.12. Ang-II infusion led to significant increase in Ki-67$^+$ mononuclear cells in the myocardium after 24 hours, indicative of increased cell proliferation, with no effect after TGF-β trap administration compared to Ang-II hearts.

Immunohistochemistry was used to identify Ki-67 positive (brown) cells in myocardial cross-sections of **(A)** saline or Ang-II animals that received either **(B)** PBS or **(D)** TGF-β trap. **(C)** Proliferation was assessed by counting the number of Ki-67$^+$ nuclei relative to the total number of nuclei in five random fields of view per sample at 40x magnification. Data are expressed as means ± SEM. n=5. Original magnification: x20. Ang-II, Angiotensin-II; PBS, phosphate-buffered saline; Trap, TGF-β trap.

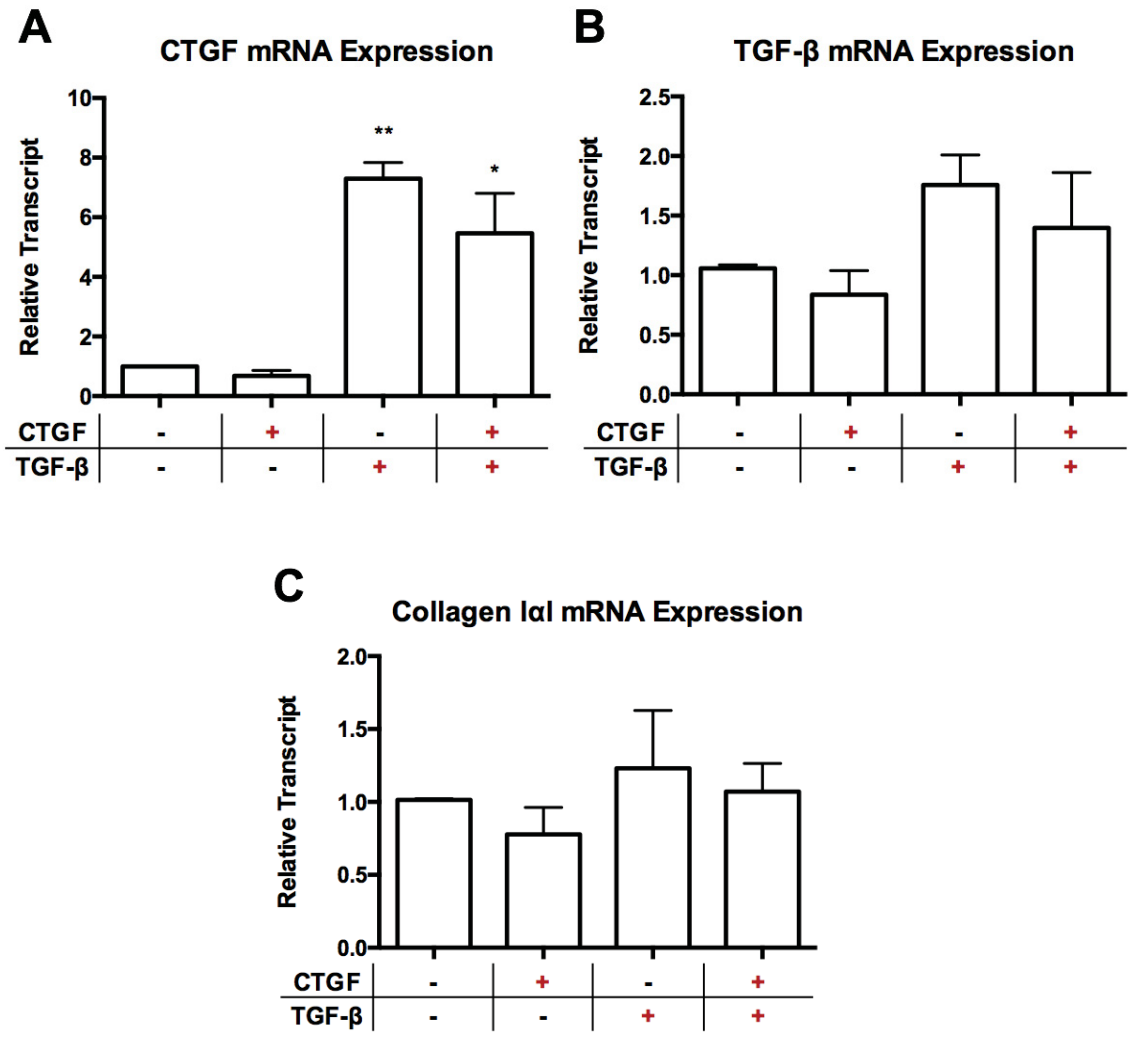

Figure 3.13. Exogenous CTGF treatment does not appear to have an effect on NIH/3T3 fibroblast production of pro-fibrotic CTGF, TGF-β, or type I collagen transcript independently or synergistically with exogenous TGF-β incubation *in vitro*. NIH/3T3 fibroblasts were incubated with exogenous CTGF only, TGF-β only, or CTGF plus TGF-β for 6 hours. Transcript levels of **(A)** CTGF, **(B)** TGF-β, and **(C)** collagen type I was obtained using qPCR analyses. Transcript levels are reported relative to both reference genes ribosomal 18S and GAPDH. Data are represented as means ± SEM and expressed relative to media control. n=3 independent experiments in triplicates.

*p<0.05, **p≤0.01. CTGF: connective tissue growth factor; GAPDH: glyceraldehyde 3-phosphate dehydrogenase; TGF-β: transforming growth factor-β.

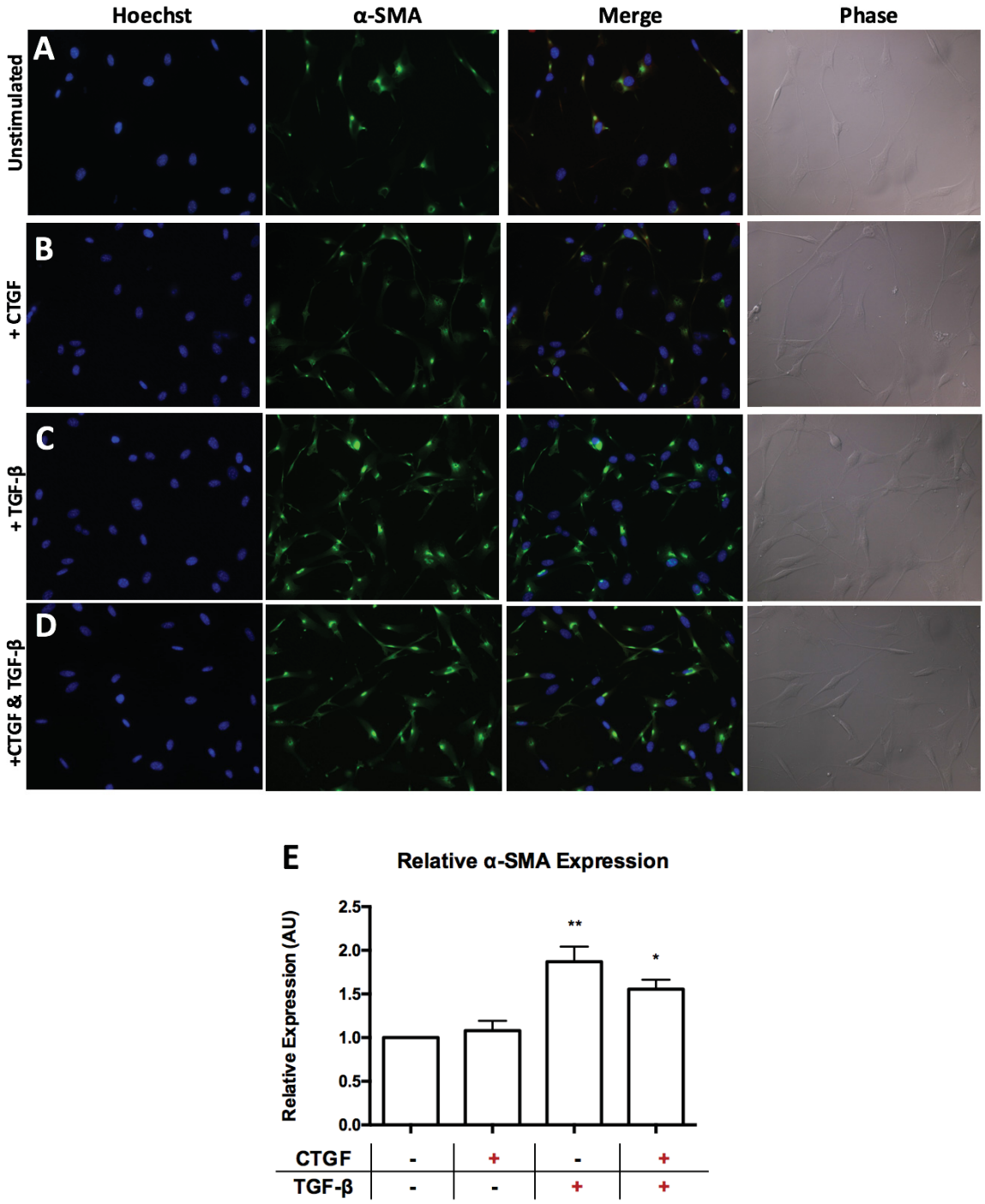

Figure 3.14. Exogenous CTGF treatment of NIH/3T3 fibroblasts does not appear to affect differentiation into α-SMA^{+} myofibroblasts independently or synergistically with exogenous TGF-β stimulation *in vitro*. NIH/3T3 fibroblasts were incubated with exogenous CTGF only, TGF-β only, or CTGF plus TGF-β for 24 hours. Representative

fields of view stained for α-SMA, Hoechst, and phase-contrast are shown for fibroblasts in **(A)** media control (1%FBS/DMEM), **(B)** exogenous CTGF, **(C)** exogenous TGF-β, and **(D)** exogenous CTGF plus TGF-β. **(E)** Graphical representation of α-SMA expression, as calculated by measuring α-SMA fluorescence intensity relative to Hoechst fluorescence intensity and represented relative to media controls. Data are represented as means ± SEM. n=3 independent experiments in triplicates. *$p<0.05$, **$p\leq0.01$, compared to media control. α-SMA: alpha-smooth muscle actin; AU: arbitrary units; CTGF: connective tissue growth factor; TGF-β: transforming growth factor-β.

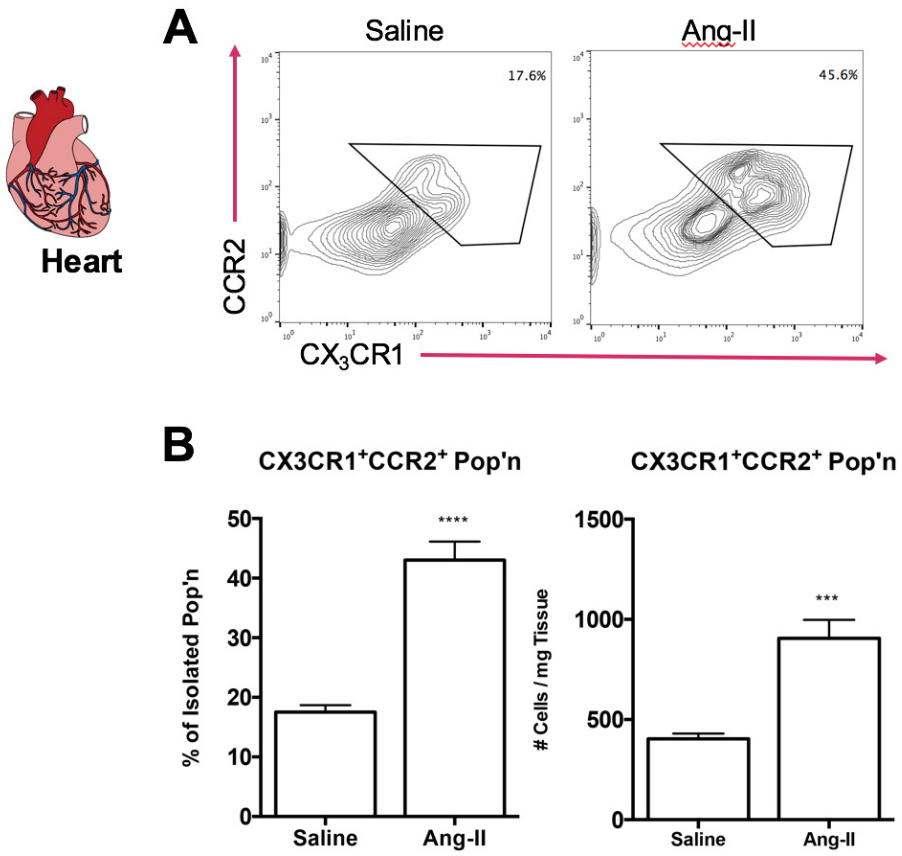

Figure 3.15. Ang-II infusion led to significant influx of $CCR2^{+}CX_3CR1^{+}$ monocytes/Mϕs in the myocardium at 3 days. (A) Representative images of flow cytometry contour plots of Mϕs in the myocardium as defined by CX_3CR1^{+} and $CCR2^{+}$ expression in saline control (left) and Ang-II (right) animals (boxed). **(B)** Quantification of $CX_3CR1^{+}CCR2^{+}$ populations in saline and Ang-II hearts as represented by the percentage of isolated mononuclear cells (left) and absolute numbers normalized per milligram of heart tissue (right). Data are expressed as means ± SEM. n=4-5. ***p<0.001, ****p<0.0001. Ang-II, Angiotensin-II; CCR2, C-C Chemokine Receptor 2; CX_3CR1, CX3C Chemokine Receptor 1; mg, milligram; Pop'n, population.

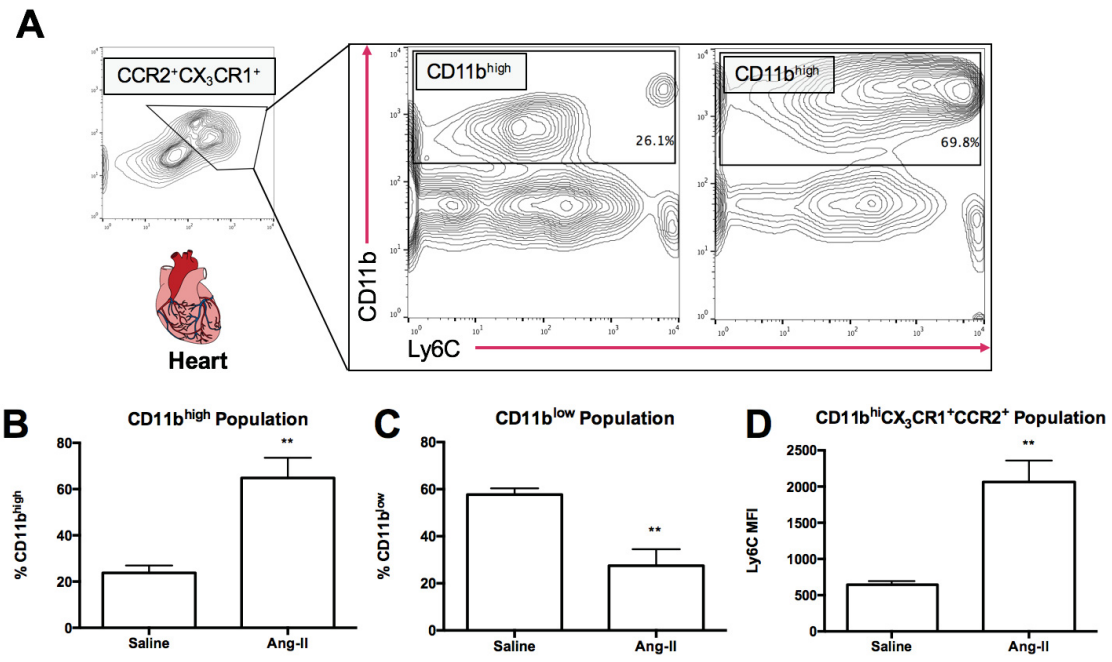

Figure 3.16. CCR2^{+}CX$_3$CR1^{+} monocytes/Mϕs demonstrated a pro-inflammatory shift towards CD11b^{high}Ly6C^{high} phenotype after 3 days of Ang-II infusion. (A) Representative images of flow cytometry contour plots of CX$_3$CR1^{+}CCR2^{+} Mϕs in the myocardium as defined by CD11b^{high} populations in saline control (left) and Ang-II (right) animals (boxed). **(B)** Quantification of CX$_3$CR1^{+}CCR2^{+} populations that expressed CD11b^{high} in saline and Ang-II hearts as represented by the percentage of CX$_3$CR1^{+}CCR2^{+} cells. **(C)** Quantification of CX$_3$CR1^{+}CCR2^{+} populations that expressed CD11b^{low} in saline and Ang-II hearts as represented by percentage of CX$_3$CR1^{+}CCR2^{+} cells. **(D)** Quantification of Ly6C expression of the CD11b^{high} CX$_3$CR1^{+}CCR2^{+} Mϕ population in saline and Ang-II hearts as represented by Ly6C MFI. Data are expressed as means ± SEM. n=4-5. **p<0.01. Ang-II, Angiotensin-II; CCR2, C-C Chemokine Receptor 2; CX$_3$CR1, CX3C Chemokine Receptor 1; Ly6C, lymphocyte antigen 6C; MFI, mean fluorescence intensity.

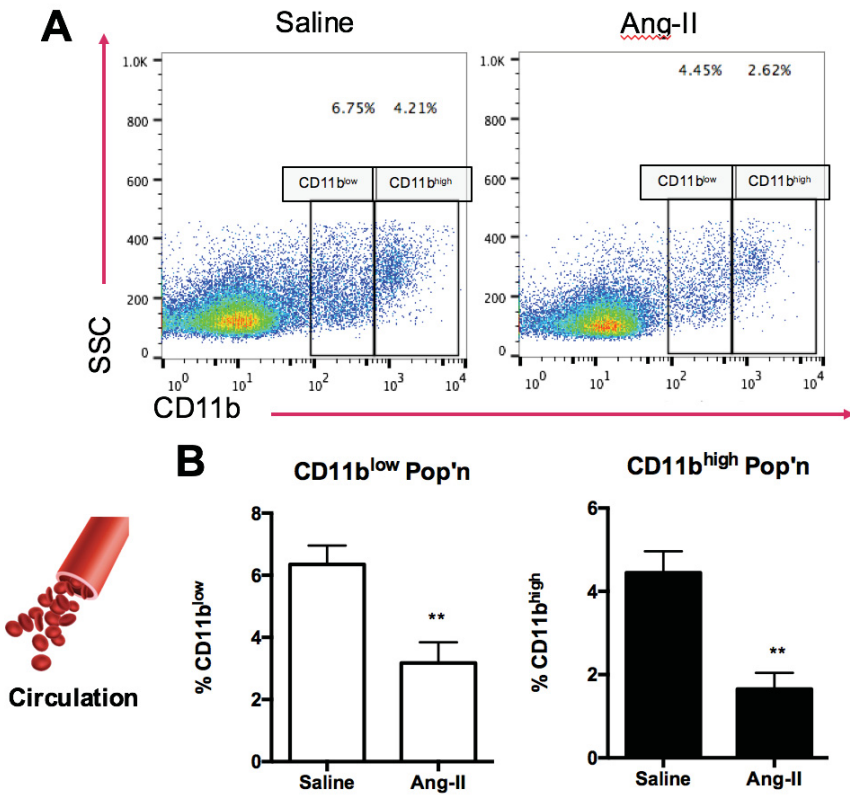

Figure 3.17. Blood CD11b^{+} monocytes displayed CD11b^{low} and CD11b^{high} subpopulations in lower proportions after Ang-II infusion. (A) Representative images of flow cytometry dot plots of monocytes in circulation as defined by CD11b^{low}SSC^{low} or CD11b^{high}SSC^{low} expression in saline control (left) and Ang-II (right) animals (boxed). **(B)** Quantification of CD11b^{low} (left) and CD11b^{high} (high) populations in saline and Ang-II hearts as represented by the percentage of isolated mononuclear cells. Data are expressed as means ± SEM. n=4-5. **p<0.01. Ang-II, Angiotensin-II; Pop'n, population; SSC, side scatter.

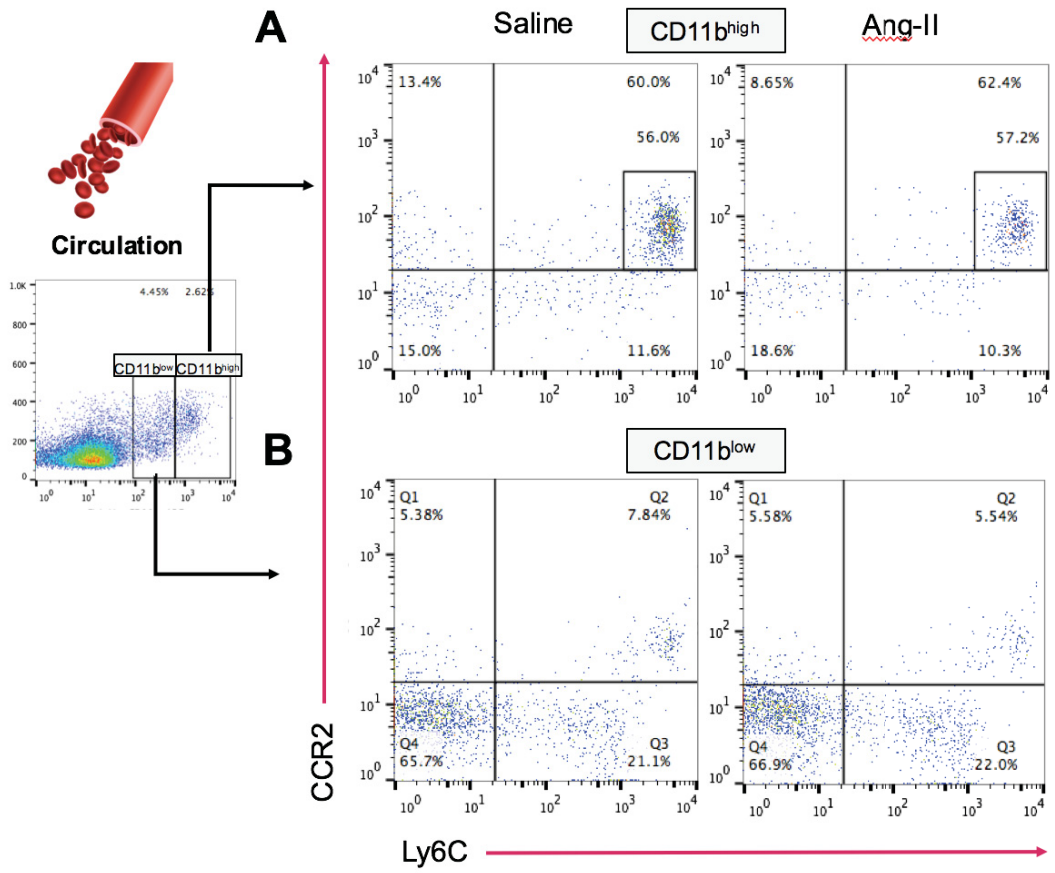

Figure 3.18. Circulatory CD11b^{high} monocytes were mainly pro-inflammatory Ly6C^{high}CCR2^{+} and present in similar proportions after Ang-II exposure. (A) Representative images of flow cytometry dot plots of CD11b^{high}SSC^{low} monocytes in circulation as defined by Ly6C^{high}CCR2^{+} expression in saline control (left) and Ang-II (right) animals (boxed). **(B)** Representative images of flow cytometry dot plots of CD11b^{low}SSC^{low} monocytes in circulation as defined by Ly6C^{high}CCR2^{+} expression in saline control (left) and Ang-II (right) animals. Ang-II, Angiotensin-II; CCR2, C-C Chemokine receptor 2; Ly6C, lymphocyte antigen 6C.

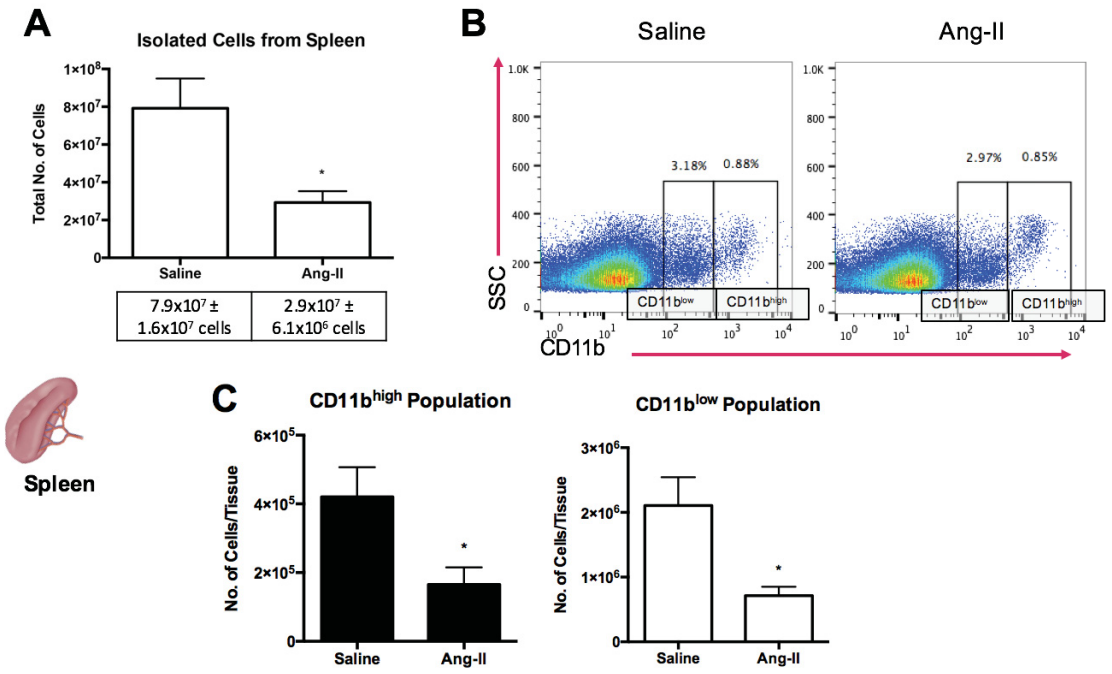

Figure 3.19. Splenic CD11b^{+} monocytes displayed CD11b^{high} and CD11b^{low} phenotypes and were present in lower numbers after Ang-II infusion. (A) Graphical representation of the total number of isolated mononuclear cells from the spleen of saline and Ang-II animals. **(B)** Representative images of flow cytometry dot plots of the monocyte population in the spleen as defined by CD11b^{high}SSC^{low} and CD11b^{low}SSC^{low} expression in saline control (left) and Ang-II (right) animals (boxed). **(C)** Graphical representation of CD11b^{high}SSC^{low} population (left) and CD11b^{low}SSC^{low} population (right) expressed as absolute number of cells normalized per spleen. Data are expressed as means ± SEM. n=4-5. *p≤0.05. Ang-II, Angiotensin-II; No., number; SSC, side scatter.

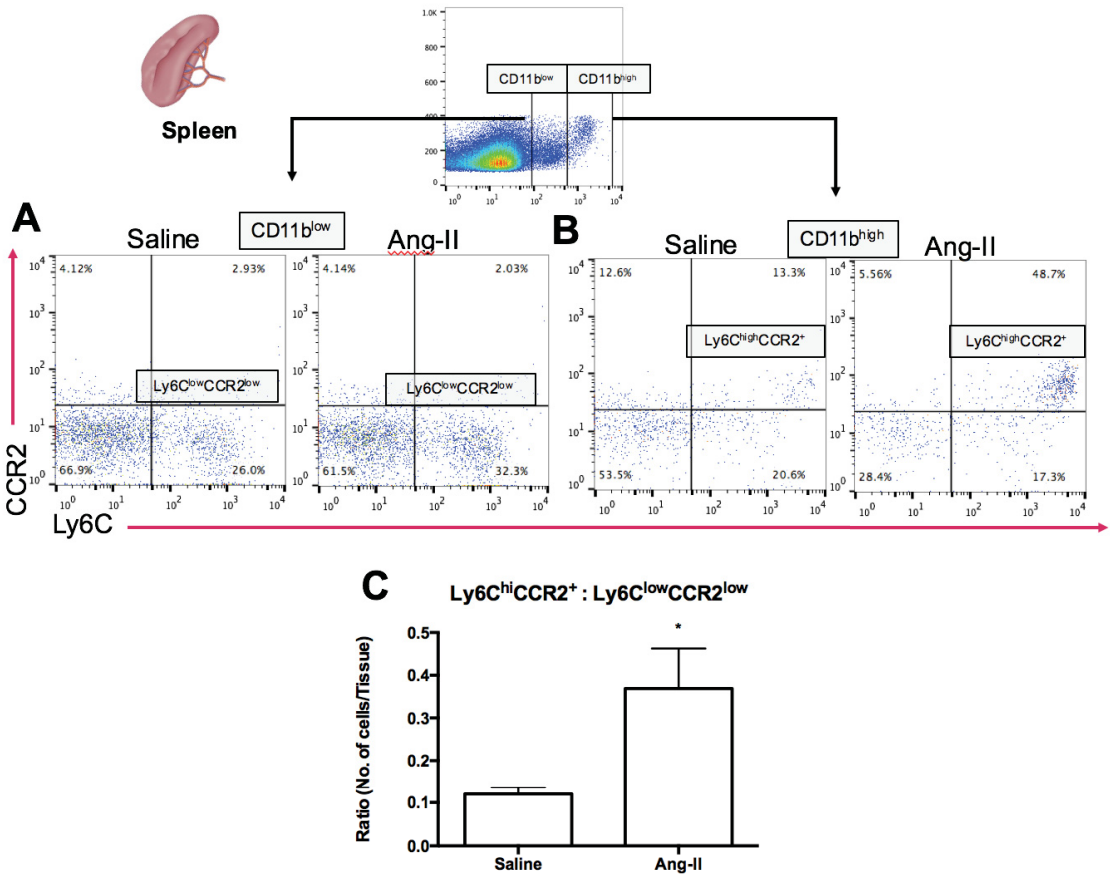

Figure 3.20. Ang-II infusion led to significant shift towards pro-inflammatory Ly6C^{high}CCR2^{+} splenic CD11b^{high} monocytes. (A) Representative images of flow cytometry dot plots of the CD11b^{low}SSC^{low} monocyte population in the spleen as defined by Ly6C^{low}CCR2^{low} expression in saline control (left) and Ang-II (right) animals. **(B)** Representative images of flow cytometry dot plots of the CD11b^{high}SSC^{low} monocyte population in the spleen as defined by Ly6C^{high}CCR2^{+} expression in saline control (left) and Ang-II (right) animals. **(C)** Graphical representation of CD11b^{high}Ly6C^{high}CCR2^{+} monocyte population relative to the CD11b^{low}Ly6C^{low}CCR2^{low} monocyte population as expressed by the ratio of absolute number of cells per spleen in saline and Ang-II mice. Data are expressed as means ± SEM. n=4-5. *p≤0.05. Ang-II, Angiotensin-II; CCR2, C-C Chemokine receptor 2; Ly6C, lymphocyte antigen 6C; No., number; SSC, side scatter.

CHAPTER 4 – DISCUSSION

4.1 Summary of Findings in the Context of the Literature

In many models of injury, a temporal relationship exists between early inflammatory responses and subsequent healing and remodeling phases. This highlights the necessity of understanding the important cellular players involved and their interactions within the environment to prevent removal of what is thought to be harmful, but in actuality may be crucial for healthy healing. Previous works by our group have demonstrated the important time-dependent course of an early inflammatory response that occurs immediately after Ang-II exposure, which precedes the increase in collagen deposition seen at 3 days – a hallmark of myocardial fibrosis[49,80,85]. This bi-phasic response has been well-established in many ischemic models of myocardial injury, such as a MI[41,176,177] . In contrast, the bi-phasic response in models of non-ischemic heart disease, such as hypertension, has not been as clearly defined. The Ang-II infusion model offers the unique opportunity to study the relationship between early molecular and cellular changes within the myocardium without confounding effects, such as tissue necrosis that are seen in models of ischemia.

In this thesis, the attention was turned towards the first 24 hours of Ang-II infusion in order to further understand the early cellular and molecular changes within the myocardium preceding cellular accumulation. Additionally, the bi-phasic response after an injury can also be attributed to the bi-phasic monocyte response demonstrated in models of MI whereby an initial inflammatory repertoire of Ly6C^{high} monocytes dominate the myocardium during the inflammatory phase followed by the recruitment of the latter reparative repertoire of Ly6C^{low} monocytes into the healing myocardium[41,177].

Thus, the latter piece of this thesis focused on changes after 3 days of Ang-II infusion, of which our previous works have characterized as the time-point in which cellular infiltration and significant collagen deposition seem to overlap[49,80,106].

4.1.1 Early Cellular and Molecular Changes in the Ang-II-Exposed Myocardium

One of the more intriguing observations noted in one of our previous works by Rosin *et al.* was the substantial upregulation of CTGF transcript immediately after Ang-II infusion *in vivo* (6 hours)[85]. This was not just a three- to four-fold change, but a substantial twenty-fold upregulation compared to saline controls. Thus, the first part of this thesis replicated this experiment in which we were able to identify a similar substantial upregulation of CTGF transcript levels after 6 hours of Ang-II exposure, as well as significant upregulation of TGF-β transcript levels. These molecular changes occurred prior to inflammatory changes in the myocardium after Ang-II exposure, indicated by accumulation of cellular infiltrate seen at 24 hours. Thus, it can be that resident cells within the myocardium are activated after Ang-II exposure either directly via AT1R, or indirectly via other signaling pathways, such as the TGF-β signaling pathway[73,74,121,122,168,178,179].

Our results have demonstrated that Ang-II infusion led to an increase in myocardial pSmad2 levels, particularly at the carboxy-termini serines 465 and 467, relative to total Smad2/3 protein levels. This is suggestive of an increase in TGF-β signaling after 6 hours of Ang-II infusion. TGF-β is a pleiotropic cytokine that has been well understood to play a central role in various fibrotic conditions[109,110,119,180,181]. As mentioned earlier, TGF-β is abundantly "stored" in the ECM in its inactive latent form

and requires proteolytic cleavage for bioactivity[109,116]. Once cleaved, active TGF-β binds to TβRII, heterodimerizes with TβRI, and in a cascade of signaling events involving Smad family protein phosphorylation, elicits downstream gene transcription, such as CTGF[163,182-185]. In the context of hypertensive-induced myocardial fibrosis, TGF-β transcript was previously shown to be upregulated 1 day after Ang-II infusion[49,85,106], while we have demonstrated TGF-β transcript to be upregulated as early as 6 hours after Ang-II infusion.

CTGF, a matricellular protein of the CCN family, has also been suggested as a key mediator of fibrosis development and its expression is generally believed to be directly downstream of TGF-β activity[163,167,185]. Given that our results have shown an early substantial elevation of CTGF transcript levels that occurred simultaneously as the 2.5-fold increase in TGF-β transcript levels, it is unlikely that this early induction of CTGF is the result of newly synthesized TGF-β given this short time course. Our findings in combination with previous work therefore suggest that this early induction of CTGF expression may be a result of latent TGF-β activation and signaling already present in the myocardial ECM[116,117,153]. Essentially, as Annes *et al.* considered, the latent TGF-β complex can be viewed as an extracellular sensor to signals by which the TGF-β peptide acts as a detector, the LTBP acts as the localizer, and the active TGF-β acting as the effector[116].

4.1.2 Mechanistic Link Between Early CTGF Upregulation and TGF-β Activation in the Ang-II Infused Myocardium

Given that Ang-II infusion led to a substantial increase in CTGF transcript levels at 6 hours and was associated with increased pSmad2 levels, this led to the hypothesis that this was a result of the activation of preformed latent TGF-β in the myocardium. These observations are associations that could have been occurring coincidentally, and thus we sought to address this hypothesis by blocking active TGF-β from downstream signaling. Zwaagstra *et al.* designed soluble single-chain bivalent TGF-β type II receptor traps with the capability of sequestering active TGF-β in the ECM[155]. In their studies, they assessed the efficacy of their TGF-β trap in tumour models. They demonstrated that administration of the TGF-β trap into established 4T1 mammary tumours *in vivo* resulted in significantly reduced tumour growth compared to the pan anti-TGF-β neutralizing antibody (1D11) likely due to TGF-β neutralization in the tumour environment[155].

In our *in vitro* NIH/3T3 fibroblast monoculture system, we were also able to show a trending reduction of exogenous TGF-β-induced upregulation of CTGF and TGF-β transcript levels using the TGF-β trap, as well as a reduction in the TGF-β induced upregulation of collagen type I transcript levels. Although not to the extent as the 1D11 antibody, these results demonstrate that upregulation of pro-fibrotic CTGF, TGF-β, and type I collagen in fibroblasts is induced by TGF-β activity. These results are expected as it is well known TGF-β activity and signaling is upstream of CTGF and collagen type I synthesis as well as plays a role in TGF-β autoinduction[117,165,167,186-190]. Thus, in our *in vivo* model of myocardial fibrosis, we were able to alter the effects of TGF-β by demonstrating a significant reduction in CTGF transcript levels after 6 hours of Ang-II

exposure with the addition of the TGF-β trap compared to PBS controls. Supporting these results, we demonstrated that pSmad2 levels were also reduced relative to total Smad2/3 levels after 6 hours of Ang-II exposure, suggestive of the participation of the TGF-β/Smad-dependent pathway in the early induction of CTGF expression.

Although the precise mechanism to which latent TGF-β is activated is unclear, signals that perturb the ECM under stress, such as proteases, matricellular proteins, integrins, oxidative stress, and/or mechanical stress, can induce proteolytic cleavage of latent TGF-β[43,116,117,165,191,192]. In this hypertensive model of myocardial fibrosis, it is possible that Ang-II-AT1R signaling acts on resident cardiac cells and induces production of ROS[58,60]. In a recent study, Pinto *et al.* revisited the cellular composition of the mouse and human heart[88]. By using genetic tracing experiments and refined flow cytometry techniques, Pinto and colleagues identified endothelial cells as the most abundant non-cardiomyocyte cell population (>60%), whilst the composition of cardiac fibroblasts were lower than previously thought (<20%)[88].

Endothelial cells and cardiomyocytes have been proposed to be potential sources of CTGF production as a result of TGF-β activation in addition to cardiac fibroblasts, as demonstrated previously by our laboratory[85]. Rosin *et al.* demonstrated an upregulation of CTGF mRNA levels in the microvascular endothelial cell line b.End3 and in isolated cardiomyocytes of neonates, which was abolished with the addition of a pan-TGF-β neutralizing antibody[85]. Our findings in this study confirmed that the early molecular changes in CTGF and TGF-β transcript levels are seen prior to cell infiltration in the myocardium. In addition, our findings here demonstrate that TGF-β is in part responsible for the induction of CTGF prior to significant cell infiltration. Endothelial cells express

both TβRII and TβRI and can transmit the TGF-β signal to the nucleus through phosphorylation of Smad2/3[169,193]. Additionally, the adult murine heart also contains latent TGF-β localized to cardiomyocytes and *in vitro* TGF-β stimulation of cardiomyocytes resulted in increased CTGF production[153,194]. Thus, it is likely possible that the initial activation of latent TGF-β and signaling initially acts on resident cardiac cells to produce the initial surge of CTGF transcript induction.

Ang-II signaling via AT1R is well-received to upregulate TGF-β production in cardiac tissue, such as in cardiomyocytes and cardiac fibroblasts[68,73,107,195]. Thus, the upregulation of TGF-β transcript levels in Ang-II hearts at 6 hours is likely a result of Ang-II signaling via AT1R as our results demonstrated that TGF-β transcript levels were not affected in Ang-II animals that received the TGF-β trap. The administration of the TGF-β trap appears to trend towards an increase in TGF-β transcript levels in Ang-II hearts. Our *in vivo* results were in contrast with our *in vitro* fibroblast monocultures, in which we were able to demonstrate a trending reduction of exogenous TGF-β autoinduction with the addition of the TGF-β trap or 1D11 antibody. One explanation could be the involvement of other autocrine and/or paracrine interactions in the myocardial environment, where the interactions between the ECM and other resident cell types present in the myocardium may be influenced[20,22]. In this dynamic myocardial environment, one may hypothesize that TGF-β neutralization in a pathological setting may promote a compensatory upregulation of TGF-β to counteract the inflammatory effects after Ang-II infusion.

In contrast to our findings seen at 6 hours after Ang-II exposure, the administration of the TGF-β trap did not affect CTGF transcript levels after 24 hours of

Ang-II infusion. A possible explanation may be that CTGF in the ECM is inducing an autoregulatory mechanism by which CTGF is regulating its own production[85,133,196]. Alternatively, Ang-II can elicit direct effects on resident cardiac cells via AT1R through a number of signaling pathways. Iwanciw *et al.* demonstrated that Ang-II-AT1R signaling induced CTGF mRNA and protein production in a human fibroblast cell line through the mitogen-activated protein kinase (MAPK)-signaling pathway[168]. RhoA/Rho kinase, p38 MAPK/Jun amino-terminal kinase (JNK) signaling, and calcineurin-dependent pathways have also been shown to induce CTGF production directly upon Ang-II stimulation[74,75]. Additionally, He *et al.* demonstrated that CTGF expression in cardiomyocytes can be regulated by Ang-II activation of the protein kinase C (PKC) pathway in an isoform-selective manner[197]. Therefore, rather than through direct TGF-β signaling, other mechanisms during the inflammatory myocardial environment may be activated that results in redundant signaling pathways.

4.1.3 Gross and Cellular Histological Changes in the Ang-II-Exposed Myocardium at 24 Hours

Fibroblast differentiation into myofibroblasts, the effector cells of the fibrotic response in various fibrotic conditions, has also been well accepted as a downstream effect of TGF-β activation either directly or synergistically with CTGF[33,39,198-200]. Traditionally, myofibroblasts were believed to be solely differentiated from resident fibroblasts, but emerging evidence has shown that fibroblasts can originate from other cellular sources, such as bone marrow derived progenitor cells or endothelial cells that underwent EMT[62,123,201]. While we did not identify the source of fibroblasts and/or

myofibroblasts in this thesis, fibroblast differentiation into myofibroblasts was not evident after 24 hours of Ang-II exposure, suggesting that myofibroblasts are not key in the early inflammatory stages of myocardial fibrosis.

In fact, cardiac fibroblasts have garnered increasing interest in respect to their participation as inflammatory cells in the pathogenesis of cardiac injury and subsequent fibrosis development[83,202]. By acting as sentinel cells, cardiac fibroblasts have the capacity to respond to stimuli under sterile inflammation, such as damage associated molecular patterns (DAMPs) or mechanical stress, and produce a repertoire of chemokines and cytokines involved in the inflammatory response[83,92,203,204]. However, these studies have addressed cardiac fibroblasts with inflammatory potential *in vitro* but their contribution in the inflammatory phase *in vivo* remains uncertain as one cannot disregard the pro-inflammatory role of other myocardial cells present as well as the difficulty in identifying cardiac fibroblasts due to limited specific markers available[95,202].

In the context of this study, Duerrschmid *et al.* demonstrated that Ang-II infusion resulted in the immediate upregulation of pro-inflammatory cytokines, such as TNF-α, IL-6, IL-1β, and MCP-1[66]. This inflammatory environment could potentially influence cardiac fibroblasts to support the inflammatory response and delaying the differentiation into myofibroblasts during the initial inflammatory phase. Additionally, Duerrschmid *et al.* demonstrated that Ang-II infusion led to delayed upregulation of anti-inflammatory and pro-fibrotic factors such as IL-4, IL-13, and TGF-β, which was seen at 7 days[66]. In previous work by our laboratory, upregulation of TGF-β transcript levels was seen to further increase from 6 hours to a peak at 3 days of Ang-II infusion[85]. Furthermore, CTGF protein expression was upregulated after 3 days of Ang-II infusion[85]. Thus, this

later increase in anti-inflammatory and pro-fibrotic factors in the myocardial environment could influence the fibroblast differentiation into α-SMA$^+$ myofibroblasts for tissue remodeling beyond 3 days of Ang-II infusion[25,39,205].

Although there was no evidence of α-SMA$^+$ myofibroblasts at 24 hours after Ang-II exposure, we have demonstrated an increase in proliferative cells at this time-point. Previous work in our laboratory using chimeric mice constitutively expressing GFP have shown a large population of accumulated infiltrating cells in the myocardium after 3 days of Ang-II exposure, largely comprised of bone marrow derived progenitor cells[85]. In the present study, we have also identified a large portion of mononuclear cells undergoing proliferation as early as 24 hours after Ang-II exposure that contributes to the increase in cell accumulation, but does not differentiate between resident or infiltrating cells or suggest the identity of the proliferative cells. Administering the TGF-β trap did not affect cell proliferation, likely suggesting that these effects are a result of direct Ang-II activation mitigating mitogenic properties on bone marrow derived progenitor cells or resident fibroblasts. Whether Ang-II is directly inducing fibroblast proliferation via the MAPK signaling cascade or indirectly by stimulating growth factors associated with fibroblast proliferation such as platelet-derived growth factor (PDGF), has yet to be fully elucidated as applications *in vivo* have been deemed as challenging due to the complexity of intervening and compensatory mechanisms[25,67,108].

Cardiac fibroblasts are important in the context of cardiac remodeling. They are the source and target of multiple stimuli and participate in the crosstalk with other immune cells and cardiomyocytes to coordinate chemical, mechanical, and electrical signals[77,206,207]. Cardiac fibroblasts can respond to IL-6, where they undergo a feed-

forward mechanism that leads to increased fibroblast proliferation[171,208]. Resident cardiac fibroblast proliferation has been suggested to be one of the main sources of myofibroblasts in the process of cardiac remodeling[205,209]. However, due to the difficulty in accurately identifying cardiac fibroblasts, the origin of myofibroblasts in the myocardium remains controversial[205]. Bone marrow derived progenitor cells have also been suggested to contribute to the fibroblast population in the myocardium after injury[62,171,210,211]. Haudek *et al.* identified spindle-shaped bone marrow derived $CD34^{+}/CD45^{+}$ precursor cells that expressed collagen type I and cardiac fibroblast marker discoidin domain-container receptor 2 (DDR2) in the Ang-II exposed hearts[62].

To further expand on the multifunctional properties of TGF-β, this pleiotropic cytokine plays a chemotactic/migratory role on monocytes to sites of injury in a concentration-dependent manner[124,212-214]. The chemotactic properties of TGF-β also appears to be context dependent, as migration of cardiac fibroblasts were not affected directly in the presence of TGF-β1 *in vitro*[122,206,215]. In our study, TGF-β trap administration did not affect cell accumulation at 24 hours despite the reduction in CTGF production observed at 6 hours, suggesting that TGF-β signaling is unlikely responsible for the migration of mononuclear cells in the context of Ang-II exposure. Thus, it is likely that in the Ang-II infusion model, other signaling mechanisms, such as the CCL2-CCR2 axis[62,66], redundancy in chemokine signaling, possibility of the CX_3CR1-dependent recruitment[80], and/or Ang-II-induced increase in vascular permeability[45,56], contribute to the accumulation of mononuclear cellular infiltrate in the myocardium.

4.1.4 Role of CTGF on Fibroblast Activity and Phenotype in vitro

CTGF has been implicated as an important fibrogenic mediator of various fibrotic conditions, such as in the lung, skin, liver, heart, and systemic tissue fibrosis[166,216,217]. Despite its association in many fibrotic conditions, the exact role of CTGF has not been fully elucidated as CTGF has no known receptor[133]. In fact, CTGF behaves like matricellular proteins by serving as adaptor proteins in the ECM and modulating cell signaling, such as its cooperation with TGF-β in promoting fibrosis[133,136,218]. In the myocardium, CTGF is not normally expressed unless induced under pathological conditions, thus implicating an important role in myocardial fibrosis[143,185,219]. A number of studies attempted to unravel the extent of which CTGF participates in mediating fibrosis in the myocardium. However, *in vitro* and *in vivo* studies have generated contradicting results in the context of cardiac remodeling[140,141,144,174].

Our *in vitro* NIH/3T3 fibroblast monoculture experiments aimed to understand the fundamental role of CTGF on fibroblasts. Upon exogenous CTGF treatment, there was no effect on pro-fibrotic gene expression as well as no discernible effect on fibroblast differentiation into α-SMA^{+} myofibroblasts. Additionally, exogenous CTGF did not provide an additive effect on TGF-β-induced fibroblast changes. This is in contrast with previous studies that have demonstrated the importance of CTGF in the progression of excessive fibrosis that leads towards diastolic heart failure[75,137,166,174,194,219]. Despite this, recent evidence has also demonstrated the negligible role of CTGF in progression of myocardial fibrosis. Accornero *et al.* generated transgenic mice with heart-specific gain or loss of CTGF to explore the role of CTGF in myocardial fibrosis[143]. Induction of pathological cardiac remodeling in models of aging, pressure overload via transverse

aortic constriction (TAC), or heart-specific TGF-β overexpression was not affected with heart-specific gain or loss of CTGF, suggesting that CTGF is unlikely playing an important role in myocardial remodeling and fibrosis[143]. Additionally, Fontes *et al.* generated conditional CTGF knockout mice that underwent TAC but was unable to prevent myocardial fibrosis and hypertrophy[144]. Implications of a cardio-protective role of CTGF has also been suggested by Gravning and colleagues, whereby transgenic mice with cardiac-restricted CTGF overexpression resulted in similar fibrosis after MI or chronic pressure-overload via abdominal aortic banding[140,173]. Moreover, other members of the CCN family of proteins may play compensatory and/or redundant roles[136,220,221]. Thus, with recent evidence suggesting minimal importance of CTGF in progression of myocardial fibrosis, the role of CTGF needs to be reconsidered.

4.1.5 Characterizing Monocyte/Mϕ Composition and Subsets in Ang-II Exposed Mice

As shown in our results after 24 hours of Ang-II exposure, mononuclear cell infiltrate in the myocardium and are likely interacting with resident cardiac cells and other infiltrating cells in a concerted effort to repair the stressed or injured myocardium. At 3 days after Ang-II exposure, previous work from our laboratory identified these mononuclear infiltrates as monocytes/Mϕs associated with progression of myocardial fibrosis[80]. At this time-point, there appears to be an overlap between collagen deposition, indicative of fibrosis, and the inflammatory response as shown in previous works from our laboratory[49,80,106]. In this study, 3 days of Ang-II infusion led to an increase in $CX_3CR1^+CCR2^+$ Mϕs in the myocardium with a pro-inflammatory shift towards increased expression of $CD11b^{high}Ly6C^{high}$. Monocytes/Mϕs play a role in essentially all

aspects of the healing response and can be described as biphasic during ischemic cardiac injury, whereby classical monocyte recruitment occurs during the inflammatory phase, followed by a shift towards non-classical monocyte accumulation to mediate the healing response[41,177,222]. In a non-ischemic model of myocardial fibrosis, Duerrschmid *et al.* demonstrated that continuous Ang-II infusion led to an initial accumulation of pro-inflammatory $CD86^{+}CD45^{+}$ M1 cells after 1 day, followed by a shift in the cardiac environment towards an accumulation of $CD301^{+}$ $CD206^{+}$ M2 cells by 1 week[66]. Thus, in the context of our study, our findings support the initial accumulation of pro-inflammatory $Ly6C^{high}$ monocytes/Mϕs in the myocardium.

The understanding of the contribution of monocyte/Mϕ accumulation in the myocardium is becoming increasingly complex with the emergence of resident cardiac Mϕs, as well as bone-marrow derived monocytes and monocyte deployment from the splenic reservoir[42,61,62,102,177,223]. Swirski *et al.* demonstrated an increase in blood monocytes and a reduction in total splenic monocytes 1 day post-MI, suggesting the large contribution of splenic monocyte deployment, with the Ang-II-AT1R signaling axis promoting this monocyte emigration[61]. In contrast, our results demonstrated a reduction in the proportion of $CD11b^{high}$ and $CD11b^{low}$ monocytes after Ang-II exposure with no effect on monocyte phenotypic changes. These differences could be attributed to our results representing the circulatory monocyte population at 3 days, at which point a large proportion of leukocytes in the blood could mainly consist of lymphocytes[42,224]. Furthermore, increase in peripheral $Ly6C^{high}$ monocytes could be a transient effect that occurred prior to 3 days[225]. Finally, the total number of mononuclear cells were reduced in the spleen after Ang-II exposure, which resulted in a reduction of $CD11b^{high}$ and

$CD11b^{low}$ monocytes. The increase in proportion of $Ly6C^{high}CCR2^{+}$ $CD11b^{high}$ monocytes indicates a pro-inflammatory shift in the Ang-II spleen and suggests the deployment of pro-inflammatory splenic monocytes in the presence of continuous Ang-II infusion.

4.2 Limitations

In an effort to further understand the cellular and molecular changes associated with hypertensive-induced myocardial fibrosis, the Ang-II infusion model represents one of the many available hypertensive models[160]. However, this animal model, like all animal models, is not without its limitations. Hypertension is a chronic disease that usually develops over a long period of time and encompasses a heterogenous etiology, thus increasing the complexity of this disease[160,226]. In contrast to the human disease, our Ang-II infusion model involves the use of young mice and conditions that result in the sudden systemic elevation of Ang-II levels. Although our mouse model results in the sustained elevation of blood pressure, this model disregards other potential confounding factors that occurs in the human disease state, such as age and genetic dispositions that may affect sodium dependency and renin status[8,160]. Additionally, it is uncertain whether the sympathetic nervous system plays a role in the Ang-II infusion model of hypertension[227].

Nevertheless, elevated Ang-II plasma concentrations are commonly associated in hypertensive and chronic kidney disease patients[228-230]. Comparison of the plasma Ang-II concentrations in mice after Ang-II infusion to plasma Ang-II concentrations in patients have been difficult due to high sequence homology between different components of the

RAAS[231]. In literature, the concentrations of plasma Ang-II in healthy patients fall within a large range, which may be due to different methodological approaches used[231-233]. Furthermore, due to many genetic dispositions and heterogeneity in etiology between individuals, the concentration of plasma Ang-II in healthy subjects and patients may range. Interestingly, unilateral renal artery stenosis is often accompanied by immediate elevation in blood pressure and consequent elevation in plasma Angiotensin II concentrations[234-236]. Renal artery stenosis has also been shown to be commonly associated in patients with chronic heart failure[237]. However, whether renal artery stenosis is involved in the progression of heart failure is still uncertain[237]. Despite this, many processes in the Ang-II signaling pathway may be similar in rodents and humans so that application from rodent experimentation to the clinical setting may be implicated with regards to understanding underlying mechanisms of hypertension, myocardial inflammation, and fibrosis.

A major limitation in our *in vitro* and *in vivo* studies using the TGF-β trap is the dosage for our *in vitro* experiments and the consideration of the TGF-β trap half-life for our *in vivo* experiments. Our *in vitro* results did not exhibit effects to the same extent as the 1D11 antibody and thus, dose-response experiments is ideal to determine the efficacy of the TGF-β trap on NIH/3T3 fibroblasts. Additionally, Zwaagstra *et al.* used the TGF-β trap to determine its efficacy in tumours, a state that is very different from our studies[155]. The TGF-β trap has a very short half-life (<1 hour) and its effect may not be maintained *in vivo* for extended periods of time, such as for our 24-hour time-point. This may be beneficial in the sense of short-term neutralization of TGF-β, as the events that occur during myocardial inflammation and fibrosis are very context and time-dependent[117,238].

As such, there exists the possibility that elimination of the TGF-β trap from the system may have occurred, which may explain the insignificant observations at 24 hours and must not be disregarded when interpreting our observations. The dosage and delivery method that we used in our experiments were based off their tumour studies and thus, the optimal dosage and delivery method should be altered in our myocardial fibrosis model.

In addition, the TGF-β trap was designed based on the human TGF-β type II receptors[155], whereas the pan TGF-β neutralizing antibody is a recombinant mouse monoclonal antibody. In this thesis, we have used both the TGF-β trap and pan TGF-β neutralizing antibody in our murine studies and *in vitro* murine fibroblasts. Thus, another limitation of this study is the use of a human-based TGF-β trap as opposed to a murine-based peptide, which may affect the interpretation of our observed results. In particular, it is necessary to consider that the differences in efficacy seen in our *in vitro* results may be due to the differences in species specificity. Potentially, the lower degree of sequence homology between human and murine TGF-β type II receptors may affect the specificity of TGF-β binding to its receptors in our experimentation.

Although the main objective of this thesis was to understand the mechanistic link between TGF-β and CTGF in the early myocardial environment, changes in the transcript levels of these early pro-fibrotic mediators does not necessarily dictate protein changes in the myocardium. This experimental technique is also extremely sensitive and is highly prone to error. Thus, further experimentation looking at protein changes temporally may provide greater insight into the mechanistic link between TGF-β signaling and CTGF protein production. Furthermore, we only assessed changes in collagen type I transcript levels, and although collagen type I comprises the majority of the collagen present in the

myocardium, we cannot disregard other types of collagen also found in the myocardium, such as collagen type III[23,151].

Our assessment of the role of CTGF *in vitro* is at a fundamental level but the use of NIH/3T3 fibroblasts does not necessarily translate to cardiac fibroblasts due to their highly adaptive nature[239]. Thus, at best, our observations can only be interpreted at a general level and further experimentation on cardiac fibroblasts is warranted. Moreover, our cell starvation protocol did not completely remove all serum and instead, included 1% FBS. Thus, when interpreting these results, careful consideration into the influence of FBS must not be disregarded as components of the serum may also affect fibroblast induction and phenotype.

Finally, our *in vivo* experiments in characterizing monocyte/Mϕ composition and subsets only uses four cell surface markers and thus, cannot disregard the possibility of other cell types that may have been included using this method. Furthermore, our observations seen in the blood did not take into consideration absolute numbers and was not normalized to a certain volume of blood taken at the time of harvest. Lastly, our method for the digestion of the heart tissue involves rigorous conditions whereby mechanical and enzymatic digestion is required to isolate mononuclear cells within the myocardium, which may have affected the monocyte/Mϕ phenotypes.

4.3 Future Directions

The overarching objective of this thesis was to further understand the close relationship between TGF-β and CTGF in the early Ang-II exposed myocardial environment. A step further was taken at understanding the monocyte/Mϕ changes that

occur after Ang-II exposure by exploring the cardiosplenic axis. With this, there are many directions of which future studies can take to fill in the knowledge gap that currently exists in the understanding of the underlying mechanisms of myocardial fibrosis. In the next few paragraphs, some future directions will be outlined.

As mentioned in the *Limitations*, administration of the TGF-β trap *in vivo* did not elicit the same response at 24 hours as it did at the 6-hour time-point and may be due to the possibility of the elimination of the TGF-β trap. Thus, further experimentation can be conducted in order to determine the optimal dosage and delivery method in this disease model. As such, longer time-points can be explored using the TGF-β trap as a therapeutic tool to limit detrimental remodeling in addition to a molecular tool. Multiple studies have attempted to block TGF-β activity in an effort to abrogate fibrosis development but have yielded both beneficial and detrimental effects[127,129,130]. Thus, the potential of short-term neutralization utilizing the TGF-β trap may result in beneficial effects. Additionally, by understanding the molecular events involved in the process of myocardial inflammation and fibrosis, time-specific administration of the TGF-β trap could perhaps prevent the inhibition of beneficial anti-inflammatory effects required after an inflammatory response, as well as limit the detrimental effects of over-induction of tissue remodeling.

Our *in vitro* experiments demonstrated minimal importance of the role of CTGF on fibroblast induction and activity. In literature, many studies have put into question as to whether CTGF is important in the progression of fibrosis[138,140,141,143,144,173,174]. Our methodology involving the starvation of fibroblasts prior to treatment included the presence of FBS in the serum could have affected our observations. Further small-scale studies could be conducted in order to eliminate the possibility of serum affecting our

results. In addition, CTGF has been demonstrated to regulate fibroblast proliferation through one of its binding domains[133,240]. Due to some technical issues, we were not able to perform the appropriate proliferative studies, of which future small-scale studies can be performed to assess proliferative capacity in the presence of CTGF. To further extend the role of CTGF on fibroblast function in the context of myocardial fibrosis, murine or human cardiac fibroblasts can be used in future *in vitro* experiments. Additionally, other resident myocardial cells, such as endothelial cells and cardiomyocytes, could be considered in future studies to determine the role of CTGF on these cell types.

Our Ang-II infusion model demonstrated early transcript upregulation of some important fibrogenic mediators and was associated with later phenotypic shifts towards pro-inflammatory Ly6C^{high}CCR2^{+} monocyte/Mϕ accumulation. As mentioned previously, the Ang-II exposed myocardium exhibits immediate upregulation of pro-inflammatory cytokines and chemokines, which later transitions into a pro-fibrotic environment[66,80]. However, these observations are strictly at the transcript level. Additionally, the population of monocytes/Mϕs can originate from multiple sources, such as proliferating cardiac resident Mϕs and/or recruitment of splenic and/or bone-marrow derived monocytes[61,100-102,241]. Recently, Sager *et al.* demonstrated in a chronic heart failure model post-MI that both proliferation of local cardiac Mϕs and monocyte recruitment contribute to the accumulation of Mϕs in the failing myocardium[242]. Additionally, they demonstrated that isolated steady-state cardiac Mϕs, monocyte-derived Mϕs, and locally derived Mϕs from the failing myocardium exhibited distinct expression patterns that deviated from the M1/M2 paradigm[242]. While there are obvious difficulties in mimicking the myocardial environment, future experiments can be designed to assess

the roles of certain factors in the early myocardial environment in the recruitment or proliferation of monocytes/Mϕs through *in vitro* studies.

Interactions between monocytes/Mϕs and resident cardiac cells, such as cardiac fibroblasts, have been demonstrated as key in dampening inflammation and progression towards remodeling[64,126,243]. As such, the interactions between monocytes/Mϕs and cardiac fibroblasts may largely influence the direction to which myocardial inflammation and fibrosis progresses. The *in vitro* fibroblast monoculture experiments explored the role of CTGF on fibroblasts only. Perhaps, the role of CTGF may be important in the presence of Mϕs and may alter Mϕ phenotypes and consequently, alter fibroblast activation and phenotype. Our laboratory has established an *in vitro* coculture system of fibroblasts and Mϕs that can be used to explore the fundamental role of CTGF in the interaction between Mϕs and fibroblasts[80,104]. This can be further extended to interactions between Mϕs and other resident cardiac cells, and in particular with cardiomyocytes and endothelial cells.

4.4 Concluding Remarks

At the end of the day, many questions asked in the laboratory setting is thought of in an applicable clinical context. In this thesis, the early molecular and cellular changes in the Ang-II exposed myocardium was explored in further detail. In the clinical setting, it is often very difficult to identify the onset of a disease, such as hypertension. Rather, the disease is often presented at a time at which the disease has progressed to a late and/or critical stage. In the context of this thesis, perhaps the most critical time is when the myocardium is presented with severe fibrosis that affects the proper function of the heart.

Despite this, understanding the underlying mechanism and cellular changes is still important to manipulate these changes in order to promote a more beneficial outcome.

Throughout this thesis, we have focused on the early mechanistic link between TGF-β signaling and its partial participation in CTGF transcript induction in the early Ang-II exposed myocardium by using a TGF-β trap. Additionally, we began to try to understand the role of CTGF on fibroblast activity and phenotype, of which CTGF appears to play minimal role in regulating fibroblast induction and differentiation into effector α-SMA^{+} myofibroblasts alone or in combination with TGF-β. Finally, we started to understand the different compositions and subsets of monocytes/Mϕs in the context of continuous Ang-II exposure in the spleen, blood, and myocardium in order to open a path for exploring possible roles of certain cytokines and mediators in influencing these phenotypic changes (Figure 4.1). We have focused on certain cell types and mediators that have been suggested to be important in the progression of myocardial inflammation and fibrosis, but in fact, the progression of a disease involves a complex web of multiple cell types, cytokines, chemokines, mediators, and redundant/compensatory signaling pathways that are likely to heavily influence one another.

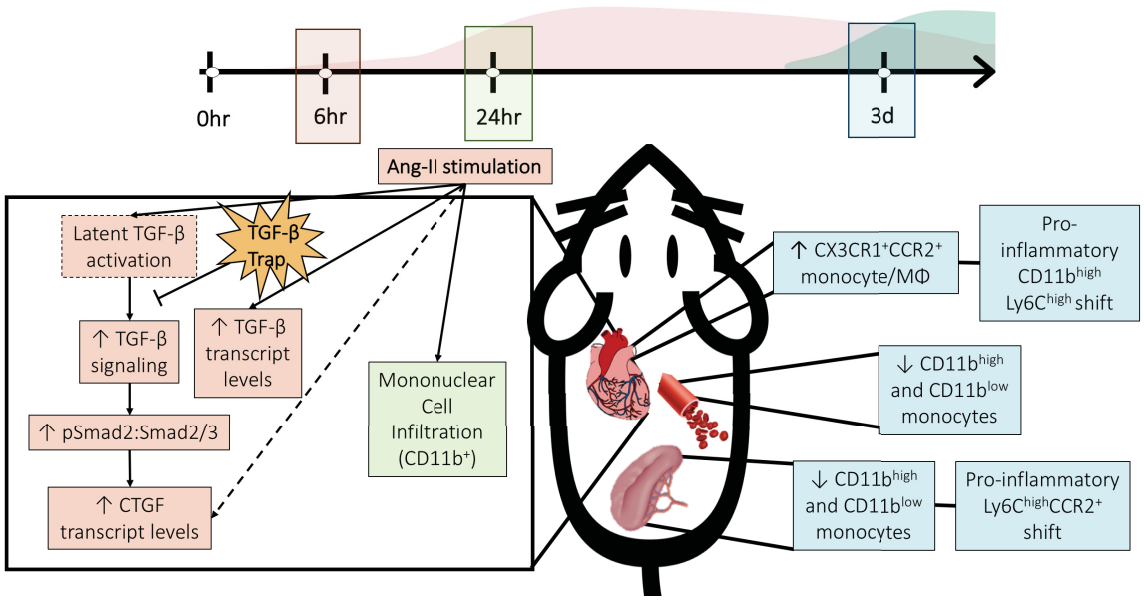

Figure 4.1. Summary of Findings. In this thesis, we demonstrated that Ang-II infusion led to onset of an inflammatory response, characterized by increase in mononuclear cell infiltration into the myocardium at 24 hours. Previous work from our laboratory have shown that myocardial fibrosis ensues at 3 days, which is characterized by an increase in collagen deposition[49,80]. Interestingly, we have shown that upregulation of TGF-β and CTGF transcript levels occur as early as 6 hours after Ang-II infusion, which occurred prior to significant cellular infiltration. We have suggested that latent TGF-β activation and signaling via the canonical Smad-dependent pathway is partially inducing early upregulation of CTGF transcript levels at 6 hours, implicating an important role for resident cardiac cells at this time-point. Finally, by extending our time-point to 3 days, we demonstrated that monocyte/Mϕ accumulate in the myocardium and largely consisted of pro-inflammatory $Ly6C^{high}$ phenotype. This pro-inflammatory phenotypic shift after Ang-II infusion is reflected in the monocyte composition in the spleen, which is represented by an increase in the ratio of $Ly6C^{high}CCR2^{+}$ monocytes to $Ly6C^{low}CCR2^{low/neg}$ monocytes. These results open a path for exploring possible roles of

certain cytokines and mediators, such as CTGF, in influencing phenotypic changes of monocytes/Mϕs and its influence and interactions with resident cardiac cells, such as fibroblasts, endothelial cells, and cardiomyocytes.

REFERENCES

1 Moodie, D. S. The Global Burden of Cardiovascular Disease. *Congenital heart disease* **11**, 213, doi:10.1111/chd.12383 (2016).

2 Gaziano, T., Reddy, K. S., Paccaud, F., Horton, S. & Chaturvedi, V. in *Disease Control Priorities in Developing Countries* (eds D. T. Jamison *et al.*) (2006).

3 Roger, V. L. Epidemiology of heart failure. *Circulation research* **113**, 646-659, doi:10.1161/CIRCRESAHA.113.300268 (2013).

4 O'Meara, E., Thibodeau-Jarry, N., Ducharme, A. & Rouleau, J. L. The epidemic of heart failure: a lucid approach to stemming the rising tide. *The Canadian journal of cardiology* **30**, S442-454, doi:10.1016/j.cjca.2014.09.032 (2014).

5 Ambrosy, A. P. *et al.* The global health and economic burden of hospitalizations for heart failure: lessons learned from hospitalized heart failure registries. *Journal of the American College of Cardiology* **63**, 1123-1133, doi:10.1016/j.jacc.2013.11.053 (2014).

6 Horwich, T. B. & Fonarow, G. C. Glucose, obesity, metabolic syndrome, and diabetes relevance to incidence of heart failure. *Journal of the American College of Cardiology* **55**, 283-293, doi:10.1016/j.jacc.2009.07.029 (2010).

7 Jessup, M. The heart failure paradox: an epidemic of scientific success. Presidential Address at the American Heart Association 2013 Scientific Sessions. *Circulation* **129**, 2717-2722, doi:10.1161/CIR.0000000000000065 (2014).

8 Drazner, M. H. The progression of hypertensive heart disease. *Circulation* **123**, 327-334, doi:10.1161/CIRCULATIONAHA.108.845792 (2011).

9 Iwano, H. & Little, W. C. Heart failure: what does ejection fraction have to do with it? *Journal of cardiology* **62**, 1-3, doi:10.1016/j.jjcc.2013.02.017 (2013).

10 Armstrong, P. W. Left ventricular dysfunction: causes, natural history, and hopes for reversal. *Heart* **84 Suppl 1**, i15-17:discussion i50 (2000).

11 Udelson, J. E. Heart failure with preserved ejection fraction. *Circulation* **124**, e540-543, doi:10.1161/CIRCULATIONAHA.111.071696 (2011).

12 Bhuiyan, T. & Maurer, M. S. Heart Failure with Preserved Ejection Fraction: Persistent Diagnosis, Therapeutic Enigma. *Current cardiovascular risk reports* **5**, 440-449, doi:10.1007/s12170-011-0184-2 (2011).

13 Little, W. C. & Zile, M. R. HFpEF: cardiovascular abnormalities not just comorbidities. *Circulation. Heart failure* **5**, 669-671, doi:10.1161/CIRCHEARTFAILURE.112.972265 (2012).

14 Aziz, F., Tk, L. A., Enweluzo, C., Dutta, S. & Zaeem, M. Diastolic heart failure: a concise review. *Journal of clinical medicine research* **5**, 327-334, doi:10.4021/jocmr1532w (2013).

15 Redfield, M. M. Heart Failure with Preserved Ejection Fraction. *The New England journal of medicine* **375**, 1868-1877, doi:10.1056/NEJMcp1511175 (2016).

16 Frohlich, E. D. & Susic, D. Pressure overload. *Heart failure clinics* **8**, 21-32, doi:10.1016/j.hfc.2011.08.005 (2012).

17 Frey, N., Katus, H. A., Olson, E. N. & Hill, J. A. Hypertrophy of the heart: a new therapeutic target? *Circulation* **109**, 1580-1589, doi:10.1161/01.CIR.0000120390.68287.BB (2004).

18 Diez, J. Mechanisms of cardiac fibrosis in hypertension. *J Clin Hypertens* **9**, 546-550 (2007).

19 Berk, B. C., Fujiwara, K. & Lehoux, S. ECM remodeling in hypertensive heart disease. *The Journal of clinical investigation* **117**, 568-575, doi:10.1172/JCI31044 (2007).

20 Brown, L. Cardiac extracellular matrix: a dynamic entity. *American journal of physiology. Heart and circulatory physiology* **289**, H973-974, doi:10.1152/ajpheart.00443.2005 (2005).

21 Li, A. H., Liu, P. P., Villarreal, F. J. & Garcia, R. A. Dynamic changes in myocardial matrix and relevance to disease: translational perspectives. *Circulation research* **114**, 916-927, doi:10.1161/CIRCRESAHA.114.302819 (2014).

22 Rienks, M., Papageorgiou, A. P., Frangogiannis, N. G. & Heymans, S. Myocardial extracellular matrix: an ever-changing and diverse entity. *Circulation research* **114**, 872-888, doi:10.1161/CIRCRESAHA.114.302533 (2014).

23 Frantz, C., Stewart, K. M. & Weaver, V. M. The extracellular matrix at a glance. *J Cell Sci* **123**, 4195-4200, doi:10.1242/jcs.023820 (2010).

24 de Souza, R. R. Aging of myocardial collagen. *Biogerontology* **3**, 325-335 (2002).

25 Sullivan, K. E. & Black, L. D. The role of cardiac fibroblasts in extracellular matrix-mediated signaling during normal and pathological cardiac development. *Journal of biomechanical engineering* **135**, 71001, doi:10.1115/1.4024349 (2013).

26 Segura, A. M., Frazier, O. H. & Buja, L. M. Fibrosis and heart failure. *Heart failure reviews* **19**, 173-185, doi:10.1007/s10741-012-9365-4 (2014).

27 Hynes, R. O. The extracellular matrix: not just pretty fibrils. *Science* **326**, 1216-1219, doi:10.1126/science.1176009 (2009).

28 Kehat, I. & Molkentin, J. D. Molecular pathways underlying cardiac remodeling during pathophysiological stimulation. *Circulation* **122**, 2727-2735, doi:10.1161/CIRCULATIONAHA.110.942268 (2010).

29 Spinale, F. G., Janicki, J. S. & Zile, M. R. Membrane-associated matrix proteolysis and heart failure. *Circulation research* **112**, 195-208, doi:10.1161/CIRCRESAHA.112.266882 (2013).

30 Moore, L., Fan, D., Basu, R., Kandalam, V. & Kassiri, Z. Tissue inhibitor of metalloproteinases (TIMPs) in heart failure. *Heart failure reviews* **17**, 693-706, doi:10.1007/s10741-011-9266-y (2012).

31 Messerli, F. H. TIMPs, MMPs and cardiovascular disease. *European heart journal* **25**, 1475-1476, doi:10.1016/j.ehj.2004.07.015 (2004).

32 Mott, J. D. & Werb, Z. Regulation of matrix biology by matrix metalloproteinases. *Current opinion in cell biology* **16**, 558-564, doi:10.1016/j.ceb.2004.07.010 (2004).

33 Fan, D., Takawale, A., Lee, J. & Kassiri, Z. Cardiac fibroblasts, fibrosis and extracellular matrix remodeling in heart disease. *Fibrogenesis Tissue Repair* **5**, 15 (2012).

34 Lopez, B. *et al.* Myocardial Collagen Cross-Linking Is Associated With Heart Failure Hospitalization in Patients With Hypertensive Heart Failure. *Journal of the American College of Cardiology* **67**, 251-260, doi:10.1016/j.jacc.2015.10.063 (2016).

35 Moon, J. C., Treibel, T. A. & Schelbert, E. B. Myocardial Fibrosis in Hypertensive Heart Failure: Does Quality Rather Than Quantity Matter? *Journal of the American College of Cardiology* **67**, 261-263, doi:10.1016/j.jacc.2015.10.070 (2016).

36 Kai, H., Kuwahara, F., Tokuda, K. & Imaizumi, T. Diastolic dysfunction in hypertensive hearts: roles of perivascular inflammation and reactive myocardial fibrosis. *Hypertens Res* **28**, 483-490, doi:10.1291/hypres.28.483 (2005).

37 Ali, S. R. *et al.* Existing cardiomyocytes generate cardiomyocytes at a low rate after birth in mice. *Proceedings of the National Academy of Sciences of the United States of America* **111**, 8850-8855, doi:10.1073/pnas.1408233111 (2014).

38 Kikuchi, K. & Poss, K. D. Cardiac regenerative capacity and mechanisms. *Annual review of cell and developmental biology* **28**, 719-741, doi:10.1146/annurev-cellbio-101011-155739 (2012).

39 Weber, K. T., Sun, Y., Bhattacharya, S. K., Ahokas, R. A. & Gerling, I. C. Myofibroblast-mediated mechanisms of pathological remodelling of the heart. *Nature reviews. Cardiology* **10**, 15-26, doi:10.1038/nrcardio.2012.158 (2013).

40 Weber, K. T. & Brilla, C. G. Factors associated with reactive and reparative fibrosis of the myocardium. *Basic research in cardiology* **87 Suppl 1**, 291-301 (1992).

41 Nahrendorf, M., Pittet, M. J. & Swirski, F. K. Monocytes: protagonists of infarct inflammation and repair after myocardial infarction. *Circulation* **121**, 2437-2445, doi:10.1161/CIRCULATIONAHA.109.916346 (2010).

42 Prabhu, S. D. & Frangogiannis, N. G. The Biological Basis for Cardiac Repair After Myocardial Infarction: From Inflammation to Fibrosis. *Circulation research* **119**, 91-112, doi:10.1161/CIRCRESAHA.116.303577 (2016).

43 Talman, V. & Ruskoaho, H. Cardiac fibrosis in myocardial infarction-from repair and remodeling to regeneration. *Cell and tissue research* **365**, 563-581, doi:10.1007/s00441-016-2431-9 (2016).

44 Mehta, P. K. & Griendling, K. K. Angiotensin II cell signaling: physiological and pathological effects in the cardiovascular system. *American journal of physiology. Cell physiology* **292**, C82-97, doi:10.1152/ajpcell.00287.2006 (2007).

45 Benigni, A., Cassis, P. & Remuzzi, G. Angiotensin II revisited: new roles in inflammation, immunology and aging. *EMBO molecular medicine* **2**, 247-257, doi:10.1002/emmm.201000080 (2010).

46 Mansur, S. J., Hage, F. G. & Oparil, S. Have the renin-angiotensin-aldosterone system perturbations in cardiovascular disease been exhausted? *Current cardiology reports* **12**, 450-463, doi:10.1007/s11886-010-0140-7 (2010).

47 Ferrario, C. M. & Strawn, W. B. Role of the renin-angiotensin-aldosterone system and proinflammatory mediators in cardiovascular disease. *The American journal of cardiology* **98**, 121-128, doi:10.1016/j.amjcard.2006.01.059 (2006).

48 Caughey, G. H. Mast cell tryptases and chymases in inflammation and host defense. *Immunological reviews* **217**, 141-154, doi:10.1111/j.1600-065X.2007.00509.x (2007).

49 Sopel, M. J., Rosin, N. L., Lee, T. D. & Legare, J. F. Myocardial fibrosis in response to Angiotensin II is preceded by the recruitment of mesenchymal progenitor cells. *Laboratory investigation; a journal of technical methods and pathology* **91**, 565-578, doi:10.1038/labinvest.2010.190 (2011).

50 Qi, G. *et al.* Angiotensin II infusion-induced inflammation, monocytic fibroblast precursor infiltration, and cardiac fibrosis are pressure dependent. *Cardiovascular toxicology* **11**, 157-167, doi:10.1007/s12012-011-9109-z (2011).

51 Lijnen, P. J., Petrov, V. V. & Fagard, R. H. Induction of cardiac fibrosis by angiotensin II. *Methods and findings in experimental and clinical pharmacology* **22**, 709-723 (2000).

52 Schnee, J. M. & Hsueh, W. A. Angiotensin II, adhesion, and cardiac fibrosis. *Cardiovascular research* **46**, 264-268 (2000).

53 Basso, N. *et al.* Protective effect of long-term angiotensin II inhibition. *American journal of physiology. Heart and circulatory physiology* **293**, H1351-1358, doi:10.1152/ajpheart.00393.2007 (2007).

54 Dai, D. F. *et al.* Overexpression of catalase targeted to mitochondria attenuates murine cardiac aging. *Circulation* **119**, 2789-2797, doi:10.1161/CIRCULATIONAHA.108.822403 (2009).

55 Benigni, A. *et al.* Disruption of the Ang II type 1 receptor promotes longevity in mice. *The Journal of clinical investigation* **119**, 524-530, doi:10.1172/JCI36703 (2009).

56 Williams, B., Baker, A. Q., Gallacher, B. & Lodwick, D. Angiotensin II increases vascular permeability factor gene expression by human vascular smooth muscle cells. *Hypertension* **25**, 913-917 (1995).

57 Alvarez, A. *et al.* Direct evidence of leukocyte adhesion in arterioles by angiotensin II. *Blood* **104**, 402-408, doi:10.1182/blood-2003-08-2974 (2004).

58 Zhang, G. X., Lu, X. M., Kimura, S. & Nishiyama, A. Role of mitochondria in angiotensin II-induced reactive oxygen species and mitogen-activated protein kinase activation. *Cardiovascular research* **76**, 204-212, doi:10.1016/j.cardiores.2007.07.014 (2007).

59 Welch, W. J. Angiotensin II-dependent superoxide: effects on hypertension and vascular dysfunction. *Hypertension* **52**, 51-56, doi:10.1161/HYPERTENSIONAHA.107.090472 (2008).

60 Chang, Y. & Wei, W. Angiotensin II in inflammation, immunity and rheumatoid arthritis. *Clinical and experimental immunology* **179**, 137-145, doi:10.1111/cei.12467 (2015).

61 Swirski, F. K. *et al.* Identification of splenic reservoir monocytes and their deployment to inflammatory sites. *Science* **325**, 612-616, doi:10.1126/science.1175202 (2009).

62 Haudek, S. B. *et al.* Monocytic fibroblast precursors mediate fibrosis in angiotensin-II-induced cardiac hypertrophy. *Journal of molecular and cellular cardiology* **49**, 499-507, doi:10.1016/j.yjmcc.2010.05.005 (2010).

63 Leuschner, F. *et al.* Angiotensin-converting enzyme inhibition prevents the release of monocytes from their splenic reservoir in mice with myocardial infarction. *Circulation research* **107**, 1364-1373, doi:10.1161/CIRCRESAHA.110.227454 (2010).

64 Ma, F. *et al.* Macrophage-stimulated cardiac fibroblast production of IL-6 is essential for TGF beta/Smad activation and cardiac fibrosis induced by angiotensin II. *PloS one* **7**, e35144, doi:10.1371/journal.pone.0035144 (2012).

65 Dai, Q., Xu, M., Yao, M. & Sun, B. Angiotensin AT1 receptor antagonists exert anti-inflammatory effects in spontaneously hypertensive rats. *British journal of pharmacology* **152**, 1042-1048, doi:10.1038/sj.bjp.0707454 (2007).

66 Duerrschmid, C., Trial, J., Wang, Y., Entman, M. L. & Haudek, S. B. Tumor necrosis factor: a mechanistic link between angiotensin-II-induced cardiac inflammation and fibrosis. *Circulation. Heart failure* **8**, 352-361, doi:10.1161/CIRCHEARTFAILURE.114.001893 (2015).

67 Olson, E. R., Shamhart, P. E., Naugle, J. E. & Meszaros, J. G. Angiotensin II-induced extracellular signal-regulated kinase 1/2 activation is mediated by protein kinase Cdelta and intracellular calcium in adult rat cardiac fibroblasts. *Hypertension* **51**, 704-711, doi:10.1161/HYPERTENSIONAHA.107.098459 (2008).

68 Gao, X. *et al.* Angiotensin II increases collagen I expression via transforming growth factor-beta1 and extracellular signal-regulated kinase in cardiac fibroblasts. *European journal of pharmacology* **606**, 115-120, doi:10.1016/j.ejphar.2008.12.049 (2009).

69 Kendall, R. T. & Feghali-Bostwick, C. A. Fibroblasts in fibrosis: novel roles and mediators. *Frontiers in pharmacology* **5**, 123, doi:10.3389/fphar.2014.00123 (2014).

70 Bai, J. *et al.* Metformin inhibits angiotensin II-induced differentiation of cardiac fibroblasts into myofibroblasts. *PloS one* **8**, e72120, doi:10.1371/journal.pone.0072120 (2013).

71 Hao, J., Wang, B., Jones, S. C., Jassal, D. S. & Dixon, I. M. C. Interaction between angiotensin II and Smad proteins in fibroblasts in failing heart and in vitro. *American journal of physiology. Heart and circulatory physiology* **279**, H3020-H3030 (2000).

72 Rodriguez-Vita, J. *et al.* Angiotensin II activates the Smad pathway in vascular smooth muscle cells by a transforming growth factor-beta-independent mechanism. *Circulation* **111**, 2509-2517, doi:10.1161/01.CIR.0000165133.84978.E2 (2005).

73 Yang, F., Chung, A. C., Huang, X. R. & Lan, H. Y. Angiotensin II induces connective tissue growth factor and collagen I expression via transforming growth factor-beta-dependent and -independent Smad pathways: the role of Smad3. *Hypertension* **54**, 877-884, doi:10.1161/HYPERTENSIONAHA.109.136531 (2009).

74 Finckenberg, P. *et al.* Angiotensin II Induces Connective Tissue Growth Factor Gene Expression via Calcineurin-Dependent Pathways. *The American journal of pathology* **163**, 355-366, doi:10.1016/s0002-9440(10)63659-0 (2003).

75 Ruperez, M. *et al.* Connective tissue growth factor is a mediator of angiotensin II-induced fibrosis. *Circulation* **108**, 1499-1505, doi:10.1161/01.CIR.0000089129.51288.BA (2003).

76 Schultz, J. E. J. *et al.* TGF-β1 mediates the hypertrophic cardiomyocyte growth induced by angiotensin II. *Journal of Clinical Investigation* **109**, 787-796, doi:10.1172/jci0214190 (2002).

77 Van Linthout, S., Miteva, K. & Tschope, C. Crosstalk between fibroblasts and inflammatory cells. *Cardiovascular research* **102**, 258-269, doi:10.1093/cvr/cvu062 (2014).

78 Frangogiannis, N. G. Emerging roles for macrophages in cardiac injury: cytoprotection, repair, and regeneration. *The Journal of clinical investigation* **125**, 2927-2930, doi:10.1172/JCI83191 (2015).

79 Wang, L. *et al.* Inhibition of Toll-like receptor 2 reduces cardiac fibrosis by attenuating macrophage-mediated inflammation. *Cardiovascular research* **101**, 383-392, doi:10.1093/cvr/cvt258 (2014).

80 Falkenham, A. *et al.* Nonclassical resident macrophages are important determinants in the development of myocardial fibrosis. *The American journal of pathology* **185**, 927-942, doi:10.1016/j.ajpath.2014.11.027 (2015).

81 Leask, A. Potential therapeutic targets for cardiac fibrosis: TGFbeta, angiotensin, endothelin, CCN2, and PDGF, partners in fibroblast activation. *Circulation research* **106**, 1675-1680, doi:10.1161/CIRCRESAHA.110.217737 (2010).

82 Widdop, R. E., Jones, E. S., Hannan, R. E. & Gaspari, T. A. Angiotensin AT2 receptors: cardiovascular hope or hype? *British journal of pharmacology* **140**, 809-824, doi:10.1038/sj.bjp.0705448 (2003).

83 Diaz-Araya, G. *et al.* Cardiac fibroblasts as sentinel cells in cardiac tissue: Receptors, signaling pathways and cellular functions. *Pharmacological research* **101**, 30-40, doi:10.1016/j.phrs.2015.07.001 (2015).

84 Xu, J. *et al.* Effects of cardiac overexpression of the angiotensin II type 2 receptor on remodeling and dysfunction in mice post-myocardial infarction. *Hypertension* **63**, 1251-1259, doi:10.1161/HYPERTENSIONAHA.114.03247 (2014).

85 Rosin, N. L., Falkenham, A., Sopel, M. J., Lee, T. D. & Legare, J. F. Regulation and role of connective tissue growth factor in AngII-induced myocardial fibrosis. *The American journal of pathology* **182**, 714-726, doi:10.1016/j.ajpath.2012.11.014 (2013).

86 Wynn, T. A. Cellular and molecular mechanisms of fibrosis. *The Journal of pathology* **214**, 199-210, doi:10.1002/path.2277 (2008).

87 Vliegen, H. W., van der Laarse, A., Cornelisse, C. J. & Eulderink, F. Myocardial changes in pressure overload-induced left ventricular hypertrophy. A study on tissue composition, polyploidization and multinucleation. *European heart journal* **12**, 488-494 (1991).

88 Pinto, A. R. *et al.* Revisiting Cardiac Cellular Composition. *Circulation research* **118**, 400-409, doi:10.1161/CIRCRESAHA.115.307778 (2016).

89 Nag, A. C. Study of non-muscle cells of the adult mammalian heart: a fine structural analysis and distribution. *Cytobios* **28**, 41-61 (1980).

90 Narmoneva, D. A., Vukmirovic, R., Davis, M. E., Kamm, R. D. & Lee, R. T. Endothelial cells promote cardiac myocyte survival and spatial reorganization: implications for cardiac regeneration. *Circulation* **110**, 962-968, doi:10.1161/01.CIR.0000140667.37070.07 (2004).

91 Hsieh, P. C., Davis, M. E., Lisowski, L. K. & Lee, R. T. Endothelial-cardiomyocyte interactions in cardiac development and repair. *Annual review of physiology* **68**, 51-66, doi:10.1146/annurev.physiol.68.040104.124629 (2006).

92 Travers, J. G., Kamal, F. A., Robbins, J., Yutzey, K. E. & Blaxall, B. C. Cardiac Fibrosis: The Fibroblast Awakens. *Circulation research* **118**, 1021-1040, doi:10.1161/CIRCRESAHA.115.306565 (2016).

93 Banerjee, I., Fuseler, J. W., Price, R. L., Borg, T. K. & Baudino, T. A. Determination of cell types and numbers during cardiac development in the neonatal and adult rat and mouse. *American journal of physiology. Heart and circulatory physiology* **293**, H1883-1891, doi:10.1152/ajpheart.00514.2007 (2007).

94 Osterreicher, C. H. *et al.* Fibroblast-specific protein 1 identifies an inflammatory subpopulation of macrophages in the liver. *Proceedings of the National Academy of Sciences of the United States of America* **108**, 308-313, doi:10.1073/pnas.1017547108 (2011).

95 Kong, P., Christia, P., Saxena, A., Su, Y. & Frangogiannis, N. G. Lack of specificity of fibroblast-specific protein 1 in cardiac remodeling and fibrosis. *American journal of physiology. Heart and circulatory physiology* **305**, H1363-1372, doi:10.1152/ajpheart.00395.2013 (2013).

96 Ali, S. R. *et al.* Developmental heterogeneity of cardiac fibroblasts does not predict pathological proliferation and activation. *Circulation research* **115**, 625-635, doi:10.1161/CIRCRESAHA.115.303794 (2014).

97 Yona, S. *et al.* Fate mapping reveals origins and dynamics of monocytes and tissue macrophages under homeostasis. *Immunity* **38**, 79-91, doi:10.1016/j.immuni.2012.12.001 (2013).

98 Swirski, F. K., Robbins, C. S. & Nahrendorf, M. Development and Function of Arterial and Cardiac Macrophages. *Trends in immunology* **37**, 32-40, doi:10.1016/j.it.2015.11.004 (2016).

99 Nahrendorf, M. & Swirski, F. K. Monocyte and macrophage heterogeneity in the heart. *Circulation research* **112**, 1624-1633, doi:10.1161/CIRCRESAHA.113.300890 (2013).

100 Epelman, S. *et al.* Embryonic and adult-derived resident cardiac macrophages are maintained through distinct mechanisms at steady state and during inflammation. *Immunity* **40**, 91-104, doi:10.1016/j.immuni.2013.11.019 (2014).

101 Heidt, T. *et al.* Differential contribution of monocytes to heart macrophages in steady-state and after myocardial infarction. *Circulation research* **115**, 284-295, doi:10.1161/CIRCRESAHA.115.303567 (2014).

102 Molawi, K. *et al.* Progressive replacement of embryo-derived cardiac macrophages with age. *The Journal of experimental medicine* **211**, 2151-2158, doi:10.1084/jem.20140639 (2014).

103 Naqvi, N. *et al.* A proliferative burst during preadolescence establishes the final cardiomyocyte number. *Cell* **157**, 795-807, doi:10.1016/j.cell.2014.03.035 (2014).

104 Falkenham, A., Myers, T., Wong, C. & Legare, J. F. Implications for the role of macrophages in a model of myocardial fibrosis: CCR2(-/-) mice exhibit an M2 phenotypic shift in resident cardiac macrophages. *Cardiovascular pathology : the official journal of the Society for Cardiovascular Pathology* **25**, 390-398, doi:10.1016/j.carpath.2016.05.006 (2016).

105 Crowley, S. D. *et al.* A role for angiotensin II type 1 receptors on bone marrow-derived cells in the pathogenesis of angiotensin II-dependent hypertension. *Hypertension* **55**, 99-108, doi:10.1161/HYPERTENSIONAHA.109.144964 (2010).

106 Falkenham, A. *et al.* Early fibroblast progenitor cell migration to the AngII-exposed myocardium is not CXCL12 or CCL2 dependent as previously thought. *The American journal of pathology* **183**, 459-469, doi:10.1016/j.ajpath.2013.04.011 (2013).

107 Rosenkranz, S. TGF-beta1 and angiotensin networking in cardiac remodeling. *Cardiovascular research* **63**, 423-432, doi:10.1016/j.cardiores.2004.04.030 (2004).

108 Bouzegrhane, F. & Thibault, G. Is angiotensin II a proliferative factor of cardiac fibroblasts? *Cardiovascular research* **53**, 304-312 (2002).

109 Biernacka, A., Dobaczewski, M. & Frangogiannis, N. G. TGF-beta signaling in fibrosis. *Growth factors* **29**, 196-202, doi:10.3109/08977194.2011.595714 (2011).

110 Dobaczewski, M., Chen, W. & Frangogiannis, N. G. Transforming growth factor (TGF)-beta signaling in cardiac remodeling. *Journal of molecular and cellular cardiology* **51**, 600-606, doi:10.1016/j.yjmcc.2010.10.033 (2011).

111 Dooley, S. & ten Dijke, P. TGF-beta in progression of liver disease. *Cell and tissue research* **347**, 245-256, doi:10.1007/s00441-011-1246-y (2012).

112 Fernandez, I. E. & Eickelberg, O. The impact of TGF-beta on lung fibrosis: from targeting to biomarkers. *Proceedings of the American Thoracic Society* **9**, 111-116, doi:10.1513/pats.201203-023AW (2012).

113 Harris, W. T. *et al.* Myofibroblast differentiation and enhanced TGF-B signaling in cystic fibrosis lung disease. *PloS one* **8**, e70196, doi:10.1371/journal.pone.0070196 (2013).

114 Brooks, W. W. & Conrad, C. H. Myocardial fibrosis in transforming growth factor beta(1)heterozygous mice. *Journal of molecular and cellular cardiology* **32**, 187-195, doi:10.1006/jmcc.1999.1065 (2000).

115 Rosenkranz, S. *et al.* Alterations of beta-adrenergic signaling and cardiac hypertrophy in transgenic mice overexpressing TGF-beta1. *American journal of physiology. Heart and circulatory physiology* **283**, H1253-H1262 (2002).

116 Annes, J. P. Making sense of latent TGFbeta activation. *Journal of Cell Science* **116**, 217-224, doi:10.1242/jcs.00229 (2003).

117 Frangogiannis, N. G. Targeting the transforming growth factor (TGF)-beta cascade in the remodeling heart: benefits and perils. *Journal of molecular and cellular cardiology* **76**, 169-171, doi:10.1016/j.yjmcc.2014.09.001 (2014).

118 Shi, M. *et al.* Latent TGF-beta structure and activation. *Nature* **474**, 343-349, doi:10.1038/nature10152 (2011).

119 Leask, A. & Abraham, D. J. TGF-beta signaling and the fibrotic response. *FASEB journal : official publication of the Federation of American Societies for Experimental Biology* **18**, 816-827, doi:10.1096/fj.03-1273rev (2004).

120 Rainer, P. P. *et al.* Cardiomyocyte-specific transforming growth factor beta suppression blocks neutrophil infiltration, augments multiple cytoprotective cascades, and reduces early mortality after myocardial infarction. *Circulation research* **114**, 1246-1257, doi:10.1161/CIRCRESAHA.114.302653 (2014).

121 Leask, A. TGFbeta, cardiac fibroblasts, and the fibrotic response. *Cardiovascular research* **74**, 207-212, doi:10.1016/j.cardiores.2006.07.012 (2007).

122 Dobaczewski, M. *et al.* Smad3 signaling critically regulates fibroblast phenotype and function in healing myocardial infarction. *Circulation research* **107**, 418-428, doi:10.1161/CIRCRESAHA.109.216101 (2010).

123 Zeisberg, E. M. *et al.* Endothelial-to-mesenchymal transition contributes to cardiac fibrosis. *Nature medicine* **13**, 952-961, doi:10.1038/nm1613 (2007).

124 Li, M. O., Wan, Y. Y., Sanjabi, S., Robertson, A. K. & Flavell, R. A. Transforming growth factor-beta regulation of immune responses. *Annual review of immunology* **24**, 99-146, doi:10.1146/annurev.immunol.24.021605.090737 (2006).

125 Travis, M. A. & Sheppard, D. TGF-beta activation and function in immunity. *Annual review of immunology* **32**, 51-82, doi:10.1146/annurev-immunol-032713-120257 (2014).

126 Mewhort, H. E. *et al.* Monocytes increase human cardiac myofibroblast-mediated extracellular matrix remodeling through TGF-beta1. *American journal of physiology. Heart and circulatory physiology* **310**, H716-724, doi:10.1152/ajpheart.00309.2015 (2016).

127 Ellmers, L. J. *et al.* Transforming growth factor-beta blockade down-regulates the renin-angiotensin system and modifies cardiac remodeling after myocardial infarction. *Endocrinology* **149**, 5828-5834, doi:10.1210/en.2008-0165 (2008).

128 Tan, S. M., Zhang, Y., Connelly, K. A., Gilbert, R. E. & Kelly, D. J. Targeted inhibition of activin receptor-like kinase 5 signaling attenuates cardiac dysfunction following myocardial infarction. *American journal of physiology. Heart and circulatory physiology* **298**, H1415-1425, doi:10.1152/ajpheart.01048.2009 (2010).

129 Ikeuchi, M. *et al.* Inhibition of TGF-beta signaling exacerbates early cardiac dysfunction but prevents late remodeling after infarction. *Cardiovascular research* **64**, 526-535, doi:10.1016/j.cardiores.2004.07.017 (2004).

130 Frantz, S. *et al.* Transforming growth factor beta inhibition increases mortality and left ventricular dilatation after myocardial infarction. *Basic research in cardiology* **103**, 485-492, doi:10.1007/s00395-008-0739-7 (2008).

131 Engebretsen, K. V. *et al.* Attenuated development of cardiac fibrosis in left ventricular pressure overload by SM16, an orally active inhibitor of ALK5. *Journal of molecular and cellular cardiology* **76**, 148-157, doi:10.1016/j.yjmcc.2014.08.008 (2014).

132 Bjornstad, J. L. *et al.* Inhibition of SMAD2 phosphorylation preserves cardiac function during pressure overload. *Cardiovascular research* **93**, 100-110, doi:10.1093/cvr/cvr294 (2012).

133 Lipson, K. E., Wong, C., Teng, Y. & Spong, S. CTGF is a central mediator of tissue remodeling and fibrosis and its inhibition can reverse the process of fibrosis. *Fibrogenesis Tissue Repair* **5**, S24, doi:10.1186/1755-1536-5-S1-S24 (2012).

134 Huang, X. R. *et al.* Smad3 mediates cardiac inflammation and fibrosis in angiotensin II-induced hypertensive cardiac remodeling. *Hypertension* **55**, 1165-1171, doi:10.1161/HYPERTENSIONAHA.109.147611 (2010).

135 Sorescu, D. Smad3 mediates angiotensin II- and TGF-beta1-induced vascular fibrosis: Smad3 thickens the plot. *Circulation research* **98**, 988-989, doi:10.1161/01.RES.0000221824.87718.c0 (2006).

136 Leask, A. & Abraham, D. J. All in the CCN family: essential matricellular signaling modulators emerge from the bunker. *J Cell Sci* **119**, 4803-4810, doi:10.1242/jcs.03270 (2006).

137 Garrett, Q. *et al.* Involvement of CTGF in TGF- b1-stimulation of myofibroblast differentiation and collagen matrix contraction in the presence of mechanical stress. *Invest Ophthalmol Vis Sci* **45**, 1109-1116 (2004).

138 Wang, Q. *et al.* Cooperative interaction of CTGF and TGF-beta in animal models of fibrotic disease. *Fibrogenesis Tissue Repair* **4**, 4, doi:10.1186/1755-1536-4-4 (2011).

139 Panek, A. N. *et al.* Connective tissue growth factor overexpression in cardiomyocytes promotes cardiac hypertrophy and protection against pressure overload. *PloS one* **4**, e6743, doi:10.1371/journal.pone.0006743 (2009).

140 Gravning, J., Ahmed, M. S., von Lueder, T. G., Edvardsen, T. & Attramadal, H. CCN2/CTGF attenuates myocardial hypertrophy and cardiac dysfunction upon chronic pressure-overload. *International journal of cardiology* **168**, 2049-2056, doi:10.1016/j.ijcard.2013.01.165 (2013).

141 Tsoutsman, T. *et al.* CCN2 plays a key role in extracellular matrix gene expression in severe hypertrophic cardiomyopathy and heart failure. *Journal of molecular and cellular cardiology* **62**, 164-178, doi:10.1016/j.yjmcc.2013.05.019 (2013).

142 Liu, S., Thompson, K. & Leask, A. CCN2 expression by fibroblasts is not required for cutaneous tissue repair. *Wound repair and regeneration : official publication of the Wound Healing Society [and] the European Tissue Repair Society* **22**, 119-124, doi:10.1111/wrr.12131 (2014).

143 Accornero, F. *et al.* Genetic Analysis of Connective Tissue Growth Factor as an Effector of Transforming Growth Factor beta Signaling and Cardiac Remodeling. *Molecular and cellular biology* **35**, 2154-2164, doi:10.1128/MCB.00199-15 (2015).

144 Fontes, M. S. *et al.* CTGF knockout does not affect cardiac hypertrophy and fibrosis formation upon chronic pressure overload. *Journal of molecular and cellular cardiology* **88**, 82-90, doi:10.1016/j.yjmcc.2015.09.015 (2015).

145 Campbell, S. E. & Katwa, L. C. Angiotensin II stimulated expression of TGF-beta1 in cardiac fibroblasts and myofibroblasts. *Journal of molecular and cellular cardiology* **29**, 1947-1958 (1997).

146 Lopez, B. *et al.* Biochemical assessment of myocardial fibrosis in hypertensive heart disease. *Hypertension* **38**, 1222-1226 (2001).

147 Ricard-Blum, S. The collagen family. *Cold Spring Harbor perspectives in biology* **3**, a004978, doi:10.1101/cshperspect.a004978 (2011).

148 Gordon, M. K. & Hahn, R. A. Collagens. *Cell and tissue research* **339**, 247-257, doi:10.1007/s00441-009-0844-4 (2010).

149 Myllyharju, J. & Kivirikko, K. I. Collagens, modifying enzymes and their mutations in humans, flies and worms. *Trends in genetics : TIG* **20**, 33-43, doi:10.1016/j.tig.2003.11.004 (2004).

150 Gonzalez-Santamaria, J. *et al.* Matrix cross-linking lysyl oxidases are induced in response to myocardial infarction and promote cardiac dysfunction. *Cardiovascular research* **109**, 67-78, doi:10.1093/cvr/cvv214 (2016).

151 Horn, M. A. & Trafford, A. W. Aging and the cardiac collagen matrix: Novel mediators of fibrotic remodelling. *Journal of molecular and cellular cardiology* **93**, 175-185, doi:10.1016/j.yjmcc.2015.11.005 (2016).

152 Rosin, N. L., Sopel, M. J., Falkenham, A., Lee, T. D. & Legare, J. F. Disruption of collagen homeostasis can reverse established age-related myocardial fibrosis. *The American journal of pathology* **185**, 631-642, doi:10.1016/j.ajpath.2014.11.009 (2015).

153 Bujak, M. & Frangogiannis, N. G. The role of TGF-beta signaling in myocardial infarction and cardiac remodeling. *Cardiovascular research* **74**, 184-195, doi:10.1016/j.cardiores.2006.10.002 (2007).

154 Euler, G. Good and bad sides of TGFbeta-signaling in myocardial infarction. *Frontiers in physiology* **6**, 66, doi:10.3389/fphys.2015.00066 (2015).

155 Zwaagstra, J. C. *et al.* Engineering and therapeutic application of single-chain bivalent TGF-beta family traps. *Molecular cancer therapeutics* **11**, 1477-1487, doi:10.1158/1535-7163.MCT-12-0060 (2012).

156 Rosin, N., Sopel, M., Falkenham, A., Myers, T. & Legare, J. F. Myocardial migration by fibroblast progenitor cells is blood pressure dependent in a model of angII myocardial fibrosis. *Hypertens Res* **35**, 449-456, doi:10.1038/hr.2011.217 (2012).

157 Underwood, R. A., Gibran, N. S., Muffley, L. A., Usui, M. L. & Olerud, J. E. Color subtractive-computer-assisted image analysis for quantification of cutaneous nerves in a diabetic mouse model. *The journal of histochemistry and cytochemistry : official journal of the Histochemistry Society* **49**, 1285-1291 (2001).

158 Midgley, A. C. *et al.* Transforming growth factor-beta1 (TGF-beta1)-stimulated fibroblast to myofibroblast differentiation is mediated by hyaluronan (HA)-facilitated epidermal growth factor receptor (EGFR) and CD44 co-localization in lipid rafts. *The Journal of biological chemistry* **288**, 14824-14838, doi:10.1074/jbc.M113.451336 (2013).

159 Pfaffl, M. W. A new mathematical model for relative quantification in real-time RT-PCR. *Nucleic acids research* **29**, e45 (2001).

160 Sarikonda, K. V., Watson, R. E., Opara, O. C. & Dipette, D. J. Experimental animal models of hypertension. *Journal of the American Society of Hypertension : JASH* **3**, 158-165, doi:10.1016/j.jash.2009.02.003 (2009).

161 Sopel, M. *et al.* Fibroblast progenitor cells are recruited into the myocardium prior to the development of myocardial fibrosis. *International journal of experimental pathology* **93**, 115-124, doi:10.1111/j.1365-2613.2011.00797.x (2012).

162 Sopel, M. J. *et al.* Treatment with activated protein C (aPC) is protective during the development of myocardial fibrosis: an angiotensin II infusion model in mice. *PloS one* **7**, e45663, doi:10.1371/journal.pone.0045663 (2012).

163 Brigstock, D. R. Connective tissue growth factor (CCN2, CTGF) and organ fibrosis: lessons from transgenic animals. *Journal of cell communication and signaling* **4**, 1-4, doi:10.1007/s12079-009-0071-5 (2010).

164 Dabek, J., Kulach, A., Monastyrska-Cup, B. & Gasior, Z. Transforming growth factor beta and cardiovascular diseases: the other facet of the 'protective cytokine'. *Pharmacological reports : PR* **58**, 799-805 (2006).

165 Kapur, N. K. Transforming growth factor-beta: governing the transition from inflammation to fibrosis in heart failure with preserved left ventricular function. *Circulation. Heart failure* **4**, 5-7, doi:10.1161/CIRCHEARTFAILURE.110.960054 (2011).

166 Iwamoto, M. *et al.* Connective tissue growth factor induction in a pressure-overloaded heart ameliorated by the angiotensin II type 1 receptor blocker olmesartan. *Hypertens Res* **33**, 1305-1311, doi:10.1038/hr.2010.189 (2010).

167 Chen, M. M., Lam, A., Abraham, J. A., Schreiner, G. F. & Joly, A. H. CTGF expression is induced by TGF-beta in cardiac fibroblasts and cardiac myocytes- a potential role in heart fibrosis. *Journal of molecular and cellular cardiology* **32**, 1805-1819, doi:10.1006/2000.1215 (2000).

168 Iwanciw, D., Rehm, M., Porst, M. & Goppelt-Struebe, M. Induction of connective tissue growth factor by angiotensin II: integration of signaling pathways. *Arteriosclerosis, thrombosis, and vascular biology* **23**, 1782-1787, doi:10.1161/01.ATV.0000092913.60428.E6 (2003).

169 Abdollah, S. *et al.* TbetaRI phosphorylation of Smad2 on Ser465 and Ser467 is required for Smad2-Smad4 complex formation and signaling. *The Journal of biological chemistry* **272**, 27678-27685 (1997).

170 Lim, H. & Zhu, Y. Z. Role of transforming growth factor-beta in the progression of heart failure. *Cellular and molecular life sciences : CMLS* **63**, 2584-2596, doi:10.1007/s00018-006-6085-8 (2006).

171 Lajiness, J. D. & Conway, S. J. Origin, development, and differentiation of cardiac fibroblasts. *Journal of molecular and cellular cardiology* **70**, 2-8, doi:10.1016/j.yjmcc.2013.11.003 (2014).

172 Leask, A. Getting to the heart of the matter: new insights into cardiac fibrosis. *Circulation research* **116**, 1269-1276, doi:10.1161/CIRCRESAHA.116.305381 (2015).

173 Gravning, J. *et al.* Myocardial connective tissue growth factor (CCN2/CTGF) attenuates left ventricular remodeling after myocardial infarction. *PloS one* **7**, e52120, doi:10.1371/journal.pone.0052120 (2012).

174 Szabo, Z. *et al.* Connective tissue growth factor inhibition attenuates left ventricular remodeling and dysfunction in pressure overload-induced heart failure. *Hypertension* **63**, 1235-1240, doi:10.1161/HYPERTENSIONAHA.114.03279 (2014).

175 Stawski, L., Haines, P., Fine, A., Rudnicka, L. & Trojanowska, M. MMP-12 deficiency attenuates angiotensin II-induced vascular injury, M2 macrophage accumulation, and skin and heart fibrosis. *PloS one* **9**, e109763, doi:10.1371/journal.pone.0109763 (2014).

176 Frangogiannis, N. G. Inflammation in cardiac injury, repair and regeneration. *Current opinion in cardiology* **30**, 240-245, doi:10.1097/HCO.0000000000000158 (2015).

177 Nahrendorf, M. *et al.* The healing myocardium sequentially mobilizes two monocyte subsets with divergent and complementary functions. *The Journal of experimental medicine* **204**, 3037-3047, doi:10.1084/jem.20070885 (2007).

178 Liu, Y. *et al.* Transforming growth factor-beta (TGF-beta)-mediated connective tissue growth factor (CTGF) expression in hepatic stellate cells requires Stat3 signaling activation. *The Journal of biological chemistry* **288**, 30708-30719, doi:10.1074/jbc.M113.478685 (2013).

179 Bonda, T. A. *et al.* Transcriptional and post-transcriptional regulation of CCN genes in failing heart. *Pharmacological reports : PR* **67**, 204-208, doi:10.1016/j.pharep.2014.08.019 (2015).

180 Ruiz-Ortega, M., Rodriguez-Vita, J., Sanchez-Lopez, E., Carvajal, G. & Egido, J. TGF-beta signaling in vascular fibrosis. *Cardiovascular research* **74**, 196-206, doi:10.1016/j.cardiores.2007.02.008 (2007).

181 Doetschman, T. *et al.* Transforming growth factor beta signaling in adult cardiovascular diseases and repair. *Cell and tissue research* **347**, 203-223, doi:10.1007/s00441-011-1241-3 (2012).

182 Attisano, L. & Wrana, J. L. Signal transduction by the TGF-beta superfamily. *Science* **296**, 1646-1647, doi:10.1126/science.1071809 (2002).

183 Shi, Y. & Massagué, J. Mechanisms of TGF-β Signaling from Cell Membrane to the Nucleus. *Cell* **113**, 685-700, doi:10.1016/s0092-8674(03)00432-x (2003).

184 Heldin, C. H. & Moustakas, A. Role of Smads in TGFbeta signaling. *Cell and tissue research* **347**, 21-36, doi:10.1007/s00441-011-1190-x (2012).

185 Daniels, A., van Bilsen, M., Goldschmeding, R., van der Vusse, G. J. & van Nieuwenhoven, F. A. Connective tissue growth factor and cardiac fibrosis. *Acta physiologica* **195**, 321-338, doi:10.1111/j.1748-1716.2008.01936.x (2009).

186 Verrecchia, F. & Mauviel, A. TGF-beta and TNF-alpha: antagonistic cytokines controlling type I collagen gene expression. *Cellular signalling* **16**, 873-880, doi:10.1016/j.cellsig.2004.02.007 (2004).

187 Pan, X., Chen, Z., Huang, R., Yao, Y. & Ma, G. Transforming growth factor beta1 induces the expression of collagen type I by DNA methylation in cardiac fibroblasts. *PloS one* **8**, e60335, doi:10.1371/journal.pone.0060335 (2013).

188 Kim, S. J. *et al.* Autoinduction of transforming growth factor beta 1 is mediated by the AP-1 complex. *Molecular and cellular biology* **10**, 1492-1497 (1990).

189 Flanders, K. C., Holder, M. G. & Winokur, T. S. Autoinduction of mRNA and protein expression for transforming growth factor-beta S in cultured cardiac cells. *Journal of molecular and cellular cardiology* **27**, 805-812 (1995).

190 Dockrell, M. E., Phanish, M. K. & Hendry, B. M. Tgf-beta auto-induction and connective tissue growth factor expression in human renal tubule epithelial cells requires N-ras. *Nephron. Experimental nephrology* **112**, e71-79, doi:10.1159/000221834 (2009).

191 Sarrazy, V. *et al.* Integrins alphavbeta5 and alphavbeta3 promote latent TGF-beta1 activation by human cardiac fibroblast contraction. *Cardiovascular research* **102**, 407-417, doi:10.1093/cvr/cvu053 (2014).

192 Buscemi, L. *et al.* The single-molecule mechanics of the latent TGF-beta1 complex. *Current biology : CB* **21**, 2046-2054, doi:10.1016/j.cub.2011.11.037 (2011).

193 Goumans, M. J. *et al.* Balancing the activation state of the endothelium via two distinct TGF-beta type I receptors. *The EMBO journal* **21**, 1743-1753, doi:10.1093/emboj/21.7.1743 (2002).

194 Koitabashi, N. *et al.* Increased connective tissue growth factor relative to brain natriuretic peptide as a determinant of myocardial fibrosis. *Hypertension* **49**, 1120-1127, doi:10.1161/HYPERTENSIONAHA.106.077537 (2007).

195 Wenzel, S., Taimor, G., Piper, H. M. & Schluter, K. D. Redox-sensitive intermediates mediate angiotensin II-induced p38 MAP kinase activation, AP-1 binding activity, and TGF-beta expression in adult ventricular cardiomyocytes. *FASEB journal : official publication of the Federation of American Societies for Experimental Biology* **15**, 2291-2293, doi:10.1096/fj.00-0827fje (2001).

196 Wang, J. F., Olson, M. E., Ball, D. K., Brigstock, D. R. & Hart, D. A. Recombinant connective tissue growth factor modulates porcine skin fibroblast gene expression. *Wound repair and regeneration : official publication of the Wound Healing Society [and] the European Tissue Repair Society* **11**, 220-229 (2003).

197 He, Z. *et al.* Differential regulation of angiotensin II-induced expression of connective tissue growth factor by protein kinase C isoforms in the myocardium. *The Journal of biological chemistry* **280**, 15719-15726, doi:10.1074/jbc.M413493200 (2005).

198 Vi, L., de Lasa, C., DiGuglielmo, G. M. & Dagnino, L. Integrin-linked kinase is required for TGF-beta1 induction of dermal myofibroblast differentiation. *The Journal of investigative dermatology* **131**, 586-593, doi:10.1038/jid.2010.362 (2011).

199 Thannickal, V. J. *et al.* Myofibroblast differentiation by transforming growth factor-beta1 is dependent on cell adhesion and integrin signaling via focal adhesion kinase. *The Journal of biological chemistry* **278**, 12384-12389, doi:10.1074/jbc.M208544200 (2003).

200 van Nieuwenhoven, F. A., Hemmings, K. E., Porter, K. E. & Turner, N. A. Combined effects of interleukin-1alpha and transforming growth factor-beta1 on modulation of human cardiac fibroblast function. *Matrix biology : journal of the International Society for Matrix Biology* **32**, 399-406, doi:10.1016/j.matbio.2013.03.008 (2013).

201 Widyantoro, B. *et al.* Endothelial cell-derived endothelin-1 promotes cardiac fibrosis in diabetic hearts through stimulation of endothelial-to-mesenchymal transition. *Circulation* **121**, 2407-2418, doi:10.1161/CIRCULATIONAHA.110.938217 (2010).

202 Shinde, A. V. & Frangogiannis, N. G. Fibroblasts in myocardial infarction: A role in inflammation and repair. *Journal of molecular and cellular cardiology* **70**, 74-82, doi:10.1016/j.yjmcc.2013.11.015 (2014).

203 Kawaguchi, M. *et al.* Inflammasome activation of cardiac fibroblasts is essential for myocardial ischemia/reperfusion injury. *Circulation* **123**, 594-604, doi:10.1161/CIRCULATIONAHA.110.982777 (2011).

204 Lindner, D. *et al.* Cardiac fibroblasts support cardiac inflammation in heart failure. *Basic research in cardiology* **109**, 428, doi:10.1007/s00395-014-0428-7 (2014).

205 Chen, W. & Frangogiannis, N. G. Fibroblasts in post-infarction inflammation and cardiac repair. *Biochimica et biophysica acta* **1833**, 945-953, doi:10.1016/j.bbamcr.2012.08.023 (2013).

206 Souders, C. A., Bowers, S. L. & Baudino, T. A. Cardiac fibroblast: the renaissance cell. *Circulation research* **105**, 1164-1176, doi:10.1161/CIRCRESAHA.109.209809 (2009).

207 Tian, Y. & Morrisey, E. E. Importance of myocyte-nonmyocyte interactions in cardiac development and disease. *Circulation research* **110**, 1023-1034, doi:10.1161/CIRCRESAHA.111.243899 (2012).

208 Fredj, S. *et al.* Role of interleukin-6 in cardiomyocyte/cardiac fibroblast interactions during myocyte hypertrophy and fibroblast proliferation. *Journal of cellular physiology* **204**, 428-436, doi:10.1002/jcp.20307 (2005).

209 Yano, T. *et al.* Intracardiac fibroblasts, but not bone marrow derived cells, are the origin of myofibroblasts in myocardial infarct repair. *Cardiovascular pathology : the official journal of the Society for Cardiovascular Pathology* **14**, 241-246, doi:10.1016/j.carpath.2005.05.004 (2005).

210 Mollmann, H. *et al.* Bone marrow-derived cells contribute to infarct remodelling. *Cardiovascular research* **71**, 661-671, doi:10.1016/j.cardiores.2006.06.013 (2006).

211 Haudek, S. B. *et al.* Bone marrow-derived fibroblast precursors mediate ischemic cardiomyopathy in mice. *Proc Natl Acad Sci U.S.A.* **103**, 18284-18289 (2006).

212 Kim, J. S. *et al.* Transforming growth factor-beta1 regulates macrophage migration via RhoA. *Blood* **108**, 1821-1829, doi:10.1182/blood-2005-10-009191 (2006).

213 Maroni, D. & Davis, J. S. Transforming growth factor Beta 1 stimulates profibrotic activities of luteal fibroblasts in cows. *Biology of reproduction* **87**, 127, doi:10.1095/biolreprod.112.100735 (2012).

214 Wahl, S. M. *et al.* Transforming growth factor type beta induces monocyte chemotaxis and growth factor production. *Proceedings of the National Academy of Sciences of the United States of America* **84**, 5788-5792 (1987).

215 Stawowy, P. *et al.* Regulation of matrix metalloproteinase MT1-MMP/MMP-2 in cardiac fibroblasts by TGF-beta1 involves furin-convertase. *Cardiovascular research* **63**, 87-97, doi:10.1016/j.cardiores.2004.03.010 (2004).

216 Sonnylal, S. *et al.* Selective expression of connective tissue growth factor in fibroblasts in vivo promotes systemic tissue fibrosis. *Arthritis and rheumatism* **62**, 1523-1532, doi:10.1002/art.27382 (2010).

217 Ponticos, M. *et al.* Pivotal role of connective tissue growth factor in lung fibrosis: MAPK-dependent transcriptional activation of type I collagen. *Arthritis and rheumatism* **60**, 2142-2155, doi:10.1002/art.24620 (2009).

218 Frangogiannis, N. G. Matricellular proteins in cardiac adaptation and disease. *Physiological reviews* **92**, 635-688, doi:10.1152/physrev.00008.2011 (2012).

219 Chuva de Sousa Lopes, S. M. *et al.* Connective tissue growth factor expression and Smad signaling during mouse heart development and myocardial infarction. *Developmental dynamics : an official publication of the American Association of Anatomists* **231**, 542-550, doi:10.1002/dvdy.20162 (2004).

220 Diez, J., Gonzalez, A. & Ravassa, S. Understanding the Role of CCN Matricellular Proteins in Myocardial Fibrosis. *Journal of the American College of Cardiology* **67**, 1569-1571, doi:10.1016/j.jacc.2016.01.029 (2016).

221 Yoon, P. O. *et al.* The opposing effects of CCN2 and CCN5 on the development of cardiac hypertrophy and fibrosis. *Journal of molecular and cellular cardiology* **49**, 294-303, doi:10.1016/j.yjmcc.2010.04.010 (2010).

222 Hilgendorf, I. *et al.* Ly-6Chigh monocytes depend on Nr4a1 to balance both inflammatory and reparative phases in the infarcted myocardium. *Circulation research* **114**, 1611-1622, doi:10.1161/CIRCRESAHA.114.303204 (2014).

223 Ismahil, M. A. *et al.* Remodeling of the mononuclear phagocyte network underlies chronic inflammation and disease progression in heart failure: critical importance of the cardiosplenic axis. *Circulation research* **114**, 266-282, doi:10.1161/CIRCRESAHA.113.301720 (2014).

224 Ma, F. *et al.* The requirement of CD8+ T cells to initiate and augment acute cardiac inflammatory response to high blood pressure. *Journal of immunology* **192**, 3365-3373, doi:10.4049/jimmunol.1301522 (2014).

225 Mellak, S. *et al.* Angiotensin II mobilizes spleen monocytes to promote the development of abdominal aortic aneurysm in Apoe-/- mice. *Arteriosclerosis, thrombosis, and vascular biology* **35**, 378-388, doi:10.1161/ATVBAHA.114.304389 (2015).

226 Lewanczuk, R. Hypertension as a chronic disease: What can be done at a regional level? *The Canadian journal of cardiology* **24**, 483-484 (2008).

227 Lohmeier, T. E. Angiotensin II infusion model of hypertension: is there an important sympathetic component? *Hypertension* **59**, 539-541, doi:10.1161/HYPERTENSIONAHA.111.188714 (2012).

228 Catt, K. J. *et al.* Angiotensin II blood-levels in human hypertension. *Lancet* **1**, 459-464 (1971).

229 Graziani, G. *et al.* Abnormal hemodynamics and elevated angiotensin II plasma levels in polydipsic patients on regular hemodialysis treatment. *Kidney international* **44**, 107-114 (1993).

230 Mitch, W. E. & Walker, W. G. Plasma renin and angiotensin II in acute renal failure. *Lancet* **2**, 328-330 (1977).

231 Schulz, A., Jankowski, J., Zidek, W. & Jankowski, V. Absolute quantification of endogenous Angiotensin II levels in human plasma using ESI-LC-MS/MS. *Clinical proteomics* **11**, 37 (2014).

232 Roig, E. *et al.* Clinical implications of increased plasma angiotensin II despite ACE inhibitor therapy in patients with congestive heart failure. *European heart journal* **21**, 53-57, doi:10.1053/euhj.1999.1740 (2000).

233 Huang, F. *et al.* Angiotensin II plasma levels are linked to disease severity and predict fatal outcomes in H7N9-infected patients. *Nature communications* **5**, 3595, doi:10.1038/ncomms4595 (2014).

234 Atkinson, A. B. *et al.* Renal artery stenosis with normal angiotensin II values. Relationship between angiotensin II and body sodium and potassium on correction of hypertension by captopril and subsequent surgery. *Hypertension* **3**, 53-58 (1981).

235 Anderson, W. P., Woods, R. L., Denton, K. M. & Alcorn, D. Renal actions of angiotensin II in renovascular hypertension. *Canadian journal of physiology and pharmacology* **65**, 1559-1565 (1987).

236 Hodsman, G. P. *et al.* Enalapril in treatment of hypertension with renal artery stenosis. Changes in blood pressure, renin, angiotensin I and II, renal function, and body composition. *The American journal of medicine* **77**, 52-60 (1984).

237 Bourantas, C. V. *et al.* Renal artery stenosis: an innocent bystander or an independent predictor of worse outcome in patients with chronic heart failure? A magnetic resonance imaging study. *European journal of heart failure* **14**, 764-772, doi:10.1093/eurjhf/hfs057 (2012).

238 Edgley, A. J., Krum, H. & Kelly, D. J. Targeting fibrosis for the treatment of heart failure: a role for transforming growth factor-beta. *Cardiovascular therapeutics* **30**, e30-40, doi:10.1111/j.1755-5922.2010.00228.x (2012).

239 Slany, A. *et al.* Plasticity of fibroblasts demonstrated by tissue-specific and function-related proteome profiling. *Clinical proteomics* **11**, 41, doi:10.1186/1559-0275-11-41 (2014).

240 Grotendorst, G. R. & Duncan, M. R. Individual domains of connective tissue growth factor regulate fibroblast proliferation and myofibroblast differentiation. *FASEB journal : official publication of the Federation of American Societies for Experimental Biology* **19**, 729-738, doi:10.1096/fj.04-3217com (2005).

241 Dutta, P. *et al.* Myocardial Infarction Activates CCR2(+) Hematopoietic Stem and Progenitor Cells. *Cell stem cell* **16**, 477-487, doi:10.1016/j.stem.2015.04.008 (2015).

242 Sager, H. B. *et al.* Proliferation and Recruitment Contribute to Myocardial Macrophage Expansion in Chronic Heart Failure. *Circulation research* **119**, 853-864, doi:10.1161/CIRCRESAHA.116.309001 (2016).

243 Holt, D. J., Chamberlain, L. M. & Grainger, D. W. Cell-cell signaling in co-cultures of macrophages and fibroblasts. *Biomaterials* **31**, 9382-9394, doi:10.1016/j.biomaterials.2010.07.101 (2010).